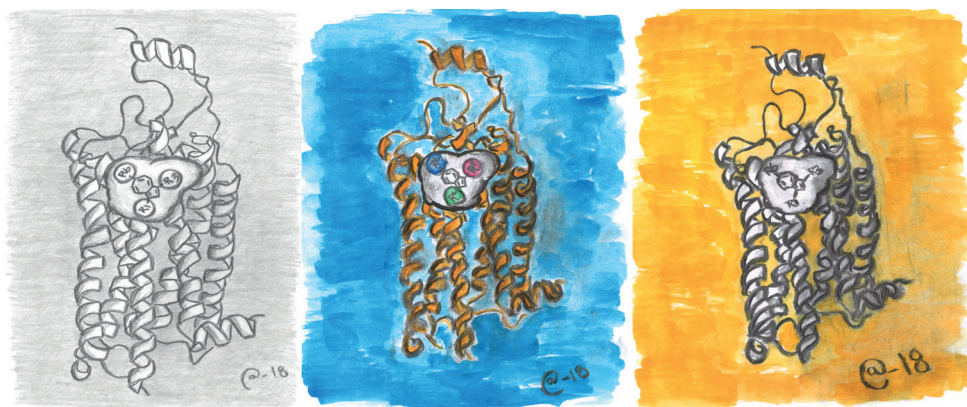AINOLEENA TURKU

Discovery of OX1 and OX2 Orexin Receptor Ligands

DIVISION OF PHARMACEUTICAL CHEMISTRY AND TECHNOLOGY
FACULTY OF PHARMACY
DOCTORAL PROGRAMME IN INTEGRATIVE LIFE SCIENCE
UNIVERSITY OF HELSINKI

Division of Pharmaceutical Chemistry and Technology
Faculty of Pharmacy
University of Helsinki
Finland

DISCOVERY OF OX$_1$ AND OX$_2$ OREXIN RECEPTOR LIGANDS

Ainoleena Turku

ACADEMIC DISSERTATION

To be presented, with the permission of the Faculty of Pharmacy of the University of Helsinki, for public examination in Auditorium 2, Viikki Infocenter Korona, on 17th of August 2018 at 12 noon.

Helsinki 2018

Supervisors   Docent Henri Xhaard, Ph.D.
                      Division of Pharmaceutical Chemistry
                      and Technology
                      Faculty of Pharmacy
                      University of Helsinki, Finland

                      Professor Jyrki P. Kukkonen,
                      B.M., M.Sc., Ph.D.
                      Department of Veterinary Biosciences
                      Faculty of Veterinary Medicine
                      University of Helsinki, Finland

Reviewers   Chris de Graaf, Ph.D.
                      Director Computational Chemistry
                      Heptares Therapeutics Ltd.
                      United Kingdom

                      Professor emeritus Mika Scheinin,
                      M.D., Ph.D.
                      Institute of Biomedicine
                      Faculty of Medicine
                      University of Turku, Finland

Opponent   Associate professor Jens Carlsson,
                      Ph.D.
                      Department of Cell and Molecular
                      Biology, BMC
                      University of Uppsala, Sweden

ABSTRACT

The main objective of this dissertation was to gain an understanding of orexin receptor activation at the molecular level and apply it in discovery of novel orexin receptor ligands. As non-peptide orexin receptor activators were almost completely unknown at the start of this study, attention was focused on them. To accomplish these goals, I utilized a combination of molecular modelling and pharmacological *in vitro* studies.

First, I studied the known orexin receptor ligands by structure- and ligand-based computational methods, and assembled the hypothesized activation features for a pharmacophore model. The model was utilized in a virtual screening, and a hit list of 395 compounds continued to a pharmacological screening phase, wherein I assessed their activities in a functional Ca^{2+}-based screening assay developed particularly for that purpose. I validated the screening hits in the competition binding and Ca^{2+} elevation assays; six compounds showed weak agonist activity and K_i's in the $1-30\ \mu M$ range (Publication I). Antagonists with sub-micromolar binding affinities were also identified.

Retrospective docking simulations of these agonistic hits and known non-peptide orexin receptor agonists (Nag26 and Yan7874, the latter of which was pharmacologically characterized in Publication II) were used to devise a working hypothesis of the binding pocket regions important for orexin receptor activation. Interactions in the antagonist binding region and two additional sub-pockets—one between TM5 and TM6, and the other approximately one helical turn above the antagonist binding site close to TM7—would be needed for orexin receptor activation (Publication I).

Relying on this, I constructed a targeted azulene-based combinatory compound library accessible to in-house chemistry. The azulene library was virtually screened at the crystal structure of OX_2 receptor, and compounds selected from

the hit list were synthesized and screened *in vitro*. I validated the hits as above, and novel antagonists, weak agonists and compounds potentiating the actions of orexin-A were identified (Publications III and IV).

The literature review focuses on the concept of GPCR activation and the orexin system: its structure, functions, and pharmaceutical applications thereof.

TIIVISTELMÄ

Väitöskirjatyöni tarkoitus oli tutkia oreksiinireseptoriaktivaatiota molekyylitasolla ja käyttää saatua tietoa uusien oreksiinireseptoriligandien löytämiseen. Aloittaessani työtäni oreksiinireseptoreja aktivoivia pienmolekyylejä ei tunnettu käytännössä lainkaan, joten keskityin ensisijaisesti niihin. Näihin tavoitteisiin päästäkseni käytin tietokoneavusteisia menetelmiä synergiassa *in vitro* -kokeiden kanssa.

Oreksiinireseptoriligandien tutkiminen rakenne- ja ligandipohjaisilla tietokoneavusteisilla menetelmillä johti mahdollisten – reseptoriaktivaation kannalta oleellisten – vuorovaikutuspisteiden tunnistamiseen ja farmakoforimallien rakentamiseen. Käytin parasta malleistani virtuaaliseulontaan, jonka perusteella 395 yhdistettä jatkoi tätä varten kehittämäämme Ca^{2+} vapautumiseen perustuvaan *in vitro* -seulontaan. Validoin seulontahitit sitoutumis- ja funktionaalisin kokein; kuusi hittiä osoittautui heikoiksi oreksiinireseptoriagonisteiksi (K_i:t 1–30 µM; osatyö I). Lisäksi löysimme oreksiinireseptoriantagonisteja, joiden sitoutumisaffiniteetit olivat nanomolaarisella tasolla.

Tutkimme yhdisteitämme ja tunnettuja ei-peptidirakenteisia oreksiinireseptoriagonisteja (Nag26 ja Yan7874; jälkimmäisen farmakologinen karakterisointi on esitetty osatyössä II) myös telakoinnin avulla. Telakointitulokset viittasivat kolmen sitoutumistaskun tärkeyteen oreksiinireseptoriaktivaation kannalta. Nämä taskut – antagonistimolekyylien sitoutumispaikka, alue TM5 ja TM6 -heliksien välissä sekä toinen alue noin yhden helikaalisen kierteen verran antagonistien sitoutumispaikan yläpuolella lähellä TM7:ää – vuorovaikuttivat kaikkien tutkittujen agonistiligandien kanssa (osatyö I).

Suunnittelimme tähän aktivaatiohypoteesiin perustuen virtuaalisen atsuleeniyhdistekirjaston, jonka synteesi olisi mahdollista osastollamme. Virtuaaliseuloin kirjaston OX2-

reseptorin kiderakenteeseen ja seulonnan tuloksista valitut yhdisteet syntetisoitiin ja testattiin *in vitro*. Validoin hitit yllä kuvatulla tavalla ja löysin uusia oreksiinireseptoriantagonisteja, heikkoja agonisteja ja yhdisteitä, jotka vahvistavat oreksiini-A-välitteistä reseptoriaktivaatiota (osatyöt III ja IV).

Työni kirjallisuuskatsaus käsittelee G-proteiinikytkentäisten reseptorien aktivaatiota sekä oreksiinijärjestelmän rakennetta ja toimintaa, sekä oreksiinijärjestelmää lääkekehityksen kohteena.

ACKNOWLEDGEMENTS

'The Road goes ever on and on

Down from the door where it began.

Now far ahead the Road has gone,

And I must follow, if I can,

Pursuing it with eager feet,

Until it joins some larger way

Where many paths and errands meet.

And whither then? I cannot say.'

Bilbo Baggins in The Fellowship of the Ring (1954)

I was caught by the Road in 2013, and as Bilbo Baggins, I did not remain unchanged either. Hereby, I would like to thank all those people who have accompanied me during this journey.

First, I wish to express my warmest gratitude to my supervisors Dr. Henri Xhaard and Prof. Jyrki Kukkonen. Without you there would not be a scientist currently known as me. Henri, we have walked together for long time, and I would not change a day (or at least not statistically significant number of days). I appreciate and admire your scientific curiosity and the preciseness of your work, and I am grateful that you have taught me the essence of being a scientist. Oh, and thanks for the beer in ISB. Jyrki, thanks for believing in my vision also in those days I did not—your company has delighted me in the good days and support made me tolerate the rainy ones.

I would like to thank my custos Prof. Jari Yli-Kauhaluoma for being the most approachable person ever. You inspired me when I was an undergraduate student and you still do.

My warm thanks go to the personnel of the day care centre Kissankello, especially Merja, Tuula, Tuija and Sari. Without you, this dissertation could not have existed within this time frame.

I am grateful to my parents for raising me up by supporting my strengths and interests. Without the can-do attitude I have learned from you, I would not have reached this far. Yes, you have surely done something right (read: Emmää ny silti tiä, mut kai te ny ootte jotai oikeenki tehny).

Finally, I would like to thank my beloved boys—Mikko, Eero and Vilho. You are the major reason I have managed to maintain sanity during this process. Thank you for your unconditional love. 'Ja kuitenkin / Kuitenkin / Yksi on suurempi muita / Nyt ja aina / Ja kun sen kohtaa et kysele hintaa / Tai kuuntele jeesusteluita / Ne ei mitään paina / Ne ei helli ja polta sun rintaa' (Vilkkumaa M., 2005).

Helsinki, July 2018

Ainoleena Turku

TABLE OF CONTENTS

LIST OF ORIGINAL PUBLICATIONS

This thesis is based on the following publications:

I   Turku, A., Borrel, A., Leino, T. O., Karhu, L., Kukkonen, J. P., Xhaard, H. Pharmacophore Model To Discover OX_1 and OX_2 Orexin Receptor Ligands. *J. Med. Chem.* **2016**, *59*, 8263–8275

II   Turku, A., Rinne, M. K., Boije af Gennäs, G., Xhaard, H., Lindholm, D., Kukkonen, J. P. Orexin Receptor Agonist Yan 7874 Is a Weak Agonist of Orexin/hypocretin Receptors and Shows Orexin Receptor-Independent Cytotoxicity. *PLoS One* **2017**, *12*, e0178526

III   Leino T. O.*, Turku A.*, Yli-Kauhaluoma J., Kukkonen J. P., Xhaard H., Wallén E. A. A. Azulene-based Compounds for Targeting Orexin Receptors. *Eur. J. Med. Chem.* **2018**, *in press*

IV   Turku A.*, Leino T. O.*, Yli-Kauhaluoma J., Kukkonen J. P., Wallén E. A. A., Xhaard H. Azulene-based Compounds as Orexin Receptor Activating Agents. (*manuscrip*t)

* These authors contributed equally

The publications are referred to in the text by their roman numerals. The reprints are published with the permission of the copyright holders.

CONTRIBUTION TO ORIGINAL PUBLICATIONS

I   Design, conduction, and analysis of the
            computational (pharmacophore modelling,
            docking simulations) as well as the
            pharmacological parts of the study together with
            H. X. and J. P. K., accordingly, and writing the
            manuscript.

II   Design of the study together with J. P. K.,
            conduction of the majority of the experiments and
            data analyses. Reviewing and editing the
            manuscript.

III   Design, conduction, and analysis of the
            computational and pharmacological parts of the
            study (together with H. X. and J. P. K.). Writing the
            manuscript together with T. O. L.

IV   As in publication III.

ADDITIONAL SCIENTIFIC INPUT

Orexin system-related publications:

Rinne M. K., Leino T. O., Turku A., Turunen P. M., Staynen Y., Xhaard H., Wallén E. A. A., Kukkonen J. P.: Pharmacological characterization of the orexin/hypocretin receptor agonist Nag26. *Eur. J. Pharmacology,* **2018** *(accepted with minor revisions)*

Karhu L., Turku A., Xhaard H.: Modeling of the OX_1R–orexin-A complex suggests two alternative binding modes. *BMC Structural Biology*, **2015**, 15 (9).

Publications of membrane-bound pyrophosphatases:

Vidilaseris K., Kiriazis A., Turku A., Ayman K., Johansson N., Leino T. O., Kiuru P. S., Boije af Gennäs G., Meri S., Yli-Kauhaluoma J., Xhaard H., Goldman A.: Structure of membrane bound pyrophosphatase from *Thermotoga maritima* in complex with imidodiphosphate and a novel inhibitor. *(submitted manuscript)*

Harborne S. P. D., Strauss J., Turku A., Watson M. A., Tuma R., Harris S. A., Goldman A.: Defining dynamics of membrane-bound pyrophosphatases by experimental and computational single-molecule FRET. *Methods in Enzymology,* **2018**, *in press*.

Shah N. R., Wilkinson C., Harborne S. P. D., Turku A., Li K.-M., Sun Y.-J., Harris S., Goldman A.: Insights into the mechanism of membrane pyrophosphatases by combining experiment and computer simulation. *Structural dynamics*, **2017**, 4 (3).

ABBREVIATIONS

1-SORA	OX_1-selective receptor antagonist
2-AG	2-arachidonoylglycerol
2-SORA	OX_2-selective receptor antagonist
5-HT$_{1A}$	5-HT$_{1A}$ serotonin receptor
5-HT$_{1B}$	5-HT$_{1B}$ serotonin receptor
A_{2A}	A_2 adenosine receptor
AC	Adenylyl cyclase
AT_1	AT_1 angiotensin receptor
AT_2	AT_2 angiotensin receptor
CB_1	CB_1 cannabinoid receptor
CCR5	CCR5 chemokine receptor
CHO	Chinese hamster ovary
CRF_1	CRF_1 corticotrophin-releasing factor receptor
CTx	Cholera toxin
CXCR4	CXCR4 chemokine receptor
DAG	Diacylglycerol
DORA	Dual orexin receptor antagonist
DR	Dorsal raphe
ECL1–3	Extracellular loops 1–3
ER	Endoplasmic reticulum
ERK	Extracellular signal-regulated kinase
ET_1	Endothelin 1
ET_B	Endothelin B receptor
FDA	Fluorescein diacetate
FN	False negative
FP	False positive
$GABA_A$	Gamma-aminobutyric acid A receptor
GPCR	G protein-coupled receptor
GRK	GPCR kinase
GSK	Glaxo Smith Kline
H	Hydrophobic feature
HBA	Hydrogen bond acceptor (feature)
HBD	Hydrogen bond donor (feature)
HBM	Hepes-buffered medium

HCRTR1	Human OX_1 receptor gene
HCRTR2	Human OX_2 receptor gene
HEK293	Human embryonic kidney cells 293
HPA	Hypothalamic–pituitary–adrenal
HTS	High throughput screening
ICL1–3	Intracellular loops 1–3
i.c.v.	Intracerebroventricular
IP_3	Inositol trisphosphate
ITSM	Immunoreceptor tyrosine-based switch motif
LC	Locus coeruleus
LDT	Laterodorsal tegmental nucleus
LH	Lateral hypothalamus
M_2	M_2 muscarinic receptor
MD	Molecular dynamics
mRNA	Messenger RNA
NCKX	Na^+/Ca^{2+}-K^+ exchanger
NCX	Na^+/Ca^{2+} exchanger
NREM	Non-rapid eye movement
NSCC	Non-selective cation channel
NTS_1	NTS_1 neurotensin receptor
OX_1	OX_1 orexin receptor
OX_2	OX_2 orexin receptor
p38 MAPK	p38 mitogen-activated protein kinase
PA	Phosphatidic acid
PAINS	Pan-assay interference compounds
PCA	Principal component analysis
PDB	Protein databank
PF	Perifornical area
PH	Posterior hypothalamus
PI	Propidium iodide
PIP_2	Phosphatidylinositol-4,5-bisphosphate
PKA	Protein kinase A
PKC	Protein kinase C
PLA_2	Phospholipase A_2
PLC	Phospholipase C
PLD	Phospholipase D
PPT	Pedunculopontine nucleus

PTx	Pertussis toxin
R	Aromatic feature
REM	Rapid eye-movement
REOS	Rapid elimination of swill
RGS	Regulator of G protein signalling
RhoGEF	Rho guanine nucleotide exchange factor
RMSD	Root mean square deviation
ROC	Receiver operating characteristic
SAR	Structure–activity relationship
TM1–TM7	Transmembrane helices 1–7
TMN	Tuberomammillary nucleus
TN	True negative
TP	True positive
TRPC	Canonical transient receptor potential
VGCC	Voltage-gated Ca^{2+} channel
VTA	Ventral tegmental area
β_1	β_1-adrenoceptor
β_2	β_2-adrenoceptor
κOR	Kappa opioid receptor
μOR	Mu opioid receptor
σ1	Sigma 1 receptor

1 INTRODUCTION

The orexin system, composed of two G protein-coupled receptors OX_1 and OX_2 and peptide agonists orexin-A and orexin-B, is connected to several physiological functions and is crucial for sleep-wake regulation. Activating orexin receptors with non-peptide ligands has proven to be challenging; however, there is a need for a discovery of such compounds for example to treat narcolepsy. One way to efficiently achieve this is by understanding orexin receptor activation at molecular level.

At the commencement of the studies for this doctoral thesis in 2013, the knowledge of orexin system was relatively scattered. At that time, amino acid sequences of orexin receptors and solution structures of orexin peptides had been published, and point mutation studies and receptor chimeras had identified the approximate location of the orthosteric binding site (Figure 1). Additionally, only one possible non-peptide orexin receptor agonist, Yan7874, had been reported in the patent literature, but conversely a variety of orexin receptor antagonists had been discovered. Thus, we aimed to utilize computational methods to merge that knowledge and identify the molecular attributes that lead to orexin receptor binding and activation. Subsequently, the goal was to apply the gained understanding and identify novel orexin receptor ligands, preferably activators.

This dissertation, a joint project between the Division of Pharmaceutical Chemistry and Technology (Faculty of Pharmacy) and the Department of Veterinary Biosciences (Faculty of Veterinary Medicine) of University of Helsinki, consists of three peer-reviewed publications and a manuscript (referred as publications I–IV). Publication I presents a pharmacophore-based virtual screening combined with a pharmacological screening and validation of the identified hits (antagonists and weak agonists with sub-micromolar binding affinities); publication II verifies the agonist activity of the

template molecule used in pharmacophore modelling. While writing these publications, Nag26, the first full non-peptide orexin receptor agonist, was discovered, and OX$_2$ receptor crystal structure in complex with small molecule antagonist suvorexant was reported (Figure 1). Together with our findings, they opened new insights into orexin receptor activation.
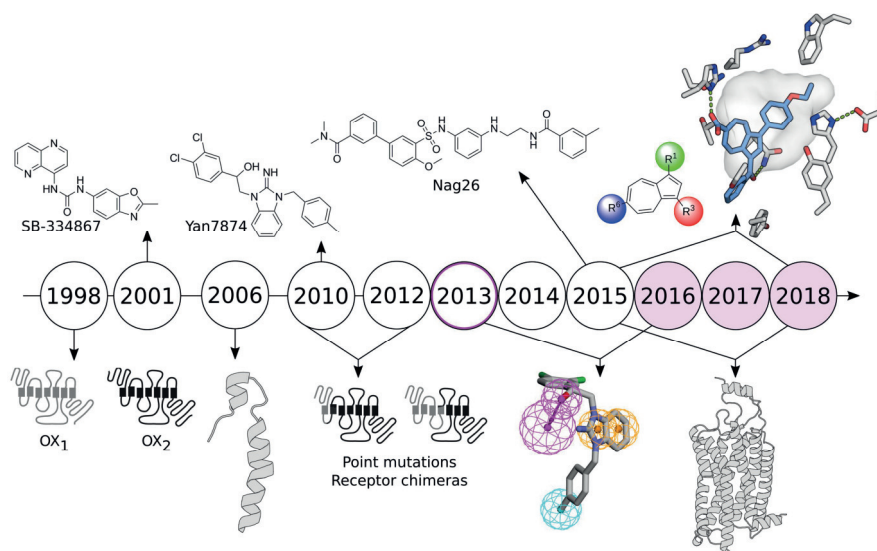
Figure 1. Orexin research timeline. 1998: The orexin system was discovered. 2001: First orexin receptor antagonists were disclosed. 2006: The NMR structure of full-length orexin-A was solved. 2010: Yan7874 was reported in a patent literature. 2010–2012: The orthosteric binding site was identified by point mutations and receptor chimeras. 2013: The studies for this dissertation started. 2014: Orexin receptor antagonist suvorexant was approved by FDA for treatment of insomnia. 2015: Nag26 was published. 2015–2018: The crystal structures of orexin receptors in complex with subtype selective and dual antagonists were solved. 2016: Publication I. 2017: Publication II. 2018: Publications III and IV. The schematic representations of OX$_1$ and OX$_2$ receptors and corresponding chimeras are modified from [1].

Inspired by the new data, we constructed a targeted virtual library of azulene-based compounds accessible to the medicinal chemistry developed in-house to identify novel orexin receptor ligands. We conducted a virtual screening at the crystal

structure of OX_2 receptor and selected a subset of the hit list compounds for synthesis. Subsequently, these compounds were pharmacologically screened and verified, and among these, orexin receptor antagonists, weak agonists, and compounds potentiating the actions of the endogenous ligand orexin-A were identified (publications III and IV).

2 REVIEW OF THE LITERATURE

2.1 G PROTEIN-COUPLED RECEPTORS

G protein-coupled receptors (GPCRs) are a large receptor family that are encoded by more than 800 genes in the human genome (about a half of which have sensory functions).[2,3] GPCRs are embedded in cell membranes throughout the human body,[4] and share a common structure: an extracellular N-terminus, seven helical transmembrane domains (TM1–TM7) linked by three extra- and intracellular loops (ECL1–3 and ICL1–3, respectively), and an intracellular C-terminus.[2,3] In general, the ligand binding on the extracellular side of the receptor triggers intricate signalling cascades inside the cell, which ultimately leads to the physiological response. Thus, GPCRs offer a molecular switch, which can be utilized to regulate a wide variety of physiological responses, making them attractive drug targets.[3,5] Indeed, the signal transduction modulated by GPCRs is essential from visual, olfactory, and gustatory sensation to neurological, cardiovascular, endocrine, and reproductive functions.

2.1.1 PHARMACOLOGICAL MODULATION OF GPCRS

Human GPCRs are divided into five main families based on their sequence similarity: Rhodopsin (class A), Secretin and Adhesion (class B), Glutamate (class C), Frizzled (class F) and Taste 2 (class T).[3,6–9] Of these, the Rhodopsin-family is both the largest and most thoroughly studied, and many endogenous ligands are known.[3] GPCR-targeted drug design has mainly focused on the Rhodopsin-family, and consequently, approximately 30% of the drugs in the market act via these GPCRs.[5,10]

Apart from the GPCR ligands found in nature (e.g. μ opioid receptor agonist morphine, reviewed in [11]), GPCRs have been originally targeted by compounds mimicking the endogenous

ligands either to achieve a similar physiological response (e.g. salbutamol, which activates the β_2-adrenoceptors in the lungs for the treatment of asthma), or to block the physiological response by competing with the endogenous ligand (e.g. propranolol, which blocks the response to noradrenalin via β-adrenoceptors in the treatment of hypertension, see e.g. [12]). Currently, GPCR-targeting ligands are typically classified as agonists (triggers a similar response to the endogenous ligand), neutral antagonists (blocks the response to the endogenous ligand without affecting the basal activity of the receptor), or inverse agonists (as antagonist, but reduces also the basal activity; reviewed in [13,14]). Furthermore, ligands can act as partial agonists; the maximal response to a partial agonist is only a fraction of the maximal response to the endogenous agonist. Finally, a biased agonist stabilizes a certain receptor conformation resulting in the activation of one signalling pathway over another.[15]

In addition to the classical agonists and antagonists acting via an orthosteric binding site (i.e. the binding site of endogenous ligand), GPCRs can be regulated with ligands targeting other binding sites.[5] Allosteric ligands are compounds, which act at a site that is topographically different from the orthosteric binding site, and thus modulate the actions of the endogenous ligand making it more or less potent (positive and negative allosteric modulators, respectively; reviewed in [14]). Furthermore, positive allosteric modulators can have some agonist activity of their own (ago-allosteric ligands, reviewed in [16]). Bitopic ligands can act simultaneously at both orthosteric and allosteric binding sites (reviewed in [17]). Bivalent ligands, instead, can bridge a dimeric construct of GPCRs and bind simultaneously at the binding sites of adjacent receptors (reviewed in [18]).

2.1.2 G PROTEIN SIGNALLING CYCLE

GPCRs signal via heterotrimeric G proteins, which are composed of α-, β-, and γ-subunits (reviewed e.g. in [19–23]; Figure

2). These subunits—and α-subunit-bound GDP—remain in complex while the G protein is in the resting state. Activation of the receptor drives the release of GDP and the binding of GTP, which triggers a conformational change in G protein structure. Typically, the conformational change leads to the dissociation of the complex to separate α- and βγ-subunits (Gα and Gβγ, respectively), which then interact with their downstream effectors. However, the complex does not necessarily fully dissociate in the downstream signalling (reviewed in [24]).

G proteins are divided into four families based on their Gα subunits: G_i, G_s, G_q, and $G_{12/13}$ (reviewed in [25]). In much simplified terms, $G\alpha_s$ and $G\alpha_i$ activate and inhibit adenylyl cyclase (AC), respectively, which leads to the alteration of the levels of the secondary messenger cAMP, and thus the functions of e.g. protein kinase A (PKA; reviewed in [26,27]). $G\alpha_q$ stimulates phospholipase C (PLC), which hydrolyses inositol phospholipids (e.g. phosphatidylinositol-4,5-bisphosphate a.k.a. PIP_2) into diacylglycerol (DAG) and inositol phosphates, such as inositol trisphosphate (IP_3, reviewed in [28–30]). DAG and IP_3 are second messengers, which activate protein kinase C (PKC) and Ca^{2+} release from endoplasmic reticulum (ER), respectively. PLC also affects functions of other membrane proteins such as ion channels via regulation of the membrane levels of inositol phospholipids. $G\alpha_{12/13}$ has mainly reported to activate Rho guanine nucleotide exchange factors (RhoGEFs; reviewed in [26]), which leads to various effects, such as the regulation of Na^+/H^+ exchanger. Apart from Gαs, Gβγ subunit can participate in signalling cascades of its own, for example, targeting some PLC isoforms and K^+ and Ca^{2+} channels (reviewed in [23,27,30]).

At the end of the G protein signalling cycle, the G protein returns to its resting state upon a hydrolysis of GTP to GDP by the Gα-subunit. The hydrolysis can be enhanced by regulator of G protein signalling proteins (RGS proteins; reviewed in [20,23,27]). Apart from the built-in catalytic activity of Gα, there are also other mechanisms to dampen any prolonged signalling, such as GPCR kinase (GRK) -catalysed receptor phosphorylation, which

then recruits intracellular regulatory proteins β-arrestins (reviewed in [23,27,31]; Figure 2). β-arrestins have intricate roles in cellular processes leading, for example, to G protein uncoupling, receptor internalization, and intracellular trafficking (recycling or degradation). Additionally, similar to G protein-GPCR–complexes, β-arrestin–GPCR complexes have signalling pathways of their own (reviewed in [27,31]).
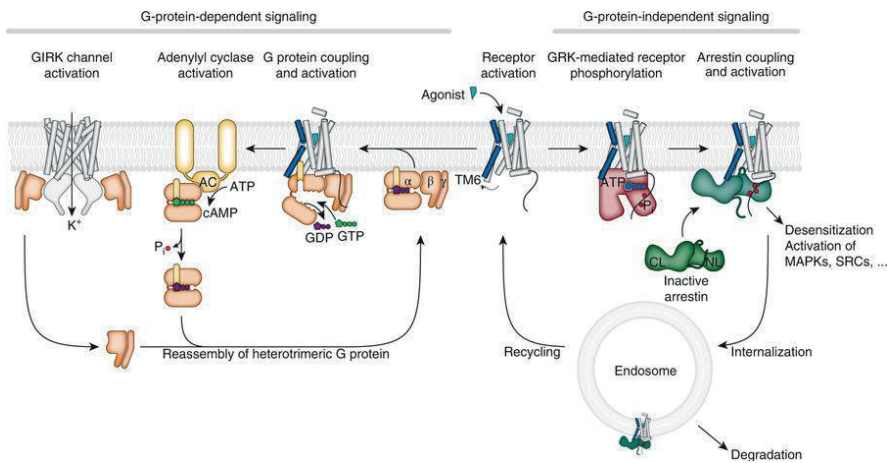
Figure 2.A schematic representation of the G protein cycle. In the resting state, the GDP-bound heterotrimeric G protein consists of α, β, and γ subunits (orange). Agonist (blue) and G protein binding to the GPCR leads to GDP release. The trimeric G protein complex remains stable until the GTP binding causes dissociation of Gα-GTP and Gβγ subunits. Subsequently, the subunits activate downstream effector proteins, such as adenylyl cyclase (AC) or G protein-coupled inwardly rectifying potassium channels (GIRKs). The signalling terminates by hydrolysis of GTP to GDP and reassociation of the G protein. Receptor activation can also lead to GRK-mediated receptor phosphorylation and, subsequently, coupling to β-arrestin (GRK in red; inactive β-arrestin in green; active β-arrestin in teal). Arrestin binding leads to desensitization and activation of several downstream effectors, such as mitogen-activated protein kinases (MAPKs). Additionally, β-arrestin activation promotes receptor internalization leading to receptor degradation or recycling. Adapted from [23] by permission from Springer Nature (Copyright 2018).

2.1.3 ACTIVE AND INACTIVE GPCR CONFORMATIONS

GPCR structures can oscillate among different conformational states, which can be represented as an equilibrium between each other (the states R, R', R'', R*, or R*G are presented in Figure 3). Additionally, current functional, structural, spectroscopic, and computational data suggest that the ability of GPCRs to regulate a variety of signalling pathways originates from the allosteric coupling between the orthosteric binding site and the intracellular G protein/β-arrestin-binding site (reviewed in [23]). How these dynamic conformational states are associated with the functional outcomes, and how they are regulated by different ligands remains not fully understood.
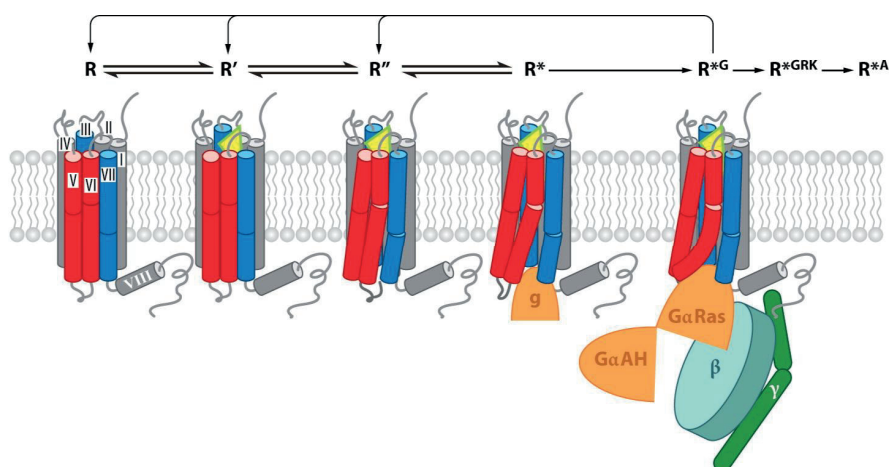
Figure 3. A schematic representation of GPCR structure, and structural changes upon receptor activation. R means the inactive state, and R' the inactive low-affinity agonist-bound state differing from R only by small local changes of the binding pocket side chains. R'' is the activated state (rearrangement of helices and side chain microswitches). R* represents activated sub-states co-crystallized with the G protein C-terminal α-helix (or its mimic; g) in the intracellular G protein-binding cavity. R*G is the distinct G protein signalling conformation of the receptor, achieved upon full engagement and activation of the GPCR–Gαβγ-complex. Other, not-presented, states include GPCR binding to G protein receptor kinases (R*GRK) and to β-arrestin (R*A). Adapted from [32] by permission from Annual Reviews Inc (Copyright 2013).

Within the last decade, GPCRs have been successfully studied by biophysical methods, such as x-ray crystallography, and the active–inactive receptor pairs have provided insights into the conformational changes occurring during receptor activation (Figure 3; reviewed in [32,33]). Currently, the structures of rhodopsin, β_1- and β_2-adrenoceptors (β_1 and β_2), A_2 adenosine (A_{2A}), M_2 muscarinic acetylcholine (M_2), μ opioid (μOR), angiotensin 2 (AT_2), and endothelin B (ET_B) receptors have been solved in both inactive (antagonist-bound or ligand free apo form) and different forms of active conformations (for rhodopsin, β_1, β_2, and A_{2A} see Table 2 in [32], for M_2 and μOR see [33–35], for AT_2 see [36], and for ET_B see [37]). Additionally, the agonist-bound structures of neurotensin 1 (NTS_1)[38], and 5-HT_{1A} and 5-HT_{1B} serotonin receptors (5-HT_{1A} and 5-HT_{1B})[39] are reported, however the antagonist-bound or apo forms of these remain currently unsolved.

Of the structures of the active receptors, only β_2 is solved as a fully active G protein-bound state,[40] and additionally rhodopsin-receptor structures in complex with C-terminal peptide of Gα representing the active receptor conformations are reported (reviewed in [32]; R* and R*G states in Figure 3). When comparing the active β_2 to the corresponding inactive conformation, the most significant structural changes are observed within the intracellular domains of TM5 and TM6: TM5 is extended by two helical turns whereas TM6 is moved outward by 14 Å (the distance between α-carbons of Glu$^{6.30}$ of the two structures).[40] Additionally, ICL2, TM5 and TM6 are in the direct contact with the G protein.[40]

The amino-acid sequences of the Rhodopsin-family GPCRs share several characteristics such as D[E]RY motif at the border between TM3 and ICL2, CWxP motif in the vicinity of the orthosteric binding site in TM6, and NPxxY motif in TM7 ([2,6], reviewed in [32]). In the inactive GPCR structures, the salt bridge between Arg$^{3.50}$-Asp$^{3.49}$ in the DRY motif of TM3 is highly conserved (reviewed in [32]; Table 1). In the aforementioned active-state structures of rhodopsin and β_2 instead, the Arg$^{3.50}$-Asp$^{3.49}$ salt bridge is broken and the arginine residue interacts

with $Tyr^{5.58}$ and the G protein. The $Arg^{3.50}$-$Tyr^{5.58}$ interaction is also present in the peptide-agonist-bound NTS_1 structure.[38] However, $Arg^{3.50}$-$Asp^{3.49}$ salt bridge is intact in NTS1, as in the all active GPCR structures solved in absence of the G protein(mimic) (reviewed in [32]).

In the inactive structures of rhodopsin and β_2 also another salt bridge, so called 'ionic lock', between $Arg^{3.50}$-$Glu^{6.30}$ is observed (Table 1; reviewed in [41]). The ionic lock stabilizes these inactive receptor conformations and breaks during the receptor activation. However, the role of ionic lock within the full receptor family is possibly less prominent, as the acidic residue in location 6.30 is conserved only among 30% of GPCRs (reviewed in [32]).

As only the β_2 and rhodopsin receptors are solved in the fully active conformations, the most of the active GPCR structures represent the pre-activated state of the receptor (i.e. their structures are solved in complex with agonist ligands but in absence of the G protein or its mimic; R" in Figure 3). These structures lack the most prominent conformational changes of receptor activation, however, they have allowed the identification of more subtle structural rearrangements, referred as microswitches (reviewed in [32]). The microswitches are considered to be subsequently connected to the larger conformational changes in the locations of TM helices, especially those of TMs 5 and 6 (Table 1; for orexin receptors, see Figure 5).

Table 1. Structural changes between active and inactive GPCRs.[32–34,36,37,42]
The residue conservation is given as a percentage within the Rhodopsin-family GPCRs (as in [32]*). The changes are presented in the order based on their location (from the intracellular to the extracellular side of the receptor).*

Structural change	Structures manifesting the change	'Microswitch'
$Arg^{3.50}$–$Asp^{3.49}$ salt bridge breaks upon activation → $Arg^{3.50}$ interacts with G_α subunit	G protein-bound states of rhodopsin and β_2 Conservation: $Arg^{3.50}$: 96% $Asp/Glu^{3.49}$: 88%	D[E]RY in TM3
Notable movement of intracellular domain of TM6 → breaks the $Arg^{3.50}$–$Glu^{6.30}$ salt bridge	G protein-bound states of rhodopsin and β_2 Conservation: $Asp/Glu^{6.30}$: 30%	D[E]RY in TM3
Active: $Tyr^{7.53}$ points towards TM3 and TM6; $Tyr^{7.53}$–$Tyr^{5.58}$ water-mediated hydrogen bond **Inactive**: $Tyr^{7.53}$ faces towards TM1, TM2 and helix 8	rhodopsin, β_2, M_2, μOR and A_{2A} Conservation: $Tyr^{7.53}$: 92% $Tyr^{5.58}$: 89%	NPxxY in TM7
$Pro^{5.50}$ moves → $Ile^{3.40}$ moves → $Phe^{6.44}$ moves and swings TM6 (intracellular domain)	β_2, 5-HT_{2B}, AT_2, and μOR	$P^{5.50}$–$I^{3.40}$–$F^{6.44}$
Ligand-dependent structural changes affecting e.g. TM6	rhodopsin, A_{2A} and ET_B Note: not universal change	CWxP in TM6

The first set of these conformational changes could occur close to the ligand binding site, where Trp[6.48] (from conserved CWxP motif) can interact directly with the bound agonist leading to movement of TM6 (reviewed in [32]). However, for β_2, for example, the conformation of Trp[6.48] is stabilized by inverse agonists and thus it is unlikely connected to the receptor activation. In the case of β_2, triggering the movement of the TM5–TM6 region is supposed to be connected with the interactions of the bound agonist and residues Ser[5.42] and Ser[5.46].[43] Additionally, in β_2, the agonists form tight hydrogen bonding interactions with Asp[3.32] in TM3 and Asn[7.39] in TM7, which could affect the conformational changes of the microswitch amino acids further away from the ligand binding site (reviewed in [32]). Notably, in the aminergic and opioid receptors, the acidic side chain Asp[3.32] is fully conserved and a critical interaction point for ligand binding and receptor activation. Of the peptide binding GPCRs, such as endothelin 1 (ET$_1$), the activating peptide ligand of endothelin receptors, can interact with Gln[3.32] and Trp[6.48] in the ET$_B$ crystal structure.[37]

The ligand binding interactions could then drive the changes in the location of the amino acid triad Pro[5.50]–Ile[3.40]–Phe[6.44] (Table 1). It is suggested that the movement of TM5 switches the conformation of Ile[3.40], which in turn moves Phe[6.44] and swings the intracellular domain of TM6 ([34], reviewed in [32]). Interestingly, Ile[3.40] is two helical turns below Asp[3.32], and in µOR their movements seem to be strongly coupled.[34]

In the structures of inactive GPCRs TM6 is in contact with TM3; this contact is detected as a shortest distance between the amino acid residues in locations 3.46 and 6.37, and it is conserved within the inactive GPCR conformations (Table 1).[33] In the active conformations, TM3 interacts with TM7 instead, with the contact point being amino acid 3.46 and the conserved Tyr[7.53] of the NPxxY motif in TM7 (Table 1).[33] Additionally, a water-mediated hydrogen bond involving Tyr[7.53] and Tyr[5.58] from TM5 is observed in many active GPCR structures, and it is suggested to stabilise the active receptor conformation (Table 1; reviewed in [32]). In the inactive conformations, Tyr[7.53] is in

31

contact with TM1 and helix 8 (locations 1.53 and 8.50, respectively).[33]

2.2 THE OREXIN SYSTEM

2.2.1 OVERVIEW

In 1998, two research groups reported individual findings regarding the orexin (hypocretin) system: de Lecea et al. identified messenger RNA (mRNA), which encoded the precursor of two peptides selectively expressed in hypothalamus;[44] while Sakurai et al. reported their findings of two hypothalamic neuropeptides activating two closely related orphan GPCRs.[45] The currently established orexin system comprises these two GPCRs, OX_1 and OX_2 receptors (OX_1 and OX_2, respectively), and the neuropeptide agonists orexin-A and orexin-B (naming according to [2]).[44,45]

2.2.2 OREXIN PEPTIDES

The human neuropeptides, orexin-A and orexin-B, are cleavage products of a single 131 residue precursor prepro-orexin.[45] Orexin-A is a 33 residue peptide with two disulphide bridges (Cys6–Cys12, Cys7–Cys14) in the N-terminal, whereas orexin-B is a linear 28 residue peptide (residues 33–66 and 69–97 of the prepro-orexin, respectively; Figure 4A). The C-terminal ends of these peptides are highly similar, including an amidated C-terminus, while the N-terminal ends show more variation.

A.
```
                              ┌──────────┐
                       ┌──┐ .   .  **  .**:.:*********:*
orexin-A    QPLPDCCRQKTCSCRLYELLHGAGNHAAGILTLX
orexin-B    ------RSGPPGLQGRLQRLLQASGNHAAGILTMX
            1.......10........20........30....
```
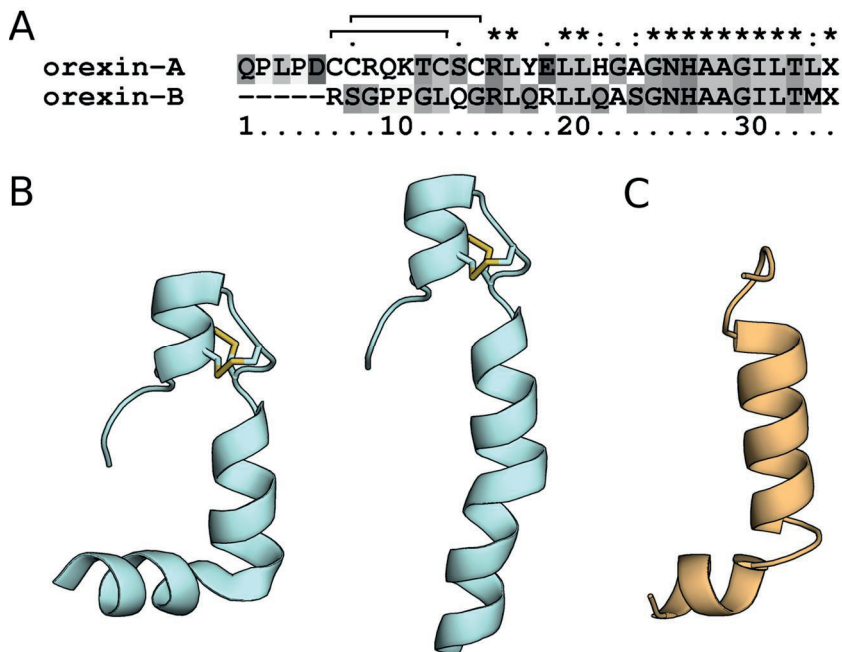
Figure 4. A. Sequence alignment of the amino acid sequences of human orexin-A and orexin-B. B. Examples of the NMR structures of bent and straight orexin-A conformations (PDB ID: 1WSO).[46] Disulphide bridges are shown as sticks (carbon: light blue, sulphur: yellow) C. The NMR structure of orexin-B (PDB ID: 1CQ0).[47] In B and C the N-terminal of the peptides are up and C-terminal down.

The NMR-structures of orexin peptides have been solved in water-based buffers. Orexin-A has three helical parts and its C terminal end adopts either straight or bent conformation in aqueous solution (Figure 4B).[46] Orexin-B, instead, consists of two helical regions, for which only one conformation is reported (Figure 4C).[47] The importance of the amino acids in orexin peptides have been thoroughly studied, and the C-terminal end, including the amidation, has been shown to be the key for the activity of these peptides.[48–52]

The native orexin peptides are equipotent towards OX_2 receptors, when studied in recombinant CHO cells.[48,52] Orexin-A has equal efficacy and potency also towards OX_1 receptors,

whereas orexin-B prefers OX_2 receptors by approximately 10-fold. The C-terminal fragment of orexin-A retaining nanomolar binding affinity for OX_1 receptors is 19 amino acids long, whereas the orexin-A truncates in lengths of 19 to 12 amino acids have been reported to retain some functional activity. [48,50–53] For orexin-B, instead, the shortest C-terminal fragment binding to orexin receptors is 15 amino acids long.[52] Especially the C-terminal amino acids 29–33, and Arg15, Tyr17, Leu20, Asn25, and His26 have shown to contribute the functional activity of orexin-A.[48,50,51] Whether the C-terminus of orexin-A is required in helical conformation for bioactivity is currently unknown, however a recent study by Karhu et al. provides evidence that orexin receptors can be activated by permanently α-helical peptides.[53] Unlike the C-terminus, no crucial amino acids have been identified in the N-termini of orexin peptides.[48–52]

2.2.3   OREXIN RECEPTORS

Human orexin receptors, OX_1 and OX_2, are composed of 425 and 444 amino acids, respectively, and they are encoded by the genes HCRTR1 and HCRTR2, respectively.[45] As GPCRs, the structures of orexin receptors consist of seven transmembrane helices and three intra- and extracellular loops, as shown by their recently reported three-dimensional structures (PDB IDs: 4ZJ8, 4ZJC, 4S0V, 5WQC, and 5WS3; Figure 5).[54–56] OX_1 and OX_2 share a 64% full-length pairwise sequence identity, and if the termini and ICL3 are excluded, the identity rises up to 80%. All currently reported orexin receptor crystal structures are solved in complex with small molecular antagonists, and thus they represent an inactive receptor conformation (Figure 5; see also Figure 3). Phylogenetically, orexin receptors belong to the β-branch of the Rhodopsin family, together with other peptide-binding GPCRs, such as neurotensin and endothelin receptors.[6]

Prior to the determination of the orexin receptor crystal structures, the ligand binding site of orexin receptors had been identified by point mutations and receptor chimeras.[1,54,57–60]

These studies showed that the orthosteric orexin-A binding site of both orexin receptors is identically located in between the TMs3–7 and involve also amino acids from ECL2 (Figure 5, grey surface). In more detail, amino acids $Gln^{3.32}$, $Val^{3.36}$, $Asp^{xl2.51}$, $Trp^{xl2.45}$, $Tyr^{5.38}$, $Phe^{5.42}$, $Tyr^{6.48}$, $Asn^{6.55}$, $His^{7.39}$, and $Tyr^{7.43}$ are shown to clearly contribute to the response to orexin-A on OX_1, and thus they were expected to be located on the orthosteric binding site (for the nomenclature, see [61,62]).[54,57] On OX_2, these and also $Thr^{5.46}$ have a role in the potency of orexin-A.[58] When considering orexin receptor antagonists almorexant, SB-674042 and EMPA (see chapter 2.5.1), instead, amino acids $Thr^{2.61}$ (on OX_2 only), $Ala/Thr^{3.33}$, $Gln^{4.60}$, $Tyr^{5.47}$, and $Ile^{6.51}$, in addition to those listed above, impart to the binding of these ligands.[57,58,60] These findings of the location of the orthosteric binding site were later confirmed by the crystal structures.

Apart from the ligand binding site, the orexin receptor crystal structures offer insights into the overall receptor conformation. One interesting observation is the amphipathic α-helix formed by the N-terminal amino acids $Glu^{1.14}$–$Arg^{1.23}$, which is suggested to contribute to the binding/recognition of orexin-A.[54] Deletion of that α-helix led to receptor constructs with no activation by orexin-A (up to 1 μM concentration), and asparagine mutations on the lipophilic phase of the helix lead to a similar outcome. The N-terminal α-helix is observed in both OX_1 and OX_2 (for OX_2, see Figure 5);[54,56] in OX_1 crystal structures it interacts with the β-hairpin structure of the ECL2, whereas in OX_2 it points in the opposite direction. In addition to the orexin receptors, the β-hairpin is present in the structures of other peptide-activated GPCRs such as CXCR4 chemokine receptor (CXCR4)[63], opioid receptors[34,64–66], NTS_1 neurotensin receptor (NTS_1)[38], endothelin B receptor (ET_B)[37], and angiotensin receptors (AT_1 and AT_2)[36]. In case of orexin receptors, the mutation of $Asp^{xl2.51}$, located in the β-hairpin, to alanine has a large effect on the efficacy of orexin-A illustrating the importance of this region.[57]
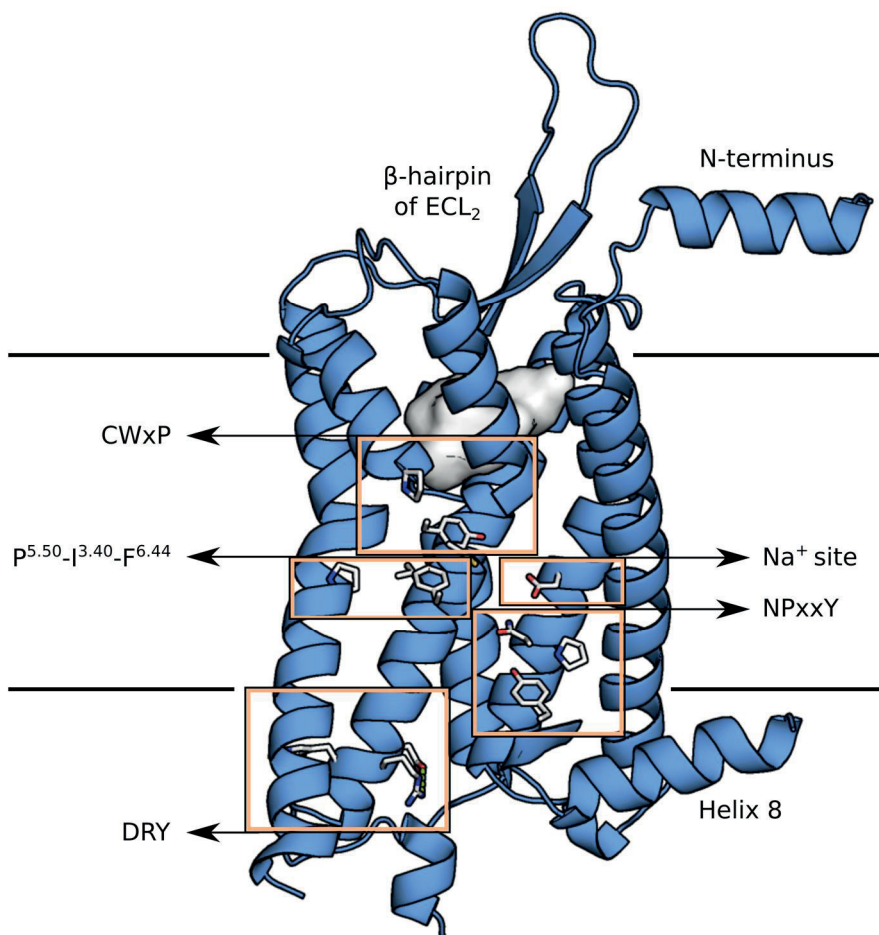
Figure 5. *Structural indicators of GPCR activation presented on OX_2 crystal structure (pdb ID: 5WS3). The receptor is shown as cobalt blue cartoon, and amino acid residues as white sticks (carbon). Red is for oxygen, blue for nitrogen and yellow for sulphur. Green dashes represent possible hydrogen bonds and the grey surface the ligand binding pocket. The black horizontal lines indicate the approximate location of the cell membrane (determined by hydrophobic surface of the receptor). Parts of TM6 and TM7 helices are hidden for clarity.*

Another feature involving β-hairpin is highly conserved disulfide bridge between it and the top of TM3 ($Cys^{3.25}$; reviewed in [67]). In orexin receptors, this bridge is observed between

Cys$^{xl2.50}$ and Cys$^{3.25}$.[54,55] Considering the other conserved motifs of Rhodopsin-family GPCRs (see chapter 2.1.3), only NPxxY in TM7 is fully conserved in the structures of orexin receptors (Figure 5).[54–56] In CWxP in TM6, there is Tyr$^{6.48}$ instead of Trp$^{6.48}$ in the orexin receptor structures, V$^{3.40}$ instead of I$^{3.40}$ in P$^{5.50}$–I$^{3.40}$–F$^{6.44}$ –triad, and Trp$^{3.51}$ instead Tyr$^{3.51}$ in the DRY motif of TM3. Additionally, in orexin receptors, R$^{6.30}$ replaces Glu$^{6.30}$, and thus ionic lock does not exist.

Allosteric Na$^+$ binding site is commonly observed in the inactive structures of Rhodopsin-family GPCRs, and it collapses during receptor activation due to the conformational rearrangements (reviewed in [42]). This binding site is located in the middle of the TM bundle close to conserved Asp$^{2.50}$ (95% conservation among these GPCRs), and involves amino acid residues in TMs 1, 2, 3, 6, and 7 (Figure 5). It is thus also connected to the conserved regions CWxP and NPxxY. Interestingly, Na$^+$ is not observed in the high resolution crystal structure of OX$_2$, and OX$_2$ function been shown to be Na$^+$-independent.[56] Asp$^{2.50}$, though, is also conserved in orexin receptors (Figure 5). Apart from OX$_2$, only the structures of visual opsins have been reported to lack the allosteric Na$^+$.[42]

Helix 8 is located to the C-terminal end of orexin receptors in parallel to the cell membrane, as commonly observed in inactive GPCR structures (for OX$_2$, see Figure 5). The location of helix 8 has not been observed to change within the active GPCR conformations either (e.g. in [37,40]), except for the active-state-mimicking AT$_2$ structure.[36] Furthermore, the CXCR4 structure lacks helix 8.[63] Helix 8 is suggested to be involved in GPCR dimerization (as shown by the structure of κ opioid receptor[68]). Apart from helix 8, the C-terminal ends and ICLs2–3 of both orexin receptor subtypes have several putative phosphorylation sites (reviewed in [69]); point mutations of a cluster of C-terminal serine and threonine residues (within amino acids 418–422 in OX$_1$) suggest that they have a role in β-arrestin binding.[70]

2.3 OREXIN SIGNALLING

2.3.1 OREXIN RECEPTOR-MEDIATED SIGNALLING CASCADES

Early on after their discovery, orexin receptors were reported to couple to Ca^{2+} elevation and phospholipase C (PLC) in recombinant CHO cells.[45,71–73] Thus, they were considered to couple with the G_q pathway in their actions ($G\alpha_q \rightarrow$ PLC $\rightarrow IP_3 \rightarrow IP_3$ receptor $\rightarrow Ca^{2+}$ release from the ER, see Figure 6), and induce the cell responses via Ca^{2+} and DAG-mediated pathways, such as those resulting from PKC activity. This was soon found to be too simplistic (see e.g. [74–77]), however, the involvement of the $G\alpha_q$ pathway in many orexin receptor-mediated responses in recombinant CHO cells is verified.[78]

In addition to the PLC pathway, orexin receptors are shown to regulate AC activity in recombinant CHO cells via both $G\alpha_s$ and $G\alpha_i$, while regulation of the phospholipase A_2 and phospholipase D cascades (PLA2 and PLD, respectively) may rely on G_q.[74–77] Apart from CHO cells, orexin functions have been studied in HEK293 and recombinant neuron-like cells, in which the coupling to Ca^{2+} elevation and PLC is also shown (reviewed in [28,79]).
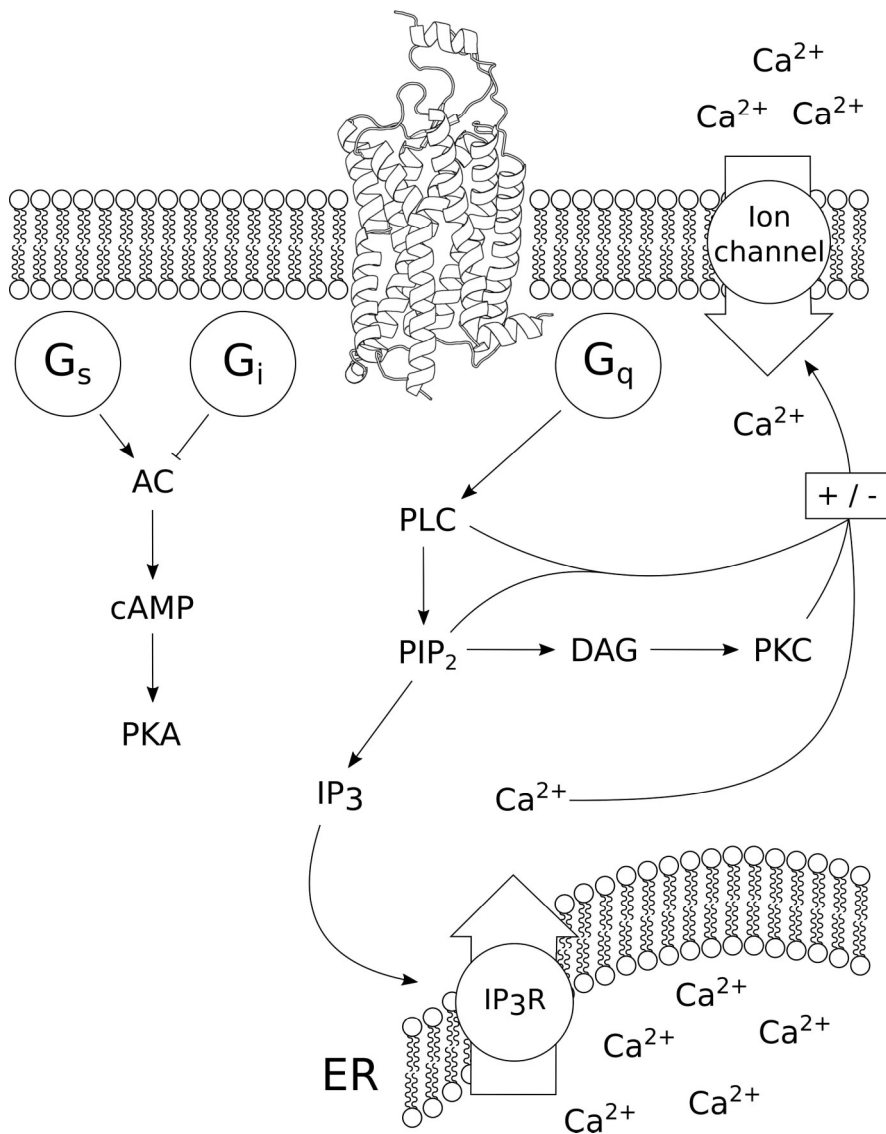
Figure 6. A simplified scheme of G protein pathways coupled by orexin receptors (as reviewed in [29,30,80,81]). G_s activates and G_i inhibits adenylyl cyclase (AC), which regulate cAMP levels and protein kinase A (PKA) activity. G_q activates phospholipase C (PLC) leading to production of diacylglycerol (DAG) and inositol trisphosphate (IP_3) from phosphatidylinositol-4,5-bisphosphate (PIP_2). IP_3 binds to IP_3 receptor (IP_3R) opening ion channels and releasing calcium ions (Ca^{2+}) from the endoplasmic reticulum (ER). DAG activates protein kinase C (PKC); PKC, PLC, PIP_2, and Ca^{2+} release from ER regulate ion channels/exchangers in the cell membrane leading to a Ca^{2+} influx.

2.3.1.1 *Phospholipase C (PLC)*

Phospholipase C (PLC) is a family of cytosolic phosphoinositide-specific enzymes (reviewed in [82]). The PLC family is divided into six subfamilies (β, γ, δ, ε, ζ, and η), which share the requirement of Ca^{2+} for activation. The most commonly studied substrate of PLCs is PIP_2, but they also hydrolyse other phosphoinositides, such as phosphatidylinositol and phosphatidylinositol-4-phosphate/phosphatidylinositol-5-phosphate (reviewed in [29]). Hydrolysis yields DAG and inositol phosphates (in case of PIP_2, IP_3), which act as secondary messengers. Additionally, PIP_2 can directly regulate several ion channels (such as voltage-gated Ca^{2+} channels [VGCC] and transient receptor potential [TRP] channels; reviewed in [83,84]).

In general, GPCRs can regulate multiple PLC isoforms, the most classical being PLCβ (via Gα_q family members and G$\beta\gamma$; reviewed in [29]). Direct measurements of PLC activity in recombinant expression systems indicate that both OX_1 and OX_2 activate PLC (see 2.3.1 above). In native orexin receptor-expressing cells, PLC activation has been directly shown in human adrenal gland tumours, and membrane preparations of human reproductive tract, rat adrenal cortex, and hypothalamus (reviewed in [29]).

2.3.1.2 *Protein kinase C (PKC)*

PLC activation leads to production of DAG and phosphatidic acid (PA), which are important lipid second messengers with many targets (reviewed in [30]). Of these, orexin receptor-mediated DAG release activates, for example, classical (cPKC) and novel (nPKC) PKCs (reviewed in [85]). Upon orexin receptor activation in recombinant cell systems, these PKCs have been reported to regulate non-selective cation channels (NSCCs), L- and N-type voltage-gated Ca^{2+} channels, inwardly rectifying K^+ channels (assessed in neuronal preparations), and PLD and protein kinases, such as extracellular signal-regulated kinases 1 and 2 (ERK1/2).[77,86–89]

2.3.1.3 Adenylyl cyclase (AC)

Apart from PLC, orexin receptors have been shown to regulate the activity of adenylyl cyclase (AC).[76,90–94] Nine plasma membrane-bound and one cytosolic AC isoforms have been reported (reviewed in [95]). Depending on the isoform, ACs are regulated by a variety of signals; the common regulator is $G\alpha_s$ (activation), but other positive or negative regulators also have an impact on ACs (such as $G\alpha_i$, $G\beta\gamma$, Ca^{2+} or PKC). Some of the orexin receptor-mediated AC regulation may relate to the ability of orexin receptors to couple to G_s proteins (reviewed in [79]), but the contribution of the other cascades, such as Ca^{2+} and PLC–PKC, cannot be ruled out. The physiological relevance of AC stimulation by orexin receptors is mostly studied in adrenocortical cells (*in vitro* and *in vivo*), and AC–PKA activation leads to glucocorticoid synthesis or release from the adrenal cortex (reviewed in [79]).

2.3.1.4 Effects of Ca^{2+} on orexin receptor signalling

PLC activation also generates IP_3, which releases Ca^{2+} from the ER into the cytosol via IP_3 receptor channels (Figure 6, reviewed in [81]). Subsequently, Ca^{2+} depletion of ER signals to the plasma membrane to allow so-called store-operated Ca^{2+} influx (often via the plasma membrane Ca^{2+} channel orai1). Apart from this, Ca^{2+} influx can occur via other plasma membrane channels, such as VGCCs, NSCCs of the TRP family, or $Na^+/Ca^{2+}(-K^+)$ exchangers (NCX, NCKX), which pump in Ca^{2+} at the expense of Na^+ (reviewed in [96]). Of these, NSCCs and TRPCs have been shown to contribute to orexin receptor-mediated Ca^{2+} influx in recombinant cell lines, whereas the involvement of VGCCs are reported in neurons (reviewed in [29,79]).

Altogether, a great extent of orexin signalling is connected with the regulation of intracellular Ca^{2+} levels, but reciprocally, these Ca^{2+} levels also have an effect on downstream orexin signalling. In CHO-hOX$_1$ cells, the effects of orexin-A to a number of intracellular pathways, such as PLC, AC, and PLD,

are strongly dependent on the intracellular Ca^{2+} concentration (studied by altering the extracellular Ca^{2+} concentration or inhibiting the receptor-operated Ca^{2+} channels).[77,86,97–100] These pathways are not stimulated by Ca^{2+} influx alone, but the Ca^{2+} influx in synergy with orexin-A, suggesting that the effect of Ca^{2+} takes place at the proximal level of orexin receptor signalling (e.g. receptor–G protein interaction). However, it is also possible that Ca^{2+} binds directly to signalling cascade components, such as PLC, and stimulates the orexin responses.

Apart from the signal transduction machinery, extracellular Ca^{2+} levels affect the binding of orexin-A to OX_1 receptors.[97] Reducing the extracellular Ca^{2+} concentration significantly inhibits the binding of $[^{125}I]$-orexin-A to OX_1 (when studied in CHO-cells) in a concentration-dependent manner. However, the blockade of the orexin receptor-mediated Ca^{2+} influx (to separate the effects of intra- and extracellular Ca^{2+}) suggests that Ca^{2+} levels affect PLC activity, not only via the stimulated orexin-A binding but also directly via the intracellular signalling machinery. It is possible that OX_1 structure has a regulatory extracellular Ca^{2+} binding site, occupancy of which enhances orexin-A binding, or that Ca^{2+} acts through receptor dimers (see below) regulating the ligand binding and/or response to orexin-A.

2.3.2 OREXIN RECEPTOR DIMERIZATION AND OLIGOMERIZATION

Numerous studies propose the formation of homodimers, heterodimers, and higher oligomers of GPCRs (reviewed in [101,102]). GPCR dimerization or oligomerization can alter the pharmacology, function, or regulation of the receptors, and is of increasing importance for the development of future drug treatments. In the case of orexins, the formation of receptor dimers/oligomers has been studied in recombinant CHO and HEK293 cells.[64,103–110] Apart from the homomers and heteromers between orexin receptor subtypes, OX_1 receptors have been reported to dimerize with CB_1 cannabinoid receptors,

κ opioid receptors (κOR), GPR103 receptors, and a complex of CRF$_1$ corticotrophin-releasing factor receptor and sigma 1 receptor (σ$_1$; not a GPCR). Of these, the complexation of OX$_1$ with κOR, GPR103, or CRF$_1$–σ$_1$ alters efficiently the cellular responses of these receptors.[64,108–110] OX$_1$–CB$_1$ complexation is also reported to occur,[104,106] however the OX$_1$–CB$_1$ synergy is not necessarily structural, but rather functional, as orexin receptor activation releases 2-arachidonoylglycerol (2-AG), a CB$_1$ receptor agonist, which could then cause the synergistic functions of these receptors by CB$_1$ receptor activation.[75,107]

2.3.3   OREXIN RECEPTOR-MEDIATED CELL DEATH

One way to classify cell death is according to particular morphological and molecular signatures, wherein the two main classes are apoptosis and necrosis (reviewed in [111]). The main markers of apoptotic cell death are fragmentation and condensation of the cells and nuclei, DNA laddering, loss of plasma membrane polarity, caspase activation, and mitochondrial membrane permeabilization. The markers of necrosis, instead, are swelling of the organelles, loss of plasma membrane integrity, and inflammation. Apoptosis is often used as a synonym for programmed cell death, whereas necrosis has been thought to be an uncontrolled form of cell death. However, the accumulating evidence indicates that necrosis can also have programmed characteristics and the physiological 'programmed' cell death non-apoptotic features (reviewed in [111,112]).

Prolonged orexin receptor stimulation has shown to induce programmed cell death in recombinant CHO cells, as well as in native cancer cell lines of colon carcinoma, neuroblastoma, and pancreatic acinar tumour.[113–116] Both orexin receptor subtypes are capable of activating programmed cell death.[114,117] In CHO cells expressing human OX$_1$, two cell-death pathways have been suggested. The first involves the phosphorylation of a tyrosine residue of the immunoreceptor tyrosine-based switch motif (ITSM) of OX$_1$ leading to apoptosis, whereas   the second

identifies p38 MAP kinase (p38 MAPK) as a carrier of both caspase-dependent and independent cell death.[113,115]

2.4 THERAPEUTIC OPPORTUNITIES FOR TARGETING THE OREXIN SYSTEM

2.4.1 ANATOMY OF THE OREXIN SYSTEM

Orexin peptides are produced by orexinergic neurons in the brain located within the lateral and posterior hypothalamus (LH and PH, respectively), and the perifornical area (PF).[44,45,118] Humans are estimated to carry approximately 70 000 orexinergic neurons, which send projections to several brain regions (Figure 7).[118–121] Orexin receptor subtypes have been suggested to have different, but partially overlapping, expression patterns. The mRNA of both orexin receptors is found, for example, in the laterodorsal tegmental nucleus (LDT), ventral tegmental area (VTA), pedunculopontine nucleus (PPT), and dorsal raphe (DR), whereas mainly OX_1 mRNA is found in the locus coeruleus (LC), and only OX_2 in the tuberomammillary nucleus (TMN).[118–121] These brain areas are involved in the regulation of arousal, but they are connected also, for example, to reward and mood (see below).
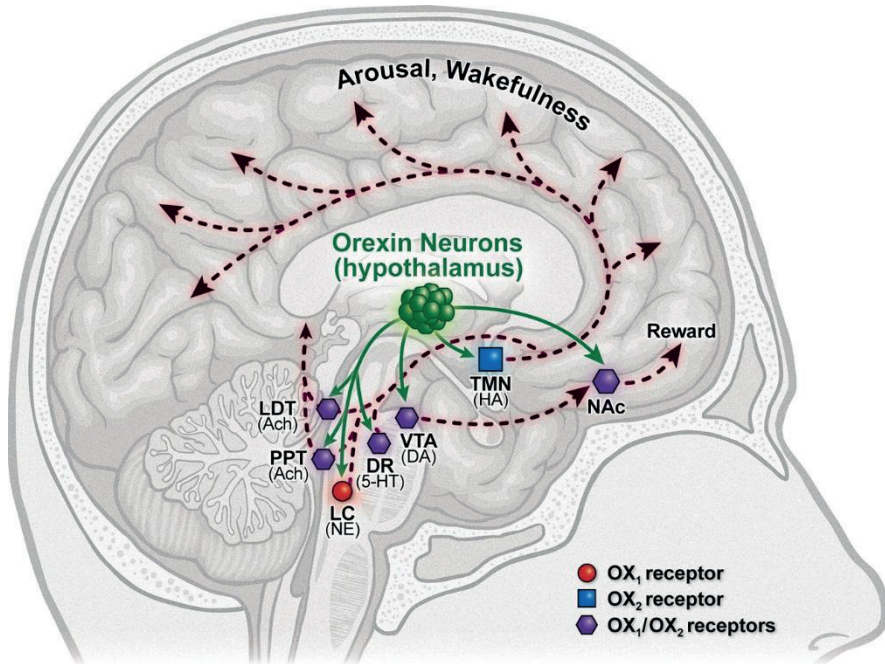
Figure 7. Expression and distribution of the orexins and orexin receptors involved in arousal and reward in the human brain. LDT: laterodorsal tegmental nucleus, VTA: ventral tegmental area, PPT: pedunculopontine nucleus, DR: raphe nucleus, LC: locus coeruleus, TMN: tuberomammillary nucleus, NAc: nucleus accumbens. The neurotransmitters in each nuclei: acetylcholine (Ach), noradrenaline (NE), serotonin (5-HT), dopamine (DA), and histamine (HA). Adapted with permission from [122]. *Copyright 2016 American Chemical Society.*

Orexinergic functions, as well as the presence of the mRNA of prepro-orexin and of orexin receptors, have been reported in several organs in periphery (reviewed in [69,123]). These organs include the gastrointestinal tract, pituitary gland, adrenal gland, pancreas, male reproductive system, and adipose tissue; however, the physiological significance of peripheral orexins remain mostly unknown. Interestingly, human neuroblastoma and colon carcinoma cells, but not healthy colon epithelium, express OX_1 receptors, and the exposure of these to orexins induces programmed cell death (see 2.3.3).[114,116]

45

2.4.2 SLEEP/WAKE REGULATION

The orexin neurons of the hypothalamus project to cholinergic and monoaminergic nuclei, which excite the wake-promoting cerebral cortex (Figure 7). The orexin system is thus essential for regulating arousal, and it is especially important for maintaining long periods of wakefulness ([44,45] reviewed in [124]). In rodent models, the activity of orexinergic neurons and extracellular levels of orexin-A are high during periods of high locomotor activity, and orexin-A injection (i.c.v.) increases wakefulness and suppresses rapid eye movement (REM) and non-rapid eye movement (NREM) sleep.[121,125,126] Furthermore, blocking the functions of the orexin system (by orexin receptor antagonists) induces sleep in mice, rats, dogs, non-human primates, and humans, which indicates that the main function of orexin system is indeed wake-promotion.[127]

The excitatory functions of the orexin system attracted attention to the possibility that the orexin system could have a role in the origin of narcolepsy. Type I narcolepsy (i.e. narcolepsy with cataplexy) is a sleep disorder with chronic, often severe sleepiness, dysregulated REM sleep, and cataplexy attacks.[128] Orexin knock-out animals show narcoleptic symptoms, which can be suppressed by administration of orexin-A, [Ala[11]]orexin-B, or the non-peptide orexin receptor agonist YNT-185 (see also chapter 2.5.2.2).[129–134] Additionally, human type I narcolepsy is associated with the loss of orexinergic neurons and correlates with low levels of orexin peptides.[135,136] Together these results indicate that narcolepsy is caused by a selective loss of the orexin neurons, but not the orexin receptors, and thus narcolepsy provides an attractive target for orexin receptor activators.

On the other hand, blockade of the arousal effects of the orexin system offers a mechanism to promote sleep, which could have advantages over the current standard pharmacotherapies. The commonly used hypnotics, such as zolpidem, zaleplon, zopiclone, and eszopiclone, act via positive allosteric modulation of $GABA_A$ receptors, which drives sleep through inhibitory ligand-gated chloride channels and CNS

depression (reviewed in [137,138]). In principle, this is a nonspecific and broadly acting approach; apart from the brain regions responsible for arousal, GABA$_A$ receptors are expressed throughout CNS functioning in a number of pathways. Targeting orexin receptors is thus a more specific way to promote sleep compared to the GABA$_A$ modulators, and currently numerous orexin receptor antagonists have been developed for insomnia treatment. The effects of these are discussed in more detail under chapter 2.5.1.

The differences in the orexin receptor subtype expression in the separate cholinergic and monoaminergic pathways suggests that they have different physiological roles in the sleep/wake regulation (Figure 7). As mentioned above, the administration of orexin-A to wild-type mice increases wakefulness and reduces both REM and NREM sleep.[121] In the OX$_1$ and OX$_2$ knockout mice, the effects of orexin-A on wakefulness and NREM sleep are significantly attenuated compared to the wild-type mice, OX$_2$ knockouts showing this more prominently. The effect of orexin-A on REM sleep, instead, is slightly reduced in both of these orexin receptor knockout mice models. In addition, the orexin null mice show greater sleep stage transitions than the OX$_2$ knockouts.[130] Altogether, this highlights the importance of both orexin receptor subtypes for the maintenance of wakefulness and sleep, but with a dominant role of OX$_2$. These findings are supported by data from narcoleptic dogs[131,139] and human clinical data of orexin receptor antagonists as insomnia treatment (see 2.5.1.2 and 2.5.1.3). Additionally, it is suggested that OX$_2$-selective blockade (by OX$_2$-selective antagonists, 2-SORAs) would produce more physiologically balanced NREM/REM profile than blockade by dual antagonists (DORAs; reviewed in [138]). However, the role of OX$_1$ in the maintenance of wakefulness and sleep is not fully clear, and thus DORA/2-SORA efficacy differentiation (i.e. whether DORAs or 2-SORAs are better sleep aids) remains partially unsolved.

2.4.3   ADDICTION AND REWARD SEEKING BEHAVIOUR

The first indication of the connection between the orexin system and addiction came from the clinical data of type I narcolepsy patients, who rarely develop stimulant abuse, even though narcolepsy is commonly treated with long-term use of amphetamines ([140], reviewed in [141]). In 2005, two research groups showed that activation of orexin neurons is correlated with morphine and cocaine seeking, and the seeking behaviour could be subsequently blocked by a selective OX_1 antagonist.[142,143] Currently, orexin neurons are suggested to be critical in high-effort drug seeking behaviour, that is, drug seeking in situations of high motivational relevance, such as during physiological need, exposure to threats (i.e. stress), or reward opportunities.[144]

Thus, the orexin system would not play a role in the primary reinforcing effects of drugs of abuse, but rather in the motivation for seeking them. The motivation for drug reward can be enhanced by various external stimuli, and it occurs in an orexin-dependent manner ([145], reviewed in [141]). Even though most of the reward/addiction studies utilize OX_1 antagonists, OX_2 also has a role in reward seeking; for example alcohol or nicotine seeking involves OX_2 receptors.[146–148]

2.4.4   STRESS AND STRESS-BASED CONDITIONS

In chronic stress, the hypothalamic–pituitary–adrenal (HPA) axis has a major role (reviewed in [149]). Orexins activate the HPA axis leading to a release of corticotrophin-releasing hormone, adrenocorticotropic hormone, and corticosterone, and sends projections to the brain regions directly responsible for the production of the corticotrophin releasing hormone. All of these factors stimulate stress behaviour and suggest a possible connection between the orexin system and chronic stress.

Dysfunctions in orexin signalling have been reported in stress-related neuropsychiatric disease states, such as anxiety (reviewed in [149,150]). Orexin neurons are needed for the development of the panic-prone state in a panic-disorder rodent

model, which can then be suppressed by silencing the prepro-orexin gene, or by a high systemic dose of OX_1 antagonist.[151–153] Furthermore, the OX_1-selective antagonist (1-SORA) ACT-335827 and dual orexin receptor antagonist almorexant have been studied in anxiety rodent model, in which they both showed similar anxiolytic-like effects, but almorexant also decreased wakefulness.[154] Thus it seems that of orexin receptors, OX_1 is the main player in anxiety. Apart from anxiety, symptoms of depression have also been reported to negatively correlate with orexin levels (e.g. [151,155–157], reviewed in [149,150]).

2.4.5 OTHER THERAPEUTIC OPPORTUNITIES

The initial findings of the physiological relevance of the orexin system were related to feeding, as the administration of orexin peptides acutely increased food consumption in rats and mice.[45] Even though the orexin-mediated effects on feeding were then later concluded to be a sum of several functions (such as those related to sleep/wake regulation, reward seeking, and mood), the orexin system also has a direct role in energy expenditure and glucose homeostasis (reviewed in [158]). Orexin neurons control multiple aspects of glucose homeostasis, such as the sympathetic nervous system output in respond to hypoglycaemia. Furthermore, orexin tone seems to promote glucose uptake and control the secretion of pancreatic islet hormones, contributing to physiologic glucose homeostasis over the longer-term. The short-term effects of orexins are possibly mostly OX_1-dependent, while the long-term control of energy expenditure acts via OX_2 signalling. However, it should be noted that most of the studies are conducted with 1-SORA SB-334867, as OX_2-selective variants have not been available until recently, and thus the role of OX_2 is not as thoroughly studied.

The orexin system has also been reported to play a role in nociception (reviewed in [159]). Orexin-A has been shown to be analgesic in rodent pain models, and this action could be blocked by the 1-SORA SB-334867.[160] These findings are supported by more recent evidence of the antinociceptive effects

of orexins in different types of pains (reviewed in [159]). Even though the pain-modulation pathways of orexins are not fully understood, the antinociceptive effects of orexin-A have been shown to be more potent than those of orexin-B, and mainly OX_1-mediated.

Prolonged orexin receptor stimulation induces programmed cell death in colon carcinoma, neuroblastoma, and pancreatic acinar tumour cell lines (chapter 2.3.3).[114–116] Furthermore, colon carcinoma cells, unlike normal colon epithelium, express OX_1 receptors. Thus, orexin receptor activation has been suggested to be useful in the treatment of colon cancer, for example.

2.5 DISCOVERY OF SMALL MOLECULE OREXIN RECEPTOR MODULATORS

2.5.1 OREXIN RECEPTOR ANTAGONISTS

The search for small molecule orexin receptor ligands started rapidly after the first indications that the orexin system can be targeted for sleep-inducing pharmacotherapies. Until 2016, over 200 patent applications concerning orexin receptor antagonists had been filed; in 2016 alone, the number of new patents was still 35 ([161], reviewed in [122]). Currently, the sleep disorders are the main indication for DORAs and 2-SORAs, whereas 1-SORAs are mainly aimed at anxiety and panic disorders (see chapter 2.4). Additionally, both orexin receptor subtypes are involved in addiction, which could imply a target for 1- and 2-SORAs, depending on the drug of abuse.

Until 2016, eight orexin receptor antagonists had reached human clinical trials, and four DORAs had completed phase II studies (reviewed in [122]). These DORAs are almorexant (Actelion Pharmaceuticals Ltd.), SB-649868 (GlaxoSmithKline a.k.a GSK), suvorexant (Merck & Co., Inc), and filorexant (Merck & Co., Inc), and they will be discussed in detail in chapter 2.5.1.3

(Figure 10). Of these, suvorexant[162] received FDA approval for the treatment of insomnia in August 2014, becoming the first orexin receptor antagonist on the market (currently in the United States and Japan).

All reported orexin receptor ligands (antagonists and agonists alike) have been initially discovered through high throughput screening (HTS; see below); whether molecular modelling has been utilized in the subsequent compound design is rarely communicated. Nevertheless, several retrospective docking studies explaining the binding of the discovered compounds is found from the literature.[54–56,163–166] An overview of binding modes of the co-crystallized antagonists and computational studies are provided in chapter 2.5.1.4.

2.5.1.1 OX_1-selective antagonists

The discovery of the very first orexin receptor antagonists was reported in 2001.[167,168] These compounds were 1,3-biaryl urea-based 1-SORAs, and they were identified by functional HTS on CHO cells expressing human OX_1 receptors. The structure-activity relationship (SAR) studies conducted around an initial HTS hit led to the discovery of SB-334867, a relatively potent and selective, and brain penetrant OX_1 ligand (Figure 8).[168] Even though SB-334867 lacked oral bioavailability and had rather wide off-target activity, it demonstrated *in vivo* efficacy in preclinical rodent models, and has remained as a commonly used research tool; SB-334867 is used in almost 500 publications concerning orexin pharmacology (see e.g. [169,170]; reviewed in [171]). Shortly after SB-334867, a discovery of SB-674042 (Figure 8) and its tritiated analogue [^{3}H]-SB-674042, the first OX_1-receptor selective radioligand, was announced.[172] Interestingly, SB-674042 is the 1-SORA utilized for determination of the OX_1 crystal structure (see chapter 2.5.1.4).[54]

Apart from 1,3-biaryl ureas, two series of tetrahydroisoquinolines, close structural analogues of the dual orexin receptor antagonist almorexant (Figure 10), and a set of

morphinan compounds have been reported as potent 1-SORAs.[154,164,173] These compounds show over 70-fold selectivity towards OX_1, and they reduce anxiety, cocaine-seeking, and physical dependence to morphine in rats.
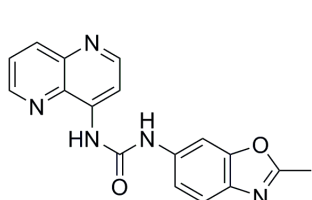
SB-334867
K_b (OX_1) 40 nM
K_b (OX_2) 1995 nM
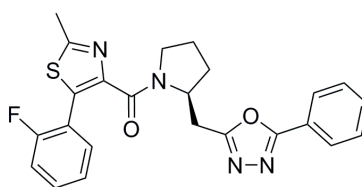
SB-674042
K_b (OX_1) 1 nM
K_b (OX_2) 129 nM
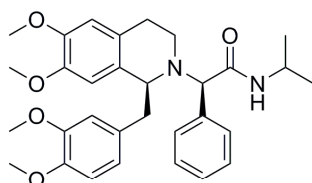
ACT-335827
IC_{50} (OX_1) 6 nM
IC_{50} (OX_2) 417 nM
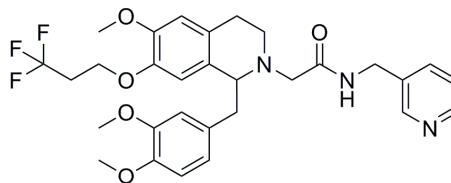
Perrey 72
K_e (OX_1) 8.5 nM
K_e (OX_2) >10 000 nM
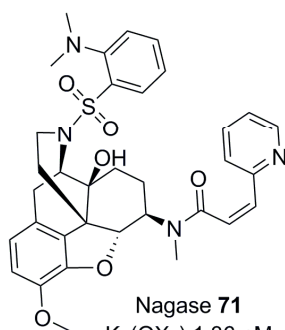
Nagase 71
K_i (OX_1) 1.36 nM
IC_{50} (OX_2) >10 000 nM

Figure 8. Examples of 1-SORAs. Affinities are as reported in [154,164,167,172,173].

2.5.1.2 OX$_2$-selective antagonists

Shortly after the first 1-SORAs, the first series of 2-SORAs were introduced by Hirose et al.[167,174] They reported a tetrahydroisoquinoline-structured HTS hit and a SAR optimization campaign leading to a 2-SORA with over 250-fold selectivity over OX$_1$ (Figure 9). About a year later, 4-phenyl-[1,3]dioxane urea compounds were identified as 2-SORAs by a similar kind of approach; the most promising compound of this series, JNJ-1037049 (Figure 9), had somewhat better binding affinities compared to the previously reported tetrahydroisoquinoline and also improved selectivity over OX$_1$.[175] Further experiments with JNJ-1037049 showed that this compound decreased the latency to persistent sleep and increased REM and NREM sleep, offering the first proof of concept of preclinical efficacy of OX$_2$-selective ligand in a rodent sleep model.[176]

In 2009, Malherbe et al. reported 2-SORA EMPA (Figure 9), and subsequently, a tritiated [^{3}H]-EMPA, the first OX$_2$ selective radioligand.[177] Quite recently, the three-dimensional structure of OX$_2$ in complex with EMPA was reported (see chapter 2.5.1.4).[56] In addition to these, benzoxazepine-scaffolded compounds have also been reported as 2-SORAs (Figure 9).[178]

In 2016, 2-SORAs were a leading trend in the patent literature of the field of orexin receptor antagonists.[161] This, however, is not too unexpected, as several 2-SORAs have provided promising preclinical data in the sleep models (e.g. references [179–181], reviewed in [122]). Until 2016, two 2-SORAs had entered clinical trials, MK-1064 by Merck and JNJ-42847922 by Janssen Pharmaceuticals (Figure 9), and until 2017 the number has doubled ([179,182], reviewed in [138]) Of these, MK-1064 has been reported to have similar effects on the sleep of healthy subjects as DORAs.[179]

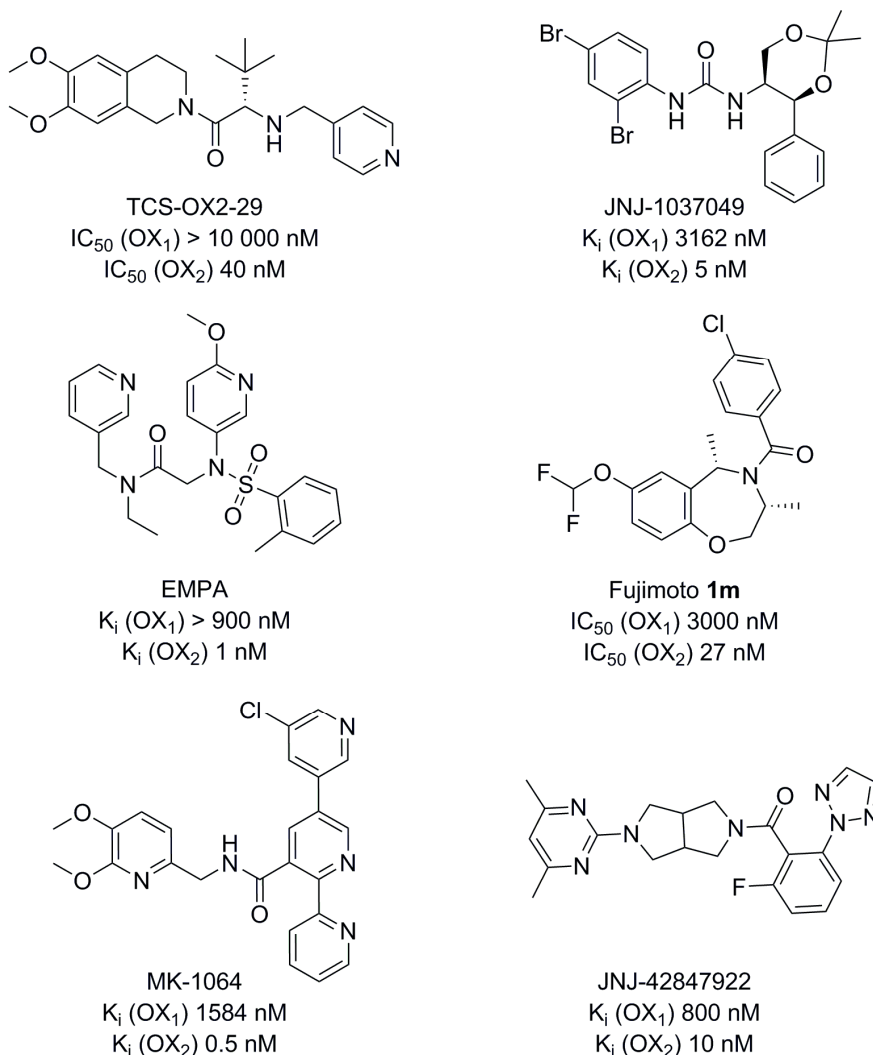Figure 9. Examples of 2-SORAs as presented in [174,175,177,179,182,183].

2.5.1.3 Dual orexin receptor antagonists

In 2003, Koberstain et al. published the first series of compounds acting as DORAs.[184] In this study, they describe a structural optimization of the tetrahydroisoquinoline compound identified by HTS, utilizing solution-phase chemistry combined with automated purification. The versatile

structural optimization led to the discovery of ACT-078573, currently known as almorexant (Figure 10).[127,184] Almorexant has a high affinity on both orexin receptor subtypes (13 nM on OX_1 and 8 nM on OX_2), efficient brain penetration, over 650-fold selectivity towards a large panel of targets, and decent bioavailability in rats and dogs. Furthermore, almorexant showed significant reductions in active wake and concomitant increases in REM and NREM sleep in these animal models and no signs of promotion of cataplexy. Thus, almorexant, as the first orexin receptor antagonist, entered clinical trials, where it was generally well tolerated and significantly improved sleep efficiency and maintenance (reviewed in [171]). Even though the development of almorexant was discontinued in 2011, due to 'infrequent transient increases in liver enzymes'[185], it offered a solid proof of concept of deploying DORAs in the treatment of insomnia.

Other DORAs have also entered clinical trials, and of these SB-649868[186], suvorexant (MK-4305),[162,187,188] and filorexant (MK-6096)[189] have been reported to have completed phase II (Figure 10; reviewed in [122]). SB-649868, reported in 2009 as a result of SAR analysis of piperidine bis-amides, is a DORA with a sub-nanomolar affinities and promising *in vivo* activity and pharmacokinetic profile in rats.[186,190] As almorexant, SB-649868 has also been reported to have a remarkably good sleep efficacy, but metabolic studies have demonstrated a risk of biologically relevant nucleophiles among its metabolic intermediates, indicating possible idiosyncratic toxicity (reviewed in [122]). After these reports, the development of SB-649868 was discontinued due to unspecified reasons (reviewed in [138]).
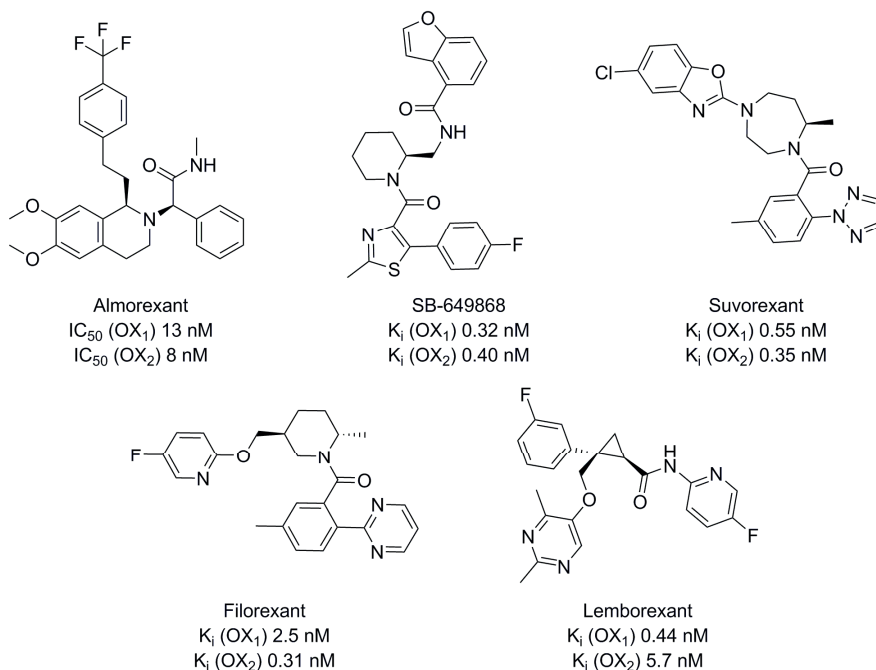
Figure 10. Examples of DORAs. Binding affinities as reported in [127,162,186,189,191].

In 2009, Whitman and co-workers reported a series of *N,N*-disubstituted-1,4-diazepanes, identified as orexin receptor ligands by HTS.[192] After a thorough structural optimization of the 'eastern' and 'western' part of the molecule, they disclosed 'compound 5' (Figure 11) with low nanomolar binding affinities towards OX_1 and OX_2. To guide further compound development, compound 5 underwent conformational analysis by NMR spectroscopy, X-ray crystallization and molecular modelling.[192] Together these studies indicated, that compound 5 adapts a U-shaped conformation due to energetically favourable intramolecular π-π-stacking interactions and the twist-boat conformation of the diazepane ring. Subsequently, the U-shape was tested by a macrocyclic compound locked into such a conformation; the higher binding affinity of the macrocycle, compared to that of the open precursor, was the first indication of orexin receptor antagonists adopting U-shaped bioactive conformation. Later, the U-shape was

established by co-crystallization of suvorexant with OX_1 and OX_2 receptors.[54,55]

The conformational studies led to the development of a series of compounds bearing modification in their central diazepane ring; the aim of these was to lock the compounds to the preferred U-shaped conformation (e.g. 'Compound 8a' in Figure 11).[193] Simultaneously, the original lead compound 5 was modified further, and after several rounds of modifications the structure of MK-4305, currently known as suvorexant, was disclosed (Figure 10; Figure 11).[162,188]

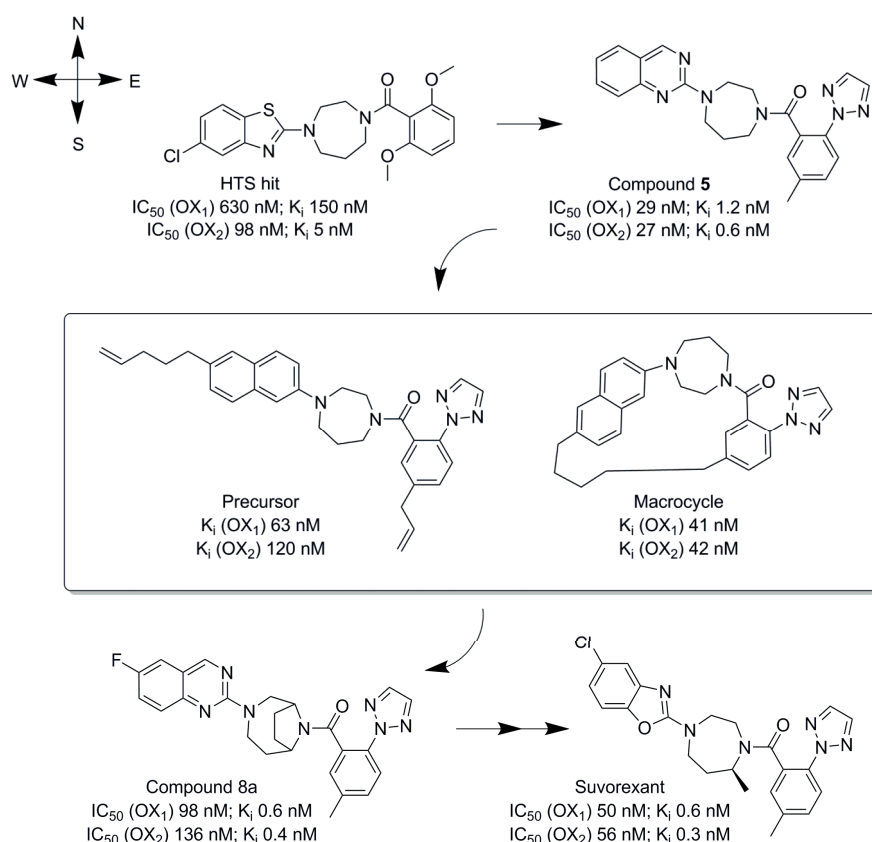Figure 11. The discovery of suvorexant. The presented structures and affinities are disclosed in [162,187,192,193].

Interestingly, suvorexant and EMPA have similar binding affinities for OX_2 (K_i's approximately 1.3 nM in [194]), but the dissociation rate of suvorexant is more than ten-fold lower than that of EMPA.[194] Furthermore, the dissociation kinetics of almorexant is even slower than that of suvorexant.[177,194] This means that the two orexin receptor antagonists that are effective in clinical trials display notably slow dissociation kinetics, which could contribute to their mechanism of action. In general, slow dissociation kinetics of antagonists of peptide receptors seems to be important for their *in vivo* efficacy (e.g. in case of neurokinin 1 receptor[195]).

At about the same time as *N,N*-disubstituted-1,4-diazepanes, piperidine ethers were reported as potent DORAs.[189,196] Guided by a thorough conformational analysis, modifications to these lead to the disclosure of the structure of MK-6096, a.k.a. filorexant (Figure 10). Filorexant bears a 2,5-*trans*-diaxial substitution in its piperidine ring allowing intramolecular π–π-stacking and U-shape formation, which is hypothesised to be crucial also for its bioactivity.[196] In addition to a favourable ADME/T profile, filorexant has shown improved efficacy in preclinical studies compared to suvorexant, likely due to its higher unbound plasma concentration *in vivo* ([189], reviewed in [122]), making it a promising clinical candidate.

Apart from tetrahydroisoquinolines, diazepanes, and piperidines, a recent study of Yoshida et al. reports the development of a series of cyclopropane-cored DORAs.[191] A detailed SAR optimization led to selection of E2006 aka lemborexant (Figure 10) for further clinical evaluation. In 2017, lemborexant was reported to have successfully entered phase II clinical trials (reviewed in [138]).

2.5.1.4 Binding modes and molecular modelling of orexin receptor antagonists

Both orexin receptor subtypes have been crystallized in complex with the DORA suvorexant (PDB IDs: 4ZJ8 and 4S0V, on OX_1

and OX₂, respectively).[54,55] Additionally, OX₁ has been crystallized with the 1-SORA SB-674042 (4ZJC)[54], whereas the structure of OX₂ is solved in complex with the 2-SORA EMPA (5WQC and 5WS3).[56] The structures of OX₁ and OX₂ in complex with suvorexant are highly similar;[54,55,197] the Cα root mean square deviation (rmsd) over 282 Cα atoms of the superimposed structures is only 0.4 Å. There is a two-amino-acid difference at the antagonist binding sites of orexin receptors—S2.61T and A3.33T in OX₁ and OX₂, respectively—making the OX₁ binding site slightly larger. Additionally, the crystal structures of OX₂ have water molecules in the binding site, but these are not detected in OX₁ structures. However, that is almost certainly due to the lower resolutions of the OX₁ structures; OX₁ structures are solved at 2.75 Å and 2.83 Å resolutions (suvorexant and SB-674042, respectively), whereas for OX₂ structures the resolutions are 2.5 Å (suvorexant), 1.96 Å and 2.3 Å (EMPA).

Suvorexant adopts almost identical U-shaped binding conformation in both orexin receptor subtypes (Figure 12A–B), and the binding conformation of SB-674042 in OX₁ is highly similar (Figure 12C). The carbonyl oxygen of all these ligands form a hydrogen bond with Asn[6.55]. In OX₂, the hydrogen bond network continues from the carbonyl oxygen of suvorexant to a crystallographic water molecule, His[7.39] and Asp[2.65] (Figure 12B). It is worth noting that the His[7.39]–Asp[2.65] salt bridge is present in all antagonist-bound orexin receptor crystal structures (Figure 12).
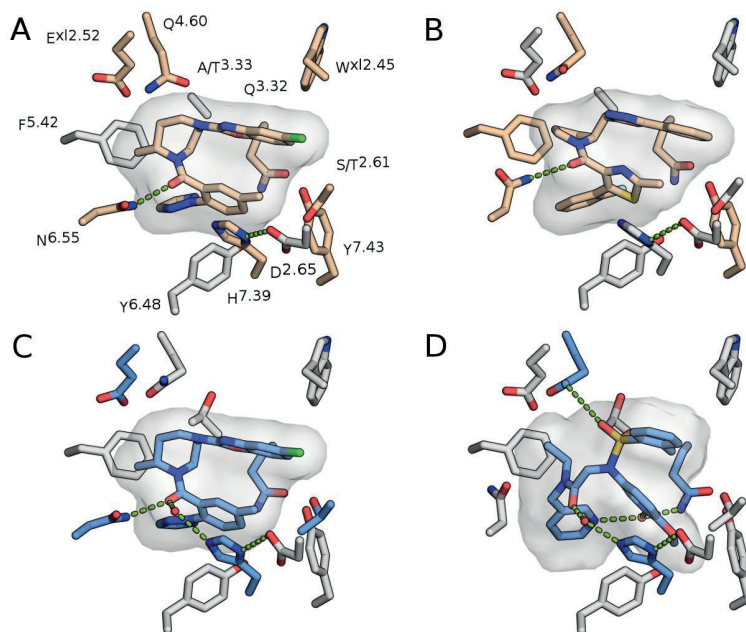
Figure 12. A. The binding pose of suvorexant in OX$_1$ (pdb ID: 4ZJ8). B. The binding pose of SB-674042 in OX$_1$ (pdb ID: 4ZJC). C. The binding pose of suvorexant in OX$_2$ (pdb ID: 4S0V). D. The binding pose of EMPA in OX$_2$ (pdb ID: 5WQC). In OX$_1$ structures (A and B) ligands and amino acid residues within 3.5 Å these ligands are shown as wheat sticks. In OX$_2$ structures (C and D) the ligands and amino acid residues within 3.5 Å of these ligands and co-crystallized water molecules are shown as cobalt blue sticks. Colour code is as follows: wheat / cobalt blue / white, carbon; red, oxygen; blue, nitrogen; yellow, sulphur; green, chlorine; light blue, fluorine. Green dashes represent possible hydrogen bonds, red spheres the crystallographic water molecules and the grey surfaces the space each ligand occupies in the binding pocket. The subset of binding site amino acid residues shown are selected based on the published point mutation data. View is from the extracellular side of the receptor, from the direction of TM7.

The 2-SORA EMPA is the only co-crystallized orexin receptor ligand reported thus far that does not adopt a U-shape and lacks direct interaction with Asn[6.55] (Figure 12D). The sulphonamide group of EMPA can instead form a hydrogen bond with Gln[4.60], and interact via crystallographic water molecules with Gln[3.32] and His[7.39].

Prior to the orexin receptor crystal structures, a couple of molecular modelling studies involving orexin receptors were published.[57,60] The study of Malherbe et al.[57] focused on the retrospective analysis the results of the orexin receptor mutants utilizing homology models and molecular docking. The study of Heifetz et al.[60] had similar aims to those of Malherbe and co-workers', but with additional molecular dynamics (MD) simulation data. Of these, the binding site amino acid residues highlighted by the computational studies are mainly verified by the crystal structures, even though the reported binding poses are not equivalent to the co-crystallized ones.

The release of the orexin receptor crystal structures led to a 'second generation' of computational studies explaining the ligand binding of orexin receptors. Several reports have been published explaining the binging interactions of a wide variety of orexin receptor ligands,[55,163,164] orexin receptor activation (see 2.5.2.2 below),[165,166,198] and subtype selectivity.[54,56] As an example, Heifetz et al. further explored the amino acid residues contributing to the binding of suvorexant to OX_2 utilizing the molecular orbital method.[163] This study identified residues $Pro^{3.29}$, $Gln^{3.32}$, $Gln^{4.60}$, $Glu^{xl2.52}$, $Phe^{5.42}$, $Ile^{6.51}$, $Asn^{6.55}$, $His^{7.39}$, and $Tyr^{7.43}$ to contribute to the binding; of these $Gln^{3.32}$, $Phe^{5.42}$, $Ile^{6.51}$, $His^{7.39}$, and $Tyr^{7.43}$ are in accordance with the mutation studies of OX_2 with almorexant and EMPA.[57] Interestingly, their results highlighted the importance of $Glu^{xl2.52}$, located within the β-hairpin structure (see chapter 2.2.3), for the binding of suvorexant. Even though there is no suitable hydrogen bond donor in the structure of suvorexant, Heifetz et al. suggested that its 1,4-diazepane ring has a positive electrostatic field, which could interact with the negative field of the side chain of $Glu^{xl2.52}$.

It is suggested that SB-674042 has improved shape-complementary with the binding site of OX_1 compared to that of OX_2 in addition to the required interactions leading to OX_1-selectivity.[54] The reported molecular docking, MD simulations, and site-directed mutagenesis studies with EMPA, instead, have suggested specifically the importance of the residues $Thr^{2.61}$ and

Thr[3.33] for their OX_2-selectivity.[54,56,57] Interestingly, the methyl groups of these residues are within 4 Å from EMPA (of its methoxy and sulphonamide groups, respectively), but the hydroxyl groups of these side chains are too far for hydrogen bonding (Figure 12D). This suggests that also in the case of EMPA, subtype selectivity may originate from the suitable binding site complementarity.

2.5.2   ACTIVATING THE OREXIN SYSTEM

Unlike the successful development of numerous orexin receptor antagonists, activation of the orexin system has relied mainly on the native orexin peptides (reviewed e.g. in [171]). However, small molecule-sized orexin receptor activators would be of interest especially in targeting narcolepsy (see chapter 2.4.2); the drugs currently used for type I narcolepsy do not target the causative deficits in orexin levels but rather act as CNS stimulants (reviewed in [138]). There are two possible ways to enhance the activity of the orexin system: orexin receptor potentiators, which enhance the actions of the endogenous orexin peptides, or direct orexin receptor agonists.

2.5.2.1 *Orexin receptor potentiators*

One series of orexin receptor potentiators is found in the literature.[199] In that study, Lee et al. reported peptoids discovered by a microarray-based, two-color, cell-binding screen, and structural optimization, which led to DORAs with low micromolar affinity. Interestingly, three compounds increased the potency of orexin-A in their assay set-up, and when studied further, the best of them, OBPt-9 (Figure 13), showed a 2.5-fold maximum potentiation of a response to a small concentration of orexin-A (corresponding to its EC_{20} in adenylyl cyclase assay). Although OBPt-9 was reported to have entered *in vivo* testing, no such a report is available to date.

Additionally, in their report, Lee et al. provide no data regarding orexin receptor mediation of the observed potentiation.

2.5.2.2 *Orexin receptor agonists*

Only one series of orexin receptor agonists with significant efficacy has been reported.[165] The lead compound of this study, Nag26 (Figure 13), has an EC_{50} of 1.62 and 0.023 μM, and an E_{max} of 100% and 98% on OX_1 and OX_2, respectively (in Ca^{2+} elevation assay in recombinant CHO cells). Nag26 was discovered by a thorough structural optimization of hits of a HTS campaign, and it bears a secondary sulphonamide, which is reported to be crucial for its activity. As the water solubility of Nag26 was not considered high enough for *in vivo* testing, it was modified further by introducing the 2-dimethylamino group on the B-ring instead of the 3-methyl of Nag26 (Figure 13). The resulting YNT-185 (Figure 13) was characterized *in vivo*, wherein it suppressed cataplexy-like episodes in orexin knockout and orexin neuron-ablated mice, and promoted wakefulness in wild-type mice upon i.c.v. administration.[134] Altogether, these results provide a proof-of-concept for treating narcolepsy–cataplexy with OX_2 agonists.

The binding interactions of Nag26 and OX_2, and possible attributes of receptor activation, have been studied by molecular docking.[165,166] Together with the disclosure of Nag26, Nagahara et al. published a docking study where they suggested Nag26 to occupy the same binding pocket as suvorexant, but adopt an extended conformation reaching its aromatic A-ring substituent towards TM5 and TM6. Thus, they hypothesized that binding of Nag26 would allow interactions leading to the inward movement of TM5 and TM6 and therewith receptor activation. Another report of molecular docking of Nag26 was published by Heifetz et al; they present two docking poses of Nag26, one similar to that of Nagahara et al. and another resembling the U-shape of suvorexant.[166] In this study, the binding interactions of Nag26 are discussed in the context of the previously published, site-directed mutagenesis data (see chapter 2.2.3). Amino acid

residues Thr[2.61], Gln[3.32], Phe[5.42], Tyr[5.47], and Tyr[6.48] have been shown to affect the potency or efficacy or both of orexin-A (investigated by alanine mutations), and these residues also interact with the Nag26 in the reported docking poses. Thus, the authors discuss the involvement of the TM3–5–6 interface, a common interaction partner with an agonist in the structures of Rhodopsin family GPCRs (see also 2.1.3), in Nag26-mediated orexin receptor activation.
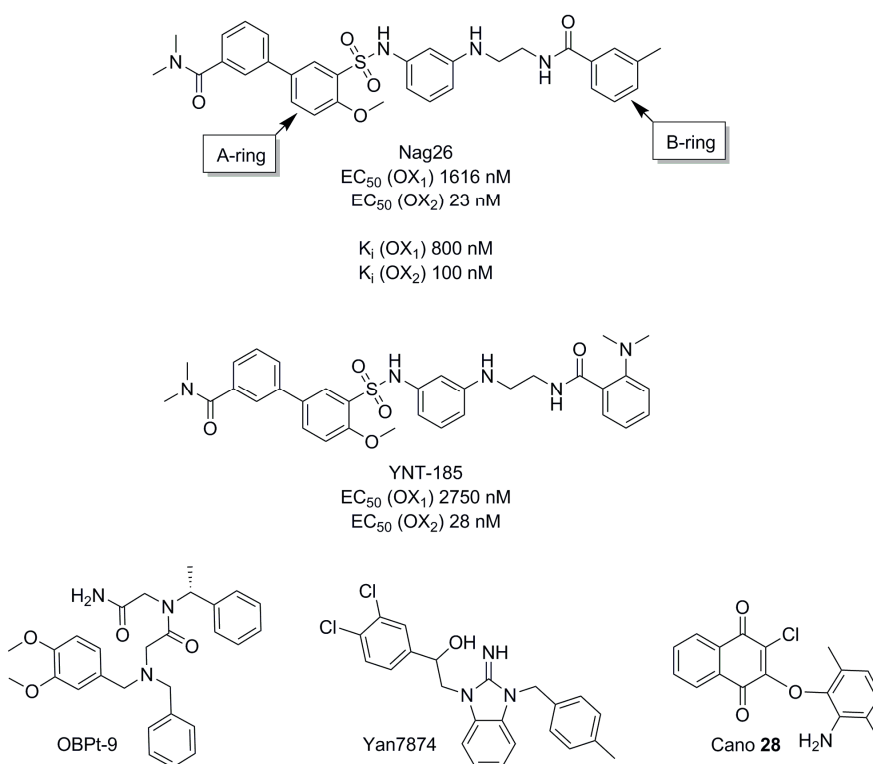
Figure 13. Orexin receptor activators—full agonists Nag26 and YNT-185, the putative potentiator OBPt-9, and the agonist hit compounds Yan7874 and Cano **28** reported in patent literature.

In addition to Nag26 and YNT-185, reports of compounds with weak orexin receptor agonism activity have been

published.[200,201] These compounds by Yanagisawa and Cano et al. are found in the patent literature, and include hardly any pharmacological data. The lead compound of Yanagisawa, Yan7874 (Figure 13), is said to produce a six-fold elevation of Ca^{2+} concentration at 10 μM compound concentration in OX_2-expressing CHO cells, and a much weaker response in OX_1-expressing cells. The patent also describes SARs for a small series of compounds showing the importance of the chiral alcohol and imine functionalities, but without disclosing any stereochemistry.

The patent of Cano et al. presents a series of 2-(2-aminophenoxy)-3-chloronaphthalene-1,4-dione compounds, whose agonist activity towards OX_2 is assessed at 50 μM concentration. The patent claims the lead compound (Figure 13) to produce 93% activation of OX_2 receptors, however, the used method is not fully described, and thus comparing the results with the other studies is not straightforward.

3 AIMS OF THE STUDY

At the commencement of this thesis work, neither small molecular orexin receptor agonists nor structural data of orexin receptors were reported in the scientific literature (Figure 1). Thus, relying on the available data, this study sought to understand binding and activation attributes of the orexin receptor ligands (by computational methods) and then subsequently apply the gained knowledge in finding novel orexin receptor ligands (preferably activators).

The specific aims were:

1.   To understand the chemical features that make small molecules and peptides bind to, and activate, orexin receptors.

2.   To develop pharmacophoric representations of the features that are important for orexin receptor binding or activation or both.

3.   To find new small molecular ligands that bind to and activate orexin receptors.

4 MATERIALS AND METHODS

The methods used in the publications I–IV are summarized in Table 2.

Table 2. Summary of the used methods.

Computational method	Publication
Pharmacophore modelling	I, IV
Molecular docking	I, III
Virtual screening	I, III
R-group analysis	III
In vitro method	
Ca^{2+} elevation assay	I–IV
Competition binding assay	I, III
Phospholipase C assay	II
Adenylyl cyclase assay	II
Cell viability measurements	II

4.1 COMPUTATIONAL METHODS

4.1.1 PHARMACOPHORE MODELLING AND VIRTUAL SCREENING

A pharmacophore model is a combination of chemical features in three dimensional space, which are required for triggering a biological response (such as binding to a receptor; reviewed e.g. in [202]). These chemical features include hydrogen bond donors and acceptors, aromatic rings, and positive, negative, or hydrophobic point features. Pharmacophore models can be constructed either by a superimposition of known bioactive

compounds of interest (a training set) and selecting the similar chemical features for the pharmacophore, or the features can be selected based on receptor-ligand interactions (so-called shared-feature and structure-based pharmacophores, respectively). The classification performance of the pharmacophore is commonly tested with a set of compounds including both active ligands and structurally related inactive compounds (a test set); each compound in the test set is overlaid with the pharmacophore model and classified either as an active (match) or inactive (non-match) based on the overlay or RMSD of the pharmacophoric features, depending on the used algorithm.

In publication I, we constructed both shared-feature and structure-based pharmacophores with Discovery Studio 3.5 software[203]. For structure-based pharmacophores, docking complexes of orexin receptor ligands and NTS$_1$-based OX$_1$ homology model[198] were used for guiding the feature selection. Docking was conducted by the Induced fit protocol of Schrödinger Glide software (2013v2).[204] A test set of 162 DORAs and 1-SORAs collected from the literature were used, in addition to 41 known decoys published together with the active ligands. Smaller subsets of these active compounds were used as a training set for common-feature pharmacophores.

The classification performance of the models was defined by calculating the sensitivity (Eq 1) and the specificity (Eq 2) of retrieving the test set compounds. Receiver operator curves (ROC) were generated, and the area under the curve (AUC) calculated by Schrödinger Maestro 2013v2 software[204].

$$sensitivity = \frac{TP}{TP + FN} \qquad (Eq.\,1)$$

$$specificity = \frac{TN}{TN + FP} \qquad (Eq.\,2)$$

In equations 1 and 2, TP refers to true positives (the number of active compounds that are correctly classified), and FN to false negatives (the number of active compounds that are incorrectly classified). TN means true negatives (the number inactive compounds that are correctly classified), and FP false positives (the number of inactive compounds that are incorrectly classified).

In publication IV, Discovery studio 4.5 software[205] and common-feature pharmacophores were employed to explain the SARs of the azulene hit compounds. The active compounds were superimposed and pharmacophore models constructed guided by the superimposition. The classification power (active compounds of publications III and IV from the inactive ones) was defined by monitoring the sensitivity and specificity (Eq1 and Eq2).

Pharmacophore models are commonly utilized as virtual screening filters to select the most promising compounds among the compound libraries for biological testing (reviewed in [202]). In publication I, the pharmacophore model with the best sensitivity and specificity factors was utilized for a virtual screen of the compound library of the Finnish Drug Discovery and Chemical Biology consortium (http://ddcb.fi/en/; v2011, about 137 000 compounds). The screening was conducted with default parameters using Discovery Studio 3.5.[203] The retrieved hit list of 800 compounds was post-processed with molecular weight (>400 g/mol passing) and reactivity filters (REOS), as well as visual examination. Additionally, the absence of possible PAINS containing structures was checked by FAF-Drugs2.[206] The final hit list consisted of 395 compounds.

4.1.2 MOLECULAR DOCKING AND DOCKING-BASED VIRTUAL SCREENING

Molecular docking aims to predict the binding mode of a ligand to a protein binding site, and it is nowadays an essential structure-based drug discovery strategy (reviewed e.g. in [207]). As a calculation, docking relies on scoring functions, both during

the exploration of the binding conformation space of a ligand and evaluation of the final binding poses. Currently applied scoring functions can be roughly divided into three classes: force-field based; empirical; and knowledge-based scoring functions. The force field-based scoring functions use classic force fields to compute the noncovalent protein–ligand interactions (e.g. van der Waals and electrostatic energies). The empirical scoring functions calculate the overall binding free energies of the protein–ligand complexes from several energetic terms, including hydrogen bond and hydrophobic interactions. Finally, the knowledge-based scoring functions consider the protein–ligand interactions as a sum of distance-dependent statistical potentials, deducted from the structural information of the solved protein–ligand complexes, between the ligand and the target.

In publications I and III, we utilized docking software Glide of the molecular modelling package Schrödinger Maestro, which applies empirical scoring function GlideScore.[204,208–210] In publication I, a homology model of OX_1 and crystal structures of OX_1 and OX_2 were utilized, and Induced Fit docking protocol used with default parameters. At an early stage, a set of reference ligands were docked to the NTS_1-based homology model of OX_1[198] to guide the pharmacophore modelling (described in 4.1.1). The binding site was defined by the centroid of the coordinates of the amino acid residues that were reported important for orexin receptor activation (see 2.2.3). The retrospective docking was conducted to the crystal structures of OX_1 and OX_2, which were published while our study was ongoing, and the binding site was defined by the location of the co-crystallized suvorexant.[54,55] Docking to the OX_2 crystal structures was conducted both in presence and absence of the binding site water molecules (waters 4021 and 4025).

Docking is also commonly utilized in virtual screening (reviewed in [207]). In the docking-based virtual screening, the compounds of a compound library are individually docked to a target binding site and ranked based on their 'fit'. The top-ranking compounds are assumed to bind better to the target,

and thus are worth undergoing biological testing. However, the docking protocols, and especially scoring, are limited by mathematical approximations, and thus monitoring the quality of the screening (e.g. enriching the library with active reference ligands and monitoring their scoring) and the post-processing of the hit lists (e.g. by additional scoring and/or filtering methods and visual examination) is utmost important.

In publication III, we conducted a docking-based virtual screen on an in-house combinatory virtual library of 70038 azulene-based compounds to OX_2, which was the only orexin receptor crystal structure available at the time.[55] The screening compounds were aimed to be synthetically accessible,[211,212] and the lipophilic azulene ring was envisaged to mimic the amphipatic α-helical C-terminus of orexin-A.[46,198] The database was built with a combinatory database building tool of Schrödinger Maestro software.[213]

For screening, Glide was used with SP parameters, and the binding site was defined by the location of co-crystallized suvorexant. To monitor the performance of the docking, the virtual library was seeded with 117 DORAs or 2-SORAs. The docking protocol retrieved 25% of the active compounds in the top 10% of the database, leading to the AUC of 0.75. Furthermore, suvorexant was docked among the active compounds, and the docked conformation compared to that present in the OX_2 crystal structure. Docked suvorexant scored in the top 1.6% of the library and its conformation was highly similar to the binding conformation in the crystal structure (pairwise heavy atom RMSD 0.54).

4.1.3   R-GROUP AND SAR ANALYSES

Structure-activity relationship (SAR) analysis relies on the assumption that the activity of the compound is a function of its structure.[214] Thus, analysing the structures of active and inactive compounds provides insights into their activity and rationalizes the structural optimization of the compounds. In publication III, this idea was utilized in post-processing of the

virtual screening hit list—it was hypothesised that the more often certain R-groups occur among the top-scoring poses, the more important this R-group would be for the activity of the compounds. Thus, we analysed the 5% top-scoring poses (i.e. 7200 poses) using the R-group analysis tool of Schrödinger Canvas.[208] The understanding gained regarding the most favourable R-groups supported the visual examination of the 200 top-scoring docking poses, and the final selection of the compounds to be synthesized.

4.2 *IN VITRO* METHODS

4.2.1 CELL CULTURE AND MEDIA

CHO-K1 cells expressing human OX_1 and OX_2 receptors (CHO-hOX1 and CHO-hOX2, respectively[72,215]) as well as ctrl CHO-K1 cells not expressing orexin receptors (ctrl CHO cells) were cultured in Ham's F12 medium (Gibco/Life Technologies, Paisley, UK) + supplements, and neuro-2a cells in Dulbecco's modified Eagle's medium (Gibco/Life Technologies) + supplements on plastic cell culture dishes (56 cm² bottom area; Greiner Bio-One GmbH, Frickenhausen, Germany) as described in [73,77].

Experiments were run in hepes-buffered medium (HBM; 137 mM NaCl, 5 mM KCl, 1.2 mM $MgCl_2$, 0.44 mM KH_2PO_4, 4.2 mM $NaHCO_3$, 20 mM Hepes, 10 mM glucose, and 1 mM $CaCl_2$, pH adjusted to 7.4 with NaOH). For Ca^{2+} measurements, HBM was supplemented with 1 mM probenecid, to inhibit probe extrusion from the cytosol, and the ligands were diluted in this same buffer containing additionally 0.05% w/v stripped bovine serum albumin (to aid in keeping the lipophilic compounds in solution). For binding, HBM with 0.1% w/v stripped bovine serum albumin (to reduce also nonspecific binding of [125I]-orexin-A) and 30 µM dyngo 4a (to block receptor internalization) was used. Furthermore, for PLC assay, HBM

supplemented with 10 mM LiCl was used, and for AC assay HBM was supplemented with 500 µM cyclic nucleotide PDE inhibitor and 3 µM PKC inhibitor.

4.2.2 CA^{2+} ELEVATION ASSAY

Intracellular Ca^{2+} elevation is a prominent response to orexin receptor activation, as reviewed in chapter 2.3.1. Thus, a fluorescence-based Ca^{2+} elevation assay was used to screen the agonist and antagonist activities of the compounds towards orexin receptors. Additionally, K_i values were determined for the most promising binding assay hits (see below) orthogonally utilizing Ca^{2+} elevation assay, as well as studying the orexin-receptor-mediation of the observed agonist activities, and the potentiation effect the hit compounds had on the Ca^{2+} responses to orexin-A.

The cells, 1.5×10^4 per well, were plated on black, clear bottom half-area 96-well plates. Twenty-four hours later, cell culture medium was removed, and the cells were treated with loading solution composed of FLIPR Calcium 4 Assay Kit (Molecular Devices, Sunnyvale, CA) dissolved in and diluted with HBM, for 60 min at 37 °C. Then, the plate was placed in a FlexStation 3 fluorescence plate reader (Molecular Devices) and intracellular Ca^{2+} levels were measured as fluorescence changes (excitation at 485 nm, emission at 525 nm) at 37 °C for 150 s.

The screening assay was designed to detect both agonist and antagonist properties of the test compounds (Figure 14). The agonist responses were detected within the first round of measurements; in the first round, the baseline was collected for 30 s of each well, after which the test compounds (in the corresponding HBM) were added and the response collected for another 120 s. To widen the detection window, the delayed agonist response was assessed for 30 s, 30 min after agonist addition. In the second round, 0.3 nM orexin-A was added to each well, revealing compounds inhibiting orexin-A response. For both tests, vehicle was included in each column of wells to serve as both negative (1st round) and positive (2nd round)

control. The responses to each compound were reported as a percentage of E_{max} of orexin-A.
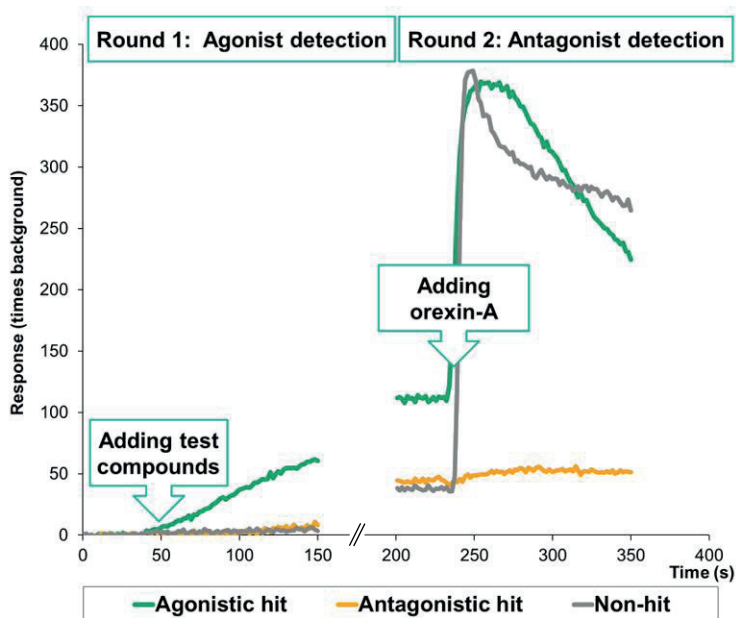

Figure 14. The design of the Ca^{2+} elevation-based screening assay. First the baseline is collected for 30 s, after which the test compounds are added, and agonists detected as a direct Ca^{2+} response (measured for 120 s; green line). Then, 30 min later, the measurement is repeated; the baseline of this round reveals possible compounds with e.g. slow association kinetics. After 30 s, 0.3 nM orexin-A is added; possible antagonists are detected by the blockade of the response to orexin-A (measured again for 120 s, orange line).

For K_i measurements, the test compounds were added in the wells according to the procedure for the first round as described above, and the plate was measured once. Then, 30 min later, 0.3 nM orexin-A was added as a stimulant (2nd addition) and the measurement was repeated.

For validation of the agonist activities, control antagonists SB-334867 and TCS-1102 were added to wells manually, when applicable, and incubated for 10–30 min before the measurement, after which the test compounds were added, and

the plate measured according to the first round procedure. SB-334867 and TCS-1102 have low nanomolar binding affinities,[168,216] and they are thus expected to block the orexin receptor-mediated fraction of the responses to the test compounds.

For potentiation studies, the orexin-A/compound and ATP/compound mixtures were added to the cells and measured as for the agonist validation. Prior to the analysis of the potentiation effect of the compounds triggering Ca^{2+} elevation on their own, the compound-mediated Ca^{2+} responses were subtracted from the responses to orexin-A/compound and ATP/compound mixtures. To rule out the effect of intracellular Ca^{2+} on the observed potentiation, two sets of controls were utilized: 10 nM ATP (no measurable Ca^{2+} elevation of its own) and 30 nM ATP (Ca^{2+} elevation of a similar magnitude than our agonistic hits at 10 µM concentration). The potentiation effects of the compounds causing no Ca^{2+} elevation were compared to the 10 nM ATP control, whereas the potentiation effects of the compounds with Ca^{2+} response were compared to 30 nM ATP control.

4.2.3 [^{125}I]-OREXIN-A COMPETITION BINDING ASSAY

Binding of the test compounds was assessed in intact cells, as on CHO cells [^{125}I]-orexin-A cannot be used with cell homogenates or membrane preparations.[97] The cells ($1.5×10^4$ per well) were plated on white clear bottom half-area 96-well plates, and 24 h later the culture medium was exchanged for HBM ± 10 µM TCS-1102 (to determine nonspecific binding), and after a 10 min incubation 0.05 nM [^{125}I]-orexin-A (publication I) or 1 nM [^{125}I]-orexin-A/orexin-A mixture (1:20, publication III) mixed with each test compound was added. Dilution series of orexin-A and SB-334867 were used as controls. After a 90 min incubation at room temperature, the medium was removed by water suction and the wells were allowed to dry at 37 °C. Scintillation cocktail (Ultima Gold; PerkinElmer) was added, and the plates

were incubated overnight and counted in a Wallac Microbeta Trilux microplate liquid scintillation counter (PerkinElmer).

4.2.4   PHOSPHOLIPASE C ASSAY

Phospholipase C assay was employed to investigate the downstream signalling of Yan7874 (publication II). The cells, 2.6×10^4 per well, were plated on clear 48-well plates. After 24 h, they were labelled with 3 µCi/mL [^{3}H]-inositol (for 20 h). The medium was removed, and the cells were incubated in HBM for 30 min at 37°C. The inhibitors TCS-1102 (orexin receptor antagonist, to check the orexin-receptor-mediation of the observed response) or UBO-QIC (G_q inhibitor, to check the G_q-mediation of the response) were also included in this incubation when applicable.

The cells were stimulated for 10 or 30 min, then the medium was rapidly removed, and the reactions stopped by ice-cold 0.4 M perchloric acid and freezing. The samples were thawed and neutralized (0.36 M KOH + 0.3 M KHCO$_3$), and the insoluble fragments spun down. Anion-exchange chromatography was used for isolation of the total inositol phosphate fraction of the supernatants, and the radioactivity determined by scintillation counting (HiSafe 3 scintillation cocktail and Wallac 1415 liquid scintillation counter; PerkinElmer).

4.2.5   ADENYLYL CYCLASE ASSAY

For AC experiments with Yan7874 (publication II), the cells were pre-treated either for 20 h with cholera toxin (CTx; 1000 ng/mL; AC inhibition studies) or for 36 h with pertussis toxin (PTx; 300 ng/mL; AC activation studies). The cells, 2.4–3.0×10^4 per well, were plated on 48-well plates. Forty-eight hours after the plating, the cells were labelled for 2 h with 5 µCi/mL [^{3}H]-adenine. Then, they were washed once with PBS, and HBM was added. The cells were incubated for 30 min at

37°C before adding the stimulants. After 10-min stimulation at 37°C, the reactions were terminated with ice-cold perchloric acid and rapid freezing. After thawing, the insoluble fragments were spun down, and the [3H]-ATP/ADP and [3H]-cAMP fractions were isolated by sequential Dowex-alumina chromatography. Radioactivity was determined from the fractions with scintillation counting as in the PLC assay.

4.2.6   CELL VIABILITY AND CELL DEATH

To assess the cell viability and death after Yan7874 treatment, microscopic observations were employed, in addition to quantitative assessment of the cell numbers, and cell viability and necrosis by a plate reader. Cells were seeded on black, clear bottom 96-well plates (0.75–1.5×10^4 per well, depending on the experiment time) for the plate reader assay, and treated with test compounds after 24 h. Bright-field microscopic observation was carried out once every 24 h up to 72 h (Olympus CKX41 microscope with Canon EOS 600D digital camera). A robust cell death was seen after 24 h of the treatment.

Phase contrast microscopy assesses only the morphological features of the cells, and thus fluorescent microscopy was used for studying the cell death more thoroughly (Nikon TE2000 with $20\times/0.75$ air objective and NIS Elements AR software; Nikon, Tokyo, Japan; and an Andor iXon 885 camera; Andor Technology Ltd., Belfast, UK). For this, the cells were stained with Hoechst, PI (propidium iodide) and FDA (fluorescein diacetate). Hoechst stains all nuclei, but the morphological markers of the nuclei can be told apart (see chapter 2.3.3). PI can only permeate damaged plasma membranes and stains thus the nuclei of necrotic cells. FDA (non-fluorescent) is hydrolysed in the cytoplasm of viable cells to fluorescent fluorescein, which stays only in the cells with intact membranes; FDA is a measure of both cell viability and membrane integrity.

For plate reader measurements, the cells were stained as above. After the incubation, the fluorescence was read using

FlexStation 3 at the wavelengths 352 nm/455 nm (Hoechst), 480 nm/525 nm (FDA), and 538/617 nm (PI).

4.2.7   DATA ANALYSIS

All data are presented as mean ± SEM. Student's non-paired or paired two-tailed *t*-test (with Bonferroni correction for multiple comparisons) was used for statistical comparisons. Significances are as follows: ns (not significant), *P > 0.05; *P < 0.05; **P < 0.01; ***P < 0.001*. Microsoft Excel was used for all data visualizations and analyses including curve fitting. For Ca^{2+} measurements, K_i values were calculated from the determined IC_{50} values using the Cheng–Prusoff equation.[217] Binding was analysed by Equation 3 and the K_i values calculated by Equation 4.

$$binding_{(compound)}$$

$$= binding_{(radioligand)}$$

$$- \frac{[compound] * binding_{(radioligand)}}{[compound] + IC_{50\,(compound)}} \quad (Eq.\,3)$$

$$K_{i\,(compound)} = \frac{IC_{50\,(compound)}}{IC_{50\,(SB\text{-}334867)}} * K_{i\,(SB\text{-}334867)} \quad (Eq.\,4)$$

5 RESULTS AND DISCUSSION

5.1 PHARMACOPHORE MODELLING (PUBLICATION I)

Orexin receptor crystal structures were unavailable at the commencement of this investigation (Figure 1). Thus, we employed homology modelling and docking of orexin peptides, orexin receptor antagonists, and patented agonist Yan7874 to gain insight into molecular features that could contribute to orexin receptor binding and activation ([198] and publication I). Even though a homology model of OX_1[198] was used, we intended to target both orexin receptor subtypes, as their binding sites are nearly identical (chapter 2.5.1.4). We sought to integrate the identified features to a pharmacophore model, which would be able to uncover both novel agonists and antagonists of orexin receptors. The hypothesis was that combining features of Yan7874 (the activation attribute), features of the major classes of orexin receptor antagonists (the binding attribute), and information on the binding site would lead to such a model (see chapter 4.1.1).

The best-performing pharmacophore model was built on the docking pose of Yan7874, and it consisted of four features: a hydrogen bond donor (HBD), two aromatic features (R1 and R2), and a hydrophobic feature (H); these features form a triangle with side lengths of 5.6 Å (HBD–R2), 7.6 Å (R2–H), and 9.4 Å (H–HBD) in three-dimensional space (Figure 15A). Additionally, exclusion volumes were added to the model based on the closest amino acid residues of the utilized docking complex. The model discriminated the test set antagonists from the decoys with 59% sensitivity (96/162 true positives) and 90% specificity (37/41 true negatives), while the area under the receiving operator curve (AUC) was 0.85.

Retrospectively, this pharmacophore model characterises not only Yan7874 but also Nag26; the secondary sulphonamide nitrogen of Nag26 maps on the HBD, the A-ring, and its

aromatic substituent on R1 and R2, and the 3-methyl substituent of the B-ring on H (Figure 15B). Interestingly, the secondary sulphonamide has been reported to be crucial for the activity of Nag26, as well as the presence of the rings A and B. Additionally, altering the substituents of these rings has a notable influence on the activity of these compounds—for example changing the B-ring substituent from 3-methyl to 4-methoxy drops the EC_{50} of the resulting compound approximately 45-fold.[165]
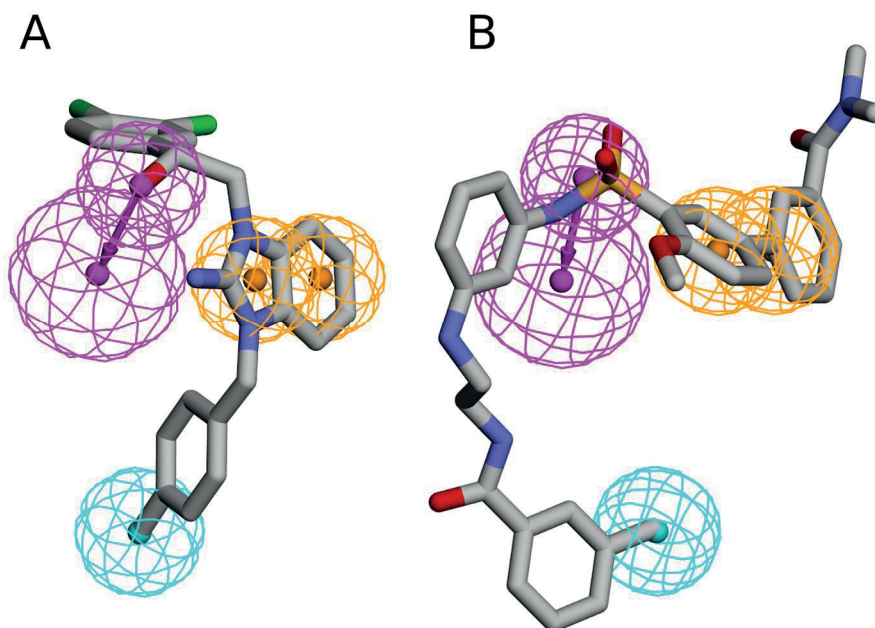

Figure 15. A. Yan7874 mapped on the pharmacophore of publication I. B. Nag26 mapped on the same pharmacophore. Hydrogen bond donor: magenta, aromatic feature, brown; hydrophobic feature, cyan, carbon, grey; nitrogen, blue; oxygen, red; sulphur, yellow; chlorine, green. The exclusion volumes are not shown for clarity.

5.2 VERIFYING THE ACTIVITY OF YAN7874 (PUBLICATION II)

To utilize Yan7874 in pharmacophore modelling, its agonist activity required verification. First, we assessed the Ca^{2+} responses and PLC activation of Yan7874 in OX_1 and OX_2-expressing cells and control CHO cells (see chapter 4.2). Yan7874 induced strong and concentration-dependent Ca^{2+} elevation, and a rather small, but concentration-dependent PLC response. When tested in the presence of orexin receptor antagonist TCS-1102, G_q inhibitor UBO-QIC, or in control cells, approximately 30–40% of these responses were shown to be orexin receptor-mediated (Figure 16; see also 4.2.2 and 4.2.4). Thus, in absence of a potent non-peptide orexin receptor agonist with full efficacy, Yan7874 was a reasonable starting point for pharmacophore modelling.
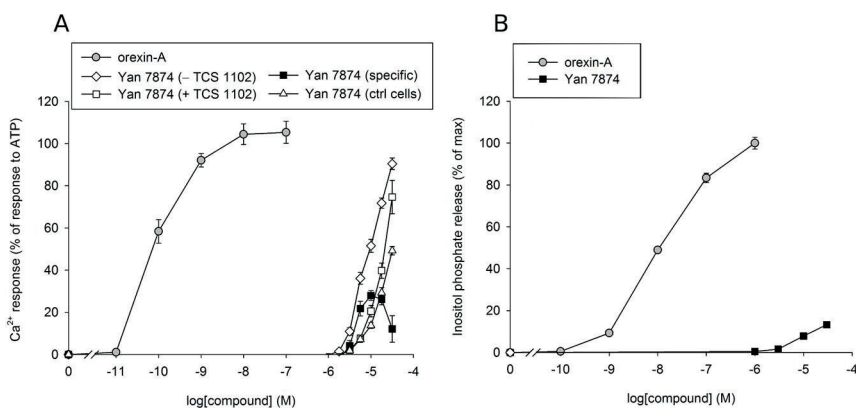

*Figure 16. A. Concentration-response curves for orexin-A and Yan7874 responses in CHO-hOX2 cells, and control CHO cells ['Yan 7874 (ctrl cells)'].
The responses are normalized to the response to 100 μM ATP to allow comparison of the Yan7874 responses in orexin receptor-expressing and non-expressing cells. Yan7874 responses are shown as such ['Yan 7874 (– TCS 1102)'], in the presence of 10 μM TCS-1102 ['Yan 7874 (+ TCS 1102)'], and as a subtraction of the latter from the former ['Yan 7874 (specific)']. B. Orexin-A and Yan7874 concentration-response curves in OX2-expressing cells normalized to the maximum response as determined by curve-fitting. The responses were normalized to the orexin-A response (100%) separately for each independent sample before averaging. n = 6.*

To characterize Yan7874 further, we assessed its G_s and G_i protein coupling by AC activation and inhibition measurements, respectively (chapter 4.2.5). Yan7874 did not couple either G_s or G_i, but caused a response mimicking mitochondrial uncoupling (an apparent increase in the AC activity, which was associated with a decrease in cellular ATP+ADP counts and an actual decrease in cellular cAMP). This suggested that Yan7874 may be cytotoxic. Thus cell growth and viability in response to Yan7874 exposure was assessed, both by visual means and quantitatively (see chapter 4.2.6). The morphological changes and the rapidity of the appearance of the toxic effects, together with the apparent decrease in the ATP levels, suggested necrotic cell death. However, the cell death driven by Yan7874 is not linked to orexin receptors, as it is equally as prominent in control cells and lacks the hallmarks of orexin receptor-mediated cell death in CHO cells (see chapter 2.3.3).

As Yan7874 drives cell death at a similar concentration range as orexin receptor activation, its usefulness as a research tool is rather limited. Also, Yan7874-mediated cell death is not mediated via orexin receptors, and thus could not be considered, for example, for development of cancer treatments.

5.3   DISCOVERY OF NOVEL OREXIN RECEPTOR MODULATORS (PUBLICATIONS I, III AND IV)

Two virtual screening campaigns were conducted to find novel orexin receptor ligands: in publication I, the pharmacophore model described in chapter 5.1 was used as a virtual screening filter, whereas in publication III a docking-based virtual screening was conducted on the crystal structure of OX_2 receptor (PDB ID: 4S0V). Both these virtual screening methods are described in detail in chapter 4.1. and the subsequent pharmacological screening in chapter 4.2.2. The screenings led to identification of orexin receptor antagonists, weak agonists, and compounds potentiating the actions of orexin-A.

5.3.1 ANTAGONISTS

In publication I we identified 21 compounds that produced over 50% inhibition of $[^{125}I]$-orexin-A, and the seven best were selected for K_i evaluation (I-8–14 in Table 3 and Figure 17). In contrast, in publication III, 12 compounds inhibited $[^{125}I]$-orexin-A binding over 30%, and K_i's were assessed for the two most promising (III-22 and III-32, Table 3 and Figure 17). All of these ligands displayed at least single-digit micromolar K_i values, the best, I-8 and I-10, reaching a nanomolar range.

Azulene (as in compounds III-22 and III-32) is an unexplored scaffold in medicinal chemistry, and only a few reports of azulene-based compounds are found in the scientific literature.[218–221] Thus, the novelty of the azulene compounds III-22 and III-32 as orexin receptor antagonists is evident. However, compounds I-8–14 are from a screening library comprising commercially available compounds, and thus some of the found ligands might resemble already known orexin receptor antagonists. The novelty of the ligands in publication I was studied using principal component analysis (PCA); I-11 and I-14 were structurally most distinct from the previously reported orexin receptor antagonists. The closest compound, instead, was I-8, which shows clear similarities to 2-SORAs (Figure 9). Even though the structure of I-8 combines different chemical scaffolds found from these antagonists, it has not been reported previously as an orexin receptor ligand.
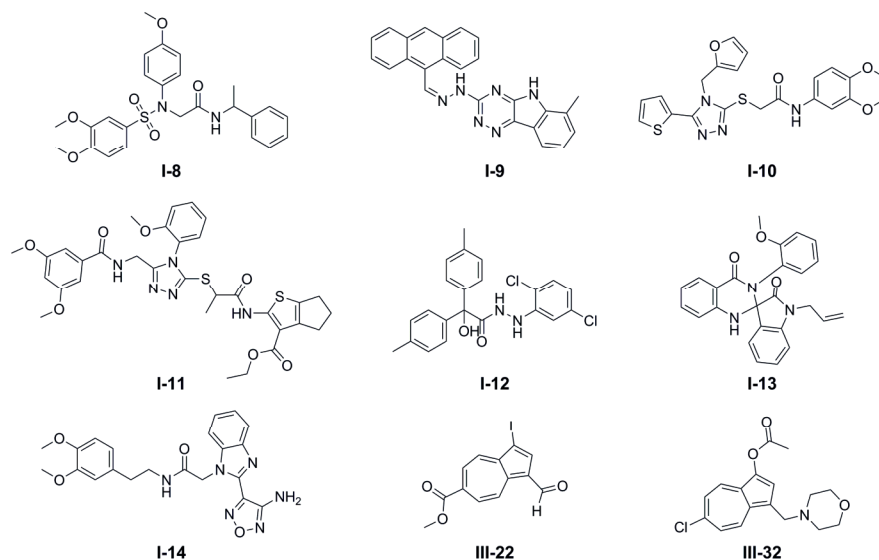
Figure 17. Antagonists identified in publications I and III.

Table 3. The K_i values of these antagonists assessed either in competition with [^{125}I]-orexin-A (binding) or as inhibition of the Ca^{2+} response to orexin-A (functional).

Compound	CHO-OX$_1$		CHO-OX$_2$	
	K_i Binding [μM]	K_i Functional [μM]	K_i Binding [μM]	K_i Functional [μM]
I-8	6.3 ± 1.2	46.7 ± 40.3	0.1 ± 0.06	0.1 ± 0.05
I-9	1.1 ± 1.0	16.2 ± 10.5	0.4 ± 0.2	11.0 ± 6.0
I-10	1.2 ± 0.1	6.0 ± 3.6	0.2 ± 0.09	0.3 ± 0.2
I-11	0.8 ± 0.2	7.0 ± 3.6	1.1 ± 0.5	1.0 ± 0.8
I-12	2.7 ± 1.6	10.3 ± 4.6	1.3 ± 0.8	1.7 ± 1.2
I-13	12.0 ± 4.4	21.6 ± 14.7	1.0 ± 0.5	1.2 ± 0.9
I-14	6.7 ± 2.4	13.1 ± 3.6	0.8 ± 0.2	0.9 ± 0.4
III-22	n.d	4.8 ± 1.8	n.d	3.6 ± 1.1
III-32	n.d	7.6 ± 2.0	n.d	8.6 ± 2.8

The K_i values of compounds I-8–14 were assessed both in the competition binding and Ca^{2+} elevation assays (Table 3). On OX_2 receptors these two methods lead generally to a similar outcome (with the exception of I-9), while on OX_1 the functional K_i values of compounds I-8–12 were notably higher than their binding assay-assessed counterparts. The reason for this is unknown, but the binding kinetics have been reported to have a role in such difference.[194] However, in the report of Mould et al. the functional K_i's were better than those from the competition binding assay, and not the reverse as in the data presented here. For compound I-9, the functional K_i values were similarly increased for both receptor subtypes, which may be due to compound-induced absorbance.

5.3.2 AGONISTS

5.3.2.1 *Identified non-peptide orexin receptor agonists*

Together with the antagonists of publications I and III, compounds with weak orexin receptor agonist activity were identified (Figure 18), and some of these compounds and their analogues were studied further in publication IV. In publication I, pharmacological screening gave rise to a set of 18 compounds, which could be potential orexin receptor agonists (i.e. they gave a signal in Ca^{2+} elevation assay, see Figure 14). Furthermore, the responses to six of these compounds were validated to be orexin receptor-mediated, and five had K_i values in the micromolar range. Two compounds are not currently disclosed, and thus their structures are not shown in Figure 18. Apart from these, the azulene studies (publications III and IV) led to a set of five compounds with orexin receptor-mediated agonist activity.
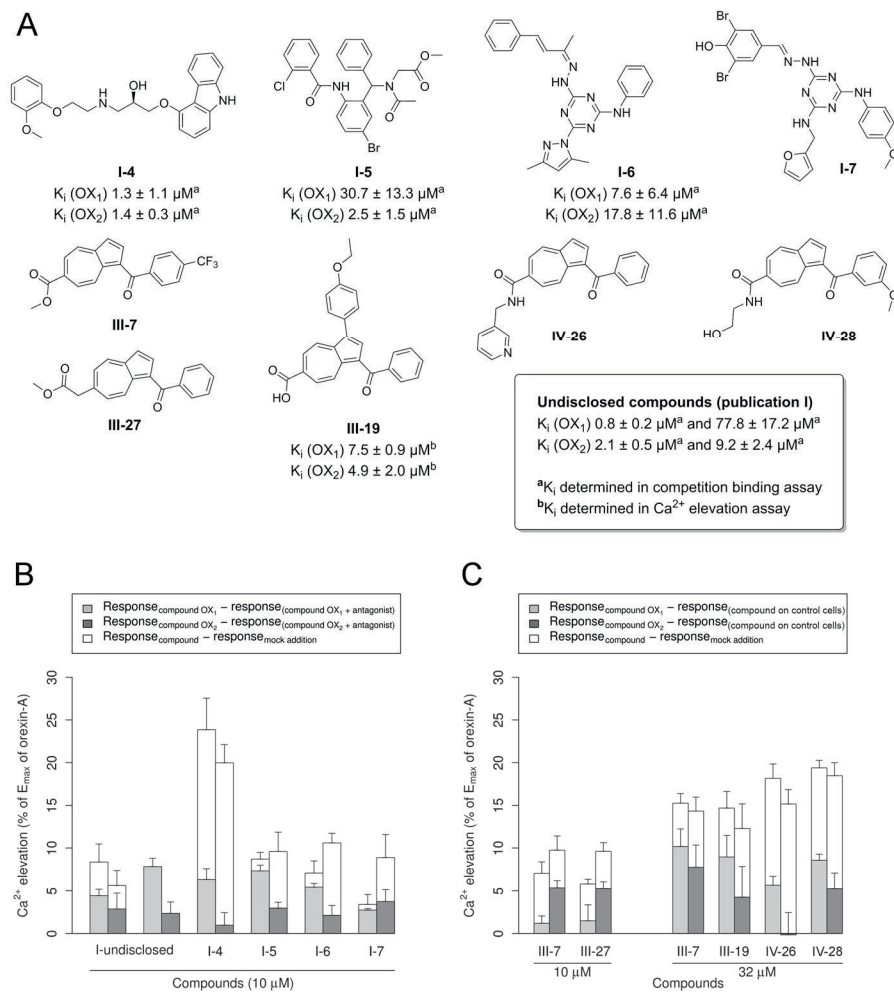
Figure 18. A. Agonistic hits of publications I, III, and IV. B and C. Total and specific Ca²⁺ responses of these hits at 10 µM (B), and 10 µM and 32 µM (C) compound concentration. Orexin-receptor-mediated responses were assessed by blockade with known antagonists (B) or in control CHO cells (C). The responses were normalized to the E_{max} of orexin-A separately before averaging. n = 3−6.

The agonist activities of these compounds are weak; at the highest concentration utilized, 10 µM in publications I and III (except III-19 a.k.a IV-37), and 32 µM in publication IV, the orexin-receptor-mediated fraction of their Ca²⁺ responses are approximately 5–10% of E_{max} of orexin-A on either one or both

receptor subtypes (Figure 18B and C). The orexin-receptor-mediated responses to azulene compounds seemed concentration-dependent (publication IV), however the solubility of these compounds unfortunately prevented full saturation. Unlike the other compounds, IV-26 was more active at 18 µM than at 32 µM concentration—at 18 µM concentration the orexin receptor-mediated activities were 7.4 ± 1.9% and 5.4 ± 1.5% of E_{max} of orexin-A on OX_1 and OX_2, respectively (publication IV).

Interestingly, compound III-19 did not show any Ca^{2+} response at 10 µM concentration, but at 32 µM an orexin-receptor-mediated response of approximately 10% on OX_1 (Figure 18), and at 45 µM approximately 20% on both receptor subtypes was detected (publication IV). This response is almost of a similar magnitude to the maximum response to Yan7874 (Figure 16), however the III-19 concentration required for the response is somewhat 4-fold higher than that of Yan7874. Additionally, also III-19 had K_i values at the micromolar level (Figure 18A).

5.3.2.2 *Insights into orexin receptor activation*

Even though the identified agonists are weak, their structural diversity offers new insights into orexin receptor activation. The only known non-peptide orexin-receptor agonist with full efficacy is Nag26, and although the structural optimization of it led to a set of compounds with weaker orexin-receptor-agonist activities, they are structurally really similar to each other (only small alterations of A- and B-ring substituents are reported in [165]). Thus, deriving a bigger picture of the molecular features required for orexin-receptor activation based only on Nag26 analogues is challenging.
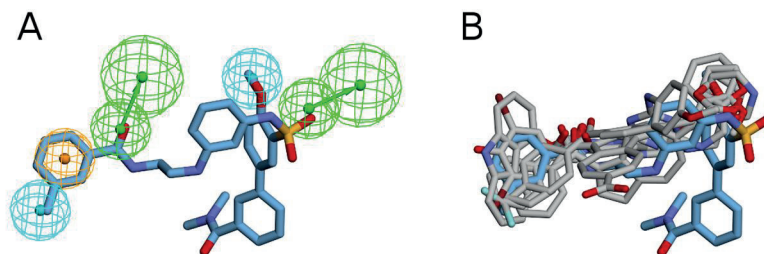
Figure 19. A. A pharmacophore describing the active ligands and the B ring fraction of Nag26 (cobalt blue). B. Active ligands (grey sticks) and Nag26 superimposed by the pharmacophore. Hydrogen bond acceptor: green, aromatic feature: brown, hydrophobic feature: cyan, nitrogen: blue, oxygen: red, sulphur: yellow, fluorine: light blue.

When studying the structures of the agonistic hit compounds, some similarities are evident; all of the compounds seem to have a (semi)aromatic core structure, polar linker regions, and aromatic group(s) in the far ends (Figure 18A). Additionally, at least one of these aromatic groups has a polar functionality. When these similarities were rationalized to a pharmacophore, it not only mapped all the active azulenes and compounds I-4 and I-7, but also the B-ring end of Nag26 (Figure 19). In the structure of Yan7874, instead, there is a chlorine atom mapping on top of one of the acceptor features, and thus it is not retrieved by the pharmacophore. However, the electron cloud of chlorine is capable of forming a halogen bond with hydrogen-bond donors, and thus the pharmacophore could be concluded to describe also Yan7874. This pharmacophore does thus represent 9/11 active ligands, and additionally, it rules out 35/42 inactive compounds (see publication IV).

Interestingly, the similar pharmacophoric features represented in Figure 19 can be mapped also on the A-ring end of Nag26. When done so, I-4, I-5, I-7, III-19, IV-26, and IV-28 are retrieved (i.e. 8/11 actives, if including Yan7874), and 33/42 inactive azulene compounds are ruled out. The azulene-based hits are especially small compounds barely reaching both ends of the described pharmacophores, a Nag26 molecule could

actually be mimicked by two of them, for example by overlaying one IV-28 molecule on the A-ring and another IV-28 molecule on the B-ring of Nag26.

Apart from pharmacophoric representations, we studied the agonist compounds by molecular docking (Figure 20; publication I; see also retrospective docking in chapter 4.1.2). When docked to the OX_2 crystal structure, all binding poses of the studied agonists overlap partially with that of the co-crystallized suvorexant (Figure 20). Compared to suvorexant, Nag26 presents an extended binding mode reaching towards a pocket between TM5 and TM6 (A-ring), and TM6 and TM7 (above the binding site of suvorexant; B-ring; Figure 20B). Yan7874 and III-19 also reach towards TM5 and TM6, but as much smaller molecules than Nag26 they do not extend towards the TM6–TM7 pocket (Figure 20C and D). Apart from the representative poses selected by the Glide gscore, however, both of these smaller ligands also show binding modes, wherein they have flipped around their vertical axes, or reach towards the TM6–TM7 pocket and not that between TM5 and TM6

All the representative poses of the agonist ligands can form a hydrogen bond with Gln[3.32] (sulphonamide oxygen of Nag26, hydroxyl group of Yan7874, and carbonyl group of III-19). It is noteworthy that the sulphonamide group of Nag26 docks approximately to the same location in the binding site than that of EMPA in the OX_2 crystal structure (one of the sulphonamide oxygens is within 4.0 Å distance from Thr[3.33]). However, the other sulphonamide oxygen of Nag26 is interacting with Gln[3.32], while that of EMPA interacts with Gln[4.60]. According to Nagahara et al., the secondary sulphonamide is crucial for the agonist activity of Nag26—in the structure of 2-SORA EMPA the sulphonamide is tertiary, and its conformational space is thus more restrained than that of Nag26. The secondary sulphonamide allows the Nag26 molecule to adopt the bent conformation observed in the docking studies (publication I and [165,166]); also the inactivity of the corresponding amide derivative of Nag26 suggests the importance of the bent conformation.[165] Additionally, the secondary sulphonamide nitrogen might be

important for not only allowing but also stabilizing the bent conformation of Nag26, for example via water-mediated intramolecular hydrogen bonds with the methoxy-oxygen of the A-ring or a carbonyl oxygen of the B-ring region of the compound.
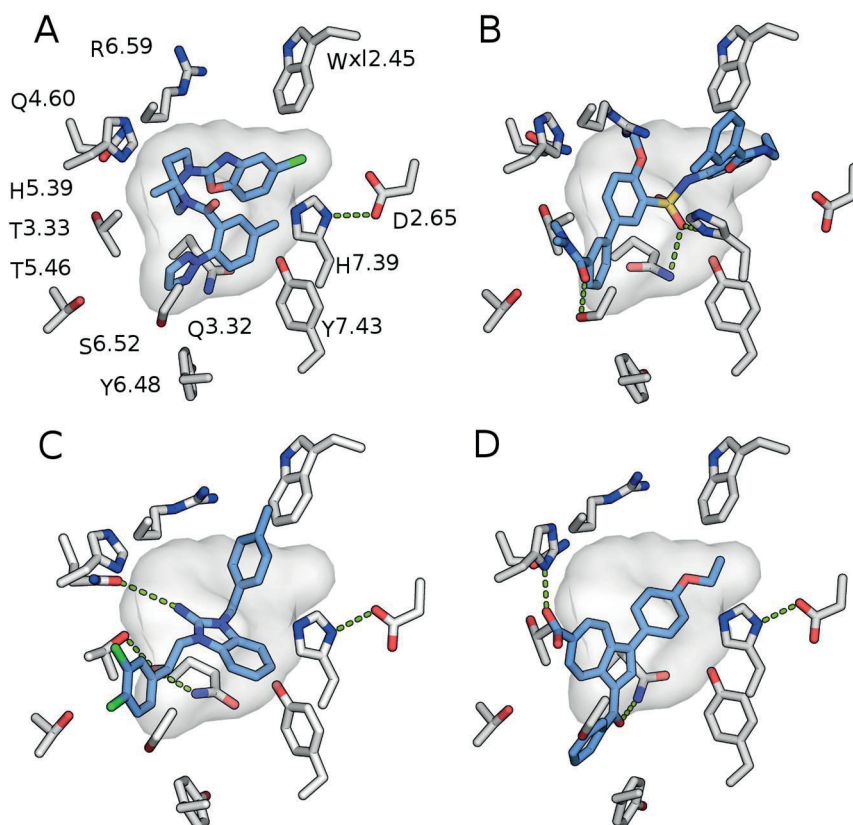
Figure 20. A. Suvorexant in complex with OX₂. B–D. Docking poses of Nag26 (B), Yan7874 (C), and III-19 (D). View from TM6, colour code as in Figure 12. The binding site water molecules are not shown for clarity.

The docking pose of Nag26 also forms a hydrogen bond with His[7.39], which flips the His[7.39] side chain away from Asp[2.65] breaking a salt bridge between TM2 and TM7. Yan7874 and III-19 could also interact with His[7.39] (aromatic π–π interaction).

The tight interactions between the agonist ligands of β_2-adrenoceptor and amino acid residues 3.32 and 7.39 are commonly observed in the corresponding crystal structures (chapter 2.1.3). Apart from these, Yan7874 can form hydrogen bonds with Thr[3.33] (hydroxyl group) and Gln[4.60] (primary amine), whereas III-19 can hydrogen bond with His[5.39] (carboxyl group). The Thr[3.33] interaction tightens the contact with TM3, and also might explain the slight OX_2 selectivity of Yan7874. In the antagonist-bound structure, His[5.39] forms a salt bridge with Glu[xl2.52] (of the β-hairpin), and interacting with His[5.39] could disturb that contact. These ligands can also interact with Tyr[6.48] (aromatic $\pi-\pi$ interaction), which is located in one of the suggested microswitch motifs of GPCR activation (Table 1).

Nag26, Yan7874, and III-19 could also interact with Ser[6.52], by a hydrogen bond (Nag26), a halogen bond (Yan7874), or an electron-deficient edge of the benzoyl group (III-19). Nag26 interacts with Ser[6.52] by its amide carbonyl functionality at the A-ring-end of the compound. The A-ring analogues of Nag26 (in Table 1 of [165]) highlight the importance of the amide carbonyl functionality in that region; amine- or methoxy-substituted phenyl groups, as well as non-substituted phenyl group as A-ring substituents led to a notable drop in both EC_{50} and E_{max}.

If the TM5 would move slightly towards the binding site, as is suggested to happen upon activation of many GPCRs, Thr[5.46] would also be within reach to interact with these ligands (similar interactions as with Ser[6.52]). Interaction with an amino acid in position 5.46 is observed in the crystal structures of β_2 agonists. Angiotensin receptors also demonstrate the importance of the pocket between TM5 and TM6. Olmesartan, an inverse agonist of angiotensin receptors, can be converted into an agonist by growing the ligand (Figure 21A; reviewed in [11]). Interestingly, the crystal structure of olmesartan in complex with AT_2 indicates that the added phenyl group would indeed reach towards the TM5–TM6 pocket (Figure 21A–C).[222]
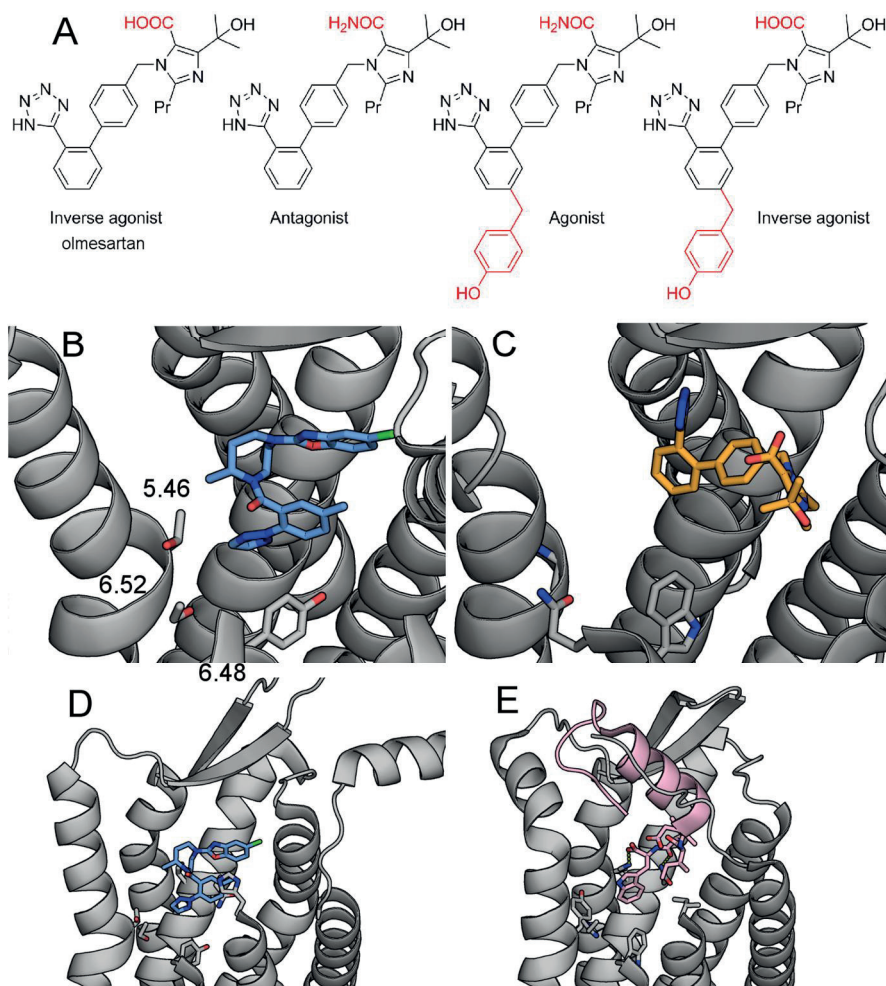
Figure 21. A. AT₁ receptor ligands presented as in [11]. B. OX₂ in complex with suvorexant (cobalt blue). C. AT₂ in complex with olmesartan (orange). D. A zoom-out of OX₂–suvorexant (cobalt blue) complex. E. ETB in complex with endothelin 1 (rose). Receptors are shown as grey cartoon; cartoon between positions 6.50–7.39 (B and C) and 6.48–7.39 (D and E) is hidden for clarity. Blue is nitrogen, red is oxygen, and green is chlorine. View as in Figure 12.

Apart from β_2 and angiotensin receptor agonists, endothelin 1 (ET_1; a peptide agonist) in complex with ET_B receptor also reaches towards TM5 and TM6 (Figure 21D and E) and interacts with amino acids in positions 3.32, 3.33, and 7.39. Interestingly, the C-terminus of ET_1 is non-helical, both in solution and when

binding to its cognate receptor.[37,223] Even though the C-terminals of orexin peptides are helical in solution, it is possible that they could also bind in such an extended conformation. Additionally, the ET_1–ET_B provides insights into the interactions involving the β-hairpin and N-terminus of the receptor; the helical part of the peptide-ligand sandwiches between these two regions (Figure 21E). As both N-terminal helix and the β-hairpin region of orexin receptors have been shown to be important for the binding/recognition of orexin-A, it is highly possible that these regions sandwich orexin-A the same way. Additionally, the TM6–TM7 pocket corresponding to the one above the binding site of suvorexant is occupied by the side chains of the helical part of ET_1, and it could be possible that a ligand (e.g. Nag26) occupying this pocked would interact with the N-terminus of the receptor as ET_1 does.

Altogether, these findings suggest the importance of three regions in the orexin receptor binding site in terms of receptor activation: (1) the 'antagonist binding site', and interactions between the ligand, TM3 and TM7, (2) the TM5–TM6 region, wherein the interaction network would be tightened by the inward movement of TM5, and (3) the TM6–TM7 region, approximately one helical turn upward from $His^{7.39}$, and with a possible interaction with the N-terminal helix of the receptor. Of the orexin receptor agonists discussed here, only Nag26 can occupy all these regions simultaneously.

5.3.3   COMPOUNDS POTENTIATING THE ACTIONS OF OREXIN-A

In general, GPCR agonists and antagonists can be structurally similar to each other (reviewed in [11]), and thus it felt only reasonable that finding one of these ligand types among structurally similar compounds lead to finding of the other. However, it was a bit unexpected to also identify compounds, which potentiated the actions of orexin-A (both binding and the functional Ca^{2+} response), as such ligands are typically considered to bind to another, allosteric, binding site (reviewed

in [14]). In Rhodopsin family GPCRs these allosteric sites can be in close proximity to the orthosteric binding sites though, and, for example, in CCR5 chemokine receptor (CCR5) and M_2, the allosteric ligands are binding just above the orthosteric pocket (i.e. the TM6–TM7 region discussed above; reviewed in [224]). Additionally, the only previously reported series of orexin receptor potentiators was also found while screening for orexin receptor antagonists.[199]
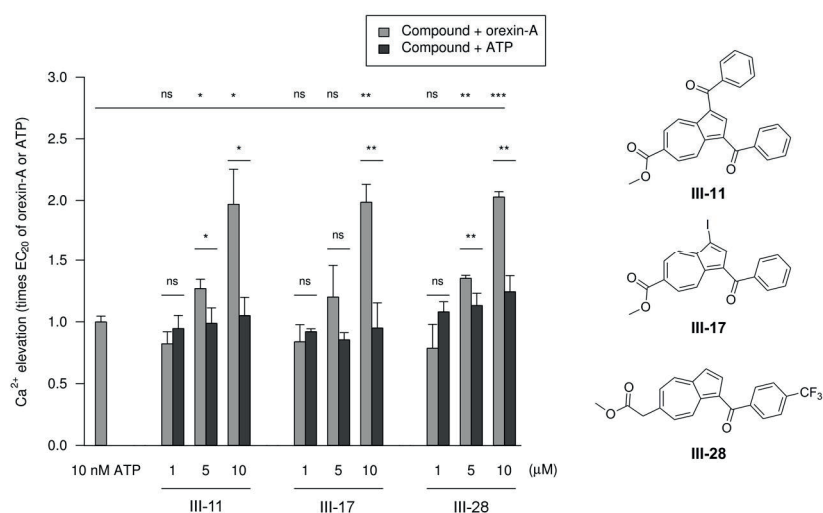

Figure 22. The effects of three most promising OX_1 receptor potentiators on the Ca^{2+} responses elicited by 0.02–0.03 nM orexin-A and 60 nM ATP (corresponding to the EC_{20} of each ligand; publication III). The responses were separately normalized to the control orexin-A or ATP responses, respectively, for each independent experiment before averaging. The significances were calculated as compared with the corresponding control. ns (not significant) $P > 0.05$, $*P < 0.05$, $**P < 0.01$, $***P < 0.001$; $n = 3−4$.

In publication III we identified a set of 12 compounds, which potentiated the binding of [^{125}I]-orexin-A in the competition binding assay. Of these, two compounds acted as weak agonists, which could lead to such a phenomenon (via e.g. receptor dimers, see below), however, the effects of the other ten could

not be explained. When studied further in the Ca^{2+} elevation assay, all these compounds, except III-19 (which was shown later to be an orexin receptor agonist at higher concentrations), potentiated the response to orexin-A, and eight of them did not trigger measurable Ca^{2+} elevation on their own. The most effective potentiators, III-11, III-17, and III-28 potentiated the Ca^{2+} response to a small, sub-EC_{50}, concentration of orexin-A approximately two-fold on OX_1 receptors (Figure 22). Additionally, none of them potentiated the effects of ATP, when studied similarly to orexin-A potentiation, indicating that the observed potentiation was orexin receptor-mediated.

To determine whether the azulene-scaffold had a crucial role to the observed potentiation effect, we studied also a set of indole-scaffolded compounds (publication IV). Interestingly, these indole analogues highlighted the importance of the location of the ester functionality in respect of the methoxybenzoyl moiety; the more linear IV-31 and IV-34 over-performed their bent counterparts. However, the tri-substituted indoles representing III-11 showed the most promising activity (approximately 1.7-fold).

In general, potentiating the actions of an endogenous ligand is a rather complex phenomenon, and currently it is not fully understood. In addition to the allosteric modulators discussed above (binding either to the nearby or distinct allosteric binding sites), the possible effectors are acting directly via receptor dimerization/oligomerization, and indirect effects affecting the orexin-A binding and the downstream signalling machinery (e.g. via Ca^{2+} levels, see 2.3.1.4).

In case of potentiating the actions of orexin-A, a few enlightening pieces of information are available. First, at low concentrations orexin-A displays self-potentiation (positive cooperativity) in the competition binding assay,[97] and a similar phenomenon was also evident with the agonist ligands (e.g. I-7 and III-7). Considering that the orexin-A peptide occupies a single site at each receptor, the self-potentiation of orexin-A binding most likely occurs through receptor dimers or oligomers, which orexin receptors have shown to form at least

in expression systems (chapter 2.3.2). Noteworthy, acting via receptor dimers would mean that also the small molecular potentiators bind to the orthosteric binding site (reviewed e.g. in [14]).

Secondly, extracellular Ca^{2+} levels affect the binding of orexin-A possibly via an allosteric Ca^{2+} binding site (see chapter 2.3.1.4). There is reported to be an allosteric Na^+ binding site in most of the Rhodopsin family GPCRs, however, OX_2 receptors have been shown to lack this (chapter 2.2.3). Additionally, molecular modelling of the OX_1–orexin-A complex[198] suggests that the His26 of orexin-A clusters close to $His^{7.39}$ and $Asp^{2.65}$, which is rather interesting, as histidine/aspartic acid clusters are known to participate in the hexahedral coordination of metal ions. However, the Ca^{2+} elevation to cytosol, caused by the agonistic ligands, cannot affect the orexin-A binding if efflux does not occur, so possibly the binding effect of extracellular Ca^{2+} is not the phenomenon dealt with here.

Thirdly, intracellular Ca^{2+} levels affect the downstream signalling effects, possibly by complexation with the receptor-G protein complex (chapter 2.3.1.4). This leads to potentiation of the detected functional responses to orexin-A (such as those mediated by PLC and AC pathways). Potentiated PLC activation affects the Ca^{2+} response detected in our assay, and represents the least interesting type of potentiation in light of the compounds tested (as it is not targeting orexin receptors). To rule out the effect of intracellular Ca^{2+}, we employed ATP controls, which mimicked the Ca^{2+} elevation of the tested ligands (10 nM ATP in case of compounds not triggering Ca^{2+} elevation, Figure 22). Thus, it is liable that the compounds potentiating the Ca^{2+} response to orexin-A significantly more than the ATP control, are acting via orexin receptors.

6 CONCLUSIONS AND FUTURE DIRECTIONS

This investigation demonstrates that molecular modelling can be utilized in finding novel ligands, also in circumstances where the amount of background knowledge is rather modest. With computer-aided methods, we succeeded to rationalise the orexin receptor binding and activation attributes and construct a pharmacophore model, which led to the identification of novel orexin receptor ligands, both antagonists with binding affinities at 0.1–1 μM range and weak agonists; the corresponding hit rates were 1.7% and 1.5%, respectively. Additionally, 30/395 of the pharmacophore-based virtual screening hits inhibited [125I]-orexin-A binding over 30% giving an overall hit rate of 7.6% for orexin receptor ligands. This demonstrates the power of the integrated screening procedure, even though the lack of precise data of the hit rates of HTS campaigns prevents a fair comparison.

The insights into orexin receptor activation provided by these compounds aided the identification of a novel set of azulene-based orexin receptor agonists with concentration-dependent activities and accessibility to further modifications by in-house chemistry. Additionally, novel antagonists and orexin receptor potentiators were identified. For the azulene screening, the hit rates were even higher: 39% for antagonists (over 30% inhibition of [125I]-orexin-A binding), 19% for potentiators, and 9.7% for agonists leading to approximately 68% hit rate for orexin receptor ligands. Even though the number sounds high, it is in line with the reported hit rates of virtual screenings for other GPCR ligands, such as those targeting β_2, A_{2A}, and CXCR4, as well as H_1 histamine and D_3 dopamine receptors (20–70% hit rates; reviewed in [32]). It should be noted, though, that hit rates can be defined using different success criteria, which heavily affect the final numbers.

In the future, much remains to be understood regarding orexin receptor activation, as well as the potentiation of the

actions of orexin-A. From the computational chemistry/molecular modelling point of view, one missing link is all-atom molecular dynamic simulations with full receptor structures and agonist ligands (Nag26, orexin-A, orexin-B) to provide insights into conformational changes occurring during orexin receptor activation. Additionally, as crystal structures of active GPCRs are available, homology modelling could be utilized to build a model of an active orexin receptor conformation, which would then be a target for molecular docking or MD studies.

From the medicinal chemistry/compound design point of view, the next step would be testing the pharmacophore hypothesis of two small ligands mimicking the features of Nag26 by studying di-azulene-scaffolded compounds, e.g. by bridging some of the current hits. The two undisclosed agonist hits from publication I should also undergo structural optimization. From the molecular biology angle, instead, the orexin receptor point mutations in regions suggested important for Nag26-mediated orexin receptor activation (TM5–TM6 and upper TM6–TM7 pockets) would indeed be interesting. These point mutations, especially in the TM6–TM7 region could also provide insights into the action of the identified potentiators. Finally, understanding the pharmacology of the orexin receptor activation and potentiation, and especially the effects of receptor dimerization/oligomerization, would be particularly helpful. Utilizing radiolabelled antagonist, such as [^{3}H]-almorexant instead of [^{125}I]-orexin-A, in the competition binding assay would possibly aid the understanding the potentiation effect mediated by our compounds.

The field of orexin research has evolved dramatically during the time frame of these studies, and knowledge of orexin receptor binding and activation has similarly expanded. Especially the solved orexin receptor crystal structures and identification of Nag26 have opened new possibilities, not only in computational drug discovery but also in understanding the phenomenon at hand. With such an accelerating trend, it feels

indeed possible that one day the field reaches the understanding of orexin receptor activation.

7 REFERENCES

(1)   Putula, J.; Turunen, P. M.; Johansson, L.; Näsman, J.; Ra, R.; Korhonen, L.; Kukkonen, J. P. Orexin/Hypocretin Receptor Chimaeras Reveal Structural Features Important for Orexin Peptide Distinction. *FEBS Lett.* **2011**, *585* (9), 1368–1374.

(2)   Foord, S. M.; Bonner, T. O. M. I.; Neubig, R. R.; Rosser, E. M.; Pin, J.; Davenport, A. P.; Spedding, M.; Harmar, A. J. International Union of Pharmacology. XLVI. G Protein-Coupled Receptor List. *Pharmacol. Rev.* **2005**, *57* (2), 279–288.

(3)   IUPHAR/BPS Guide to PHARMACOLOGY. G protein-coupled receptors. http://www.guidetopharmacology.org/GRAC/FamilyDisplayForwar d?familyId=694. (accessed Feb 2, 2018).

(4)   Vassilatis, D. K.; Hohmann, J. G.; Zeng, H.; Li, F.; Ranchalis, J. E.; Mortrud, M. T.; Brown, A.; Rodriguez, S. S.; Weller, J. R.; Wright, A. C.; Bergmann, J. E.; Gaitanaris, G. a. The G Protein-Coupled Receptor Repertoires of Human and Mouse. *Proc. Natl. Acad. Sci. U. S. A.* **2003**, *100* (8), 4903–4908.

(5)   Hauser, A. S.; Attwood, M. M.; Rask-Andersen, M.; Schiöth, H. B.; Gloriam, D. E. Trends in GPCR Drug Discovery: New Agents, Targets and Indications. *Nat. Rev. Drug Discov.* **2017**, *16* (12), 829–842.

(6)   Fredriksson, R. The G-Protein-Coupled Receptors in the Human Genome Form Five Main Families. Phylogenetic Analysis, Paralogon Groups, and Fingerprints. *Mol. Pharmacol.* **2003**, *63* (6), 1256–1272.

(7)   Schiöth, H. B.; Fredriksson, R. The GRAFS Classification System of G-Protein Coupled Receptors in Comparative Perspective. *Gen. Comp. Endocrinol.* **2005**, *142* (1–2 SPEC. ISS.), 94–101.

(8)   Nordström, K. J. V; Sällman Almén, M.; Edstam, M. M.; Fredriksson, R.; Schiöth, H. B. Independent HHsearch, Needleman–Wunsch-Based, and Motif Analyses Reveal the Overall Hierarchy for Most of the G Protein-Coupled Receptor Families. *Mol. Biol. Evol.* **2011**, *28* (9), 2471–2480.

(9)   Munk, C.; Isberg, V.; Mordalski, S.; Harpsøe, K.; Rataj, K.; Hauser, A. S.; Kolb, P.; Bojarski, A. J.; Vriend, G.; Gloriam, D. E. GPCRdb: The G Protein-Coupled Receptor Database – an Introduction. *Br. J. Pharmacol.* **2016**, *173* (14), 2195–2207.

(10)   Overington, J. P.; Al-Lazikani, B.; Hopkins, A. L. How Many Drug Targets Are There? *Nat. Rev. Drug Discov.* **2006**, *5* (12), 993–996.

(11)   Dosa, P. I.; Amin, E. A. Tactical Approaches to Interconverting GPCR Agonists and Antagonists. *J. Med. Chem.* **2016**, *59* (3), 810–840.

(12)   Williams, D. A.; Lemke, T. L. Drugs Affecting Adrenergic Neurotransmission. In *Foye's Principles of Medicinal Chemistry*; Lippincott Williams 6 Wilkins, 2002; pp 292–314.

(13)   Fujioka, M.; Omori, N. Subtleties in GPCR Drug Discovery: A Medicinal Chemistry Perspective. *Drug Discov. Today* **2012**, *17* (19–20), 1133–1138.

(14)   Wootten, D.; Christopoulos, A.; Sexton, P. M. Emerging Paradigms in GPCR Allostery: Implications for Drug Discovery. *Nat. Rev. Drug Discov.* **2013**, *12* (8), 630–644.

(15)   Shonberg, J.; Lopez, L.; Scammells, P. J.; Christopoulos, A.; Capuano, B.; Lane, J. R. Biased Agonism at G Protein-Coupled Receptors: The Promise and the Challenges-A Medicinal Chemistry Perspective. *Med. Res. Rev.* **2014**, *34* (6), 1286–1330.

(16)   Shonberg, J.; Kling, R. C.; Gmeiner, P.; Löber, S. GPCR Crystal Structures: Medicinal Chemistry in the Pocket. *Bioorganic Med. Chem.* **2015**, *23* (14), 3880–3906.

(17)   Lane, J. R.; Sexton, P. M.; Christopoulos, A. Bridging the Gap: Bitopic Ligands of G-Protein-Coupled Receptors. *Trends Pharmacol. Sci.* **2013**, *34* (1), 59–66.

(18)   Shonberg, J.; Scammells, P. J.; Capuano, B. Design Strategies for Bivalent Ligands Targeting GPCRs. *ChemMedChem* **2011**, *6* (6), 963–974.

(19)   Oldham, W. M.; Hamm, H. E. Heterotrimeric G Protein Activation by G-Protein-Coupled Receptors. *Nat. Rev. Mol. Cell Biol.* **2008**, *9* (1), 60–71.

(20)   Oldham, W. M.; Hamm, H. E. Structural Basis of Function in Heterotrimeric G Proteins. *Q. Rev. Biophys.* **2006**, *39* (2), 117–166.

(21)   Hepler, J. R.; Gilman, a G. G Proteins. *Trends Biochem. Sci.* **1992**, *17* (October), 383–387.

(22)   Kristiansen, K. Molecular Mechanisms of Ligand Binding, Signaling, and Regulation within the Superfamily of G-Protein-Coupled Receptors: Molecular Modeling and Mutagenesis Approaches to Receptor Structure and Function. *Pharmacol. Ther.* **2004**, *103* (1), 21–80.

(23)   Hilger, D.; Masureel, M.; Kobilka, B. K. Structure and Dynamics of GPCR Signaling Complexes. *Nat. Struct. Mol. Biol.* **2018**, *25* (1), 4–12.

(24)   Lambert, N. A. Dissociation of Heterotrimeric G Proteins in Cells. *Sci. Signal.* **2008**, *1* (25), re5 LP-re5.

(25)   Simon, M. I.; Strathmann, M. P.; Gautam, N. Diversity of G Proteins in Signal Transduction. *Science (80-.).* **1991**, *252* (1971), 802–808.

(26)   Iyengar, R.; Hildebrandt, J. D. G Protein Pathways. Part A, Receptors. *Science (80-.).* **2002**, *296*, 1636–1639.

References

(27) Pierce, K. L.; Premont, R. T.; Lefkowitz, R. J. Seven-Transmembrane Receptors. *Nat. Rev. Mol. Cell Biol.* **2002**, *3* (9), 639–650.

(28) Kukkonen, J. P. Orexin/Hypocretin Signaling. In *Behavioral Neuroscience of Orexin/Hypocretin. Current Topics in Behavioral Neurosciences*; Lawrence, A., de Lecea, L., Eds.; Springer, Cham, 2017.

(29) Kukkonen, J. P.; Leonard, C. S. Orexin / Hypocretin Receptor Signalling Cascades. *Br. J. Pharmacol.* **2014**, *171*, 314–331.

(30) Kukkonen, J. P. Physiology of the Orexinergic/Hypocretinergic System: A Revisit in 2012. *AJP Cell Physiol.* **2013**, *301*, 2–32.

(31) Shenoy, S. K.; Lefkowitz, R. J. B-Arrestin-Mediated Receptor Trafficking and Signal Transduction. *Trends Pharmacol. Sci.* **2011**, *32* (9), 521–533.

(32) Katritch, V.; Cherezov, V.; Stevens, R. C. Structure-Function of the G Protein–Coupled Receptor Superfamily. *Annu. Rev. Pharmacol. Toxicol.* **2013**, *53*, 531–556.

(33) Venkatakrishnan, A. J.; Deupi, X.; Lebon, G.; Heydenreich, F. M.; Flock, T.; Miljus, T.; Balaji, S.; Bouvier, M.; Veprintsev, D. B.; Tate, C. G.; Schertler, G. F. X.; Babu, M. M. Diverse Activation Pathways in Class A GPCRs Converge near the G-Protein-Coupling Region. *Nature* **2016**, *536* (7617), 484–487.

(34) Huang, W.; Manglik, A.; Venkatakrishnan, a J.; Laeremans, T.; Feinberg, E. N.; Sanborn, A. L.; Gmeiner, P.; Kato, H. E.; Livingston, K. E.; Thorsen, T. S.; Kling, R. C.; Husbands, S. M.; Traynor, J. R.; Weis, W. I.; Steyaert, J.; Dror, R. O.; Kobilka, B. K. Structural Insights into Mu-Opioid Receptor Activation. *Nature* **2015**, *524*, 315–321.

(35) Kruse, A. C.; Ring, A. M.; Manglik, A.; Hu, J.; Hu, K.; Eitel, K.; Hübner, H.; Pardon, E.; Valant, C.; Sexton, P. M.; Christopoulos, A.; Felder, C. C.; Gmeiner, P.; Steyaert, J.; Weis, W. I.; Garcia, K. C.; Wess, J.; Kobilka, B. K. Activation and Allosteric Modulation of a Muscarinic Acetylcholine Receptor. *Nature* **2013**, *504* (7478), 101–106.

(36) Zhang, H.; Han, G. W.; Batyuk, A.; Ishchenko, A.; White, K. L.; Patel, N.; Sadybekov, A.; Zamlynny, B.; Rudd, M. T.; Hollenstein, K.; Tolstikova, A.; White, T. A.; Hunter, M. S.; Weierstall, U.; Liu, W.; Babaoglu, K.; Moore, E. L.; Katz, R. D.; Shipman, J. M.; Garcia-Calvo, M.; Sharma, S.; Sheth, P.; Soisson, S. M.; Stevens, R. C.; Katritch, V.; Cherezov, V. Structural Basis for Selectivity and Diversity in Angiotensin II Receptors. *Nature* **2017**, *544* (7650), 327–332.

(37) Shihoya, W.; Nishizawa, T.; Okuta, A.; Tani, K.; Dohmae, N.; Fujiyoshi, Y.; Nureki, O.; Doi, T. Activation Mechanism of Endothelin ET B Receptor by Endothelin-1. *Nature* **2016**, *537* (7620), 363–368.

(38) White, J. F.; Noinaj, N.; Shibata, Y.; Love, J.; Kloss, B.; Xu, F.; Gvozdenovic-Jeremic, J.; Shah, P.; Shiloach, J.; Tate, C. G.;

Grisshammer, R. Structure of the Agonist-Bound Neurotensin Receptor. *Nature* **2012**, *490* (7421), 508–513.

(39) Wang, C.; Jiang, Y.; Ma, J.; Wu, H.; Wacker, D.; Katritch, V.; Han, G. W.; Liu, W.; Huang, X.-P.; Vardy, E.; McCorvy, J. D.; Gao, X.; Zhou, X. E.; Melcher, K.; Zhang, C.; Bai, F.; Yang, H.; Yang, L.; Jiang, H.; Roth, B. L.; Cherezov, V.; Stevens, R. C.; Xu, H. E. Structural Basis for Molecular Recognition at Serotonin Receptors. *Science (80-.).* **2013**, *340* (6132), 610–614.

(40) Rasmussen, S. G. F.; Devree, B. T.; Zou, Y.; Kruse, A. C.; Chung, K. Y.; Kobilka, T. S.; Thian, F. S.; Chae, P. S.; Pardon, E.; Calinski, D.; Mathiesen, J. M.; Shah, S. T. A.; Lyons, J. A.; Caffrey, M.; Gellman, S. H.; Steyaert, J.; Skiniotis, G.; Weis, W. I.; Sunahara, R. K.; Kobilka, B. K. Crystal Structure of the β 2 Adrenergic Receptor-Gs Protein Complex. *Nature* **2011**, *477* (7366), 549–557.

(41) Vogel, R.; Mahalingam, M.; Lüdeke, S.; Huber, T.; Siebert, F.; Sakmar, T. P. Functional Role of the "Ionic Lock"-An Interhelical Hydrogen-Bond Network in Family A Heptahelical Receptors. *J. Mol. Biol.* **2008**, *380* (4), 648–655.

(42) Katritch, V.; Fenalti, G.; Abola, E. E.; Roth, B. L.; Cherezov, V.; Stevens, R. C. Allosteric Sodium in Class A GPCR Signaling. *Trends Biochem. Sci.* **2014**, *39* (5), 233–244.

(43) Katritch, V.; Reynolds, K. a; Cherezov, V.; Hanson, M. a; Roth, C. B.; Yeager, M.; Abagyan, R. Analysis of Full and Partial Agonists Binding to Beta2-Adrenergic Receptor Suggests a Role of Transmembrane Helix V in Agonist-Specific Conformational Changes. *J. Mol. Recognit.* **2009**, *22* (4), 307–318.

(44) de Lecea, L.; Kilduff, T. S.; Peyron, C.; Gao, X.-B.; Foye, P. E.; Danielsson, P. E.; Fukuhara, C.; Battenberg, E. L. F.; Gautvik, V. T.; Bartlett II, F. S.; Frankel, W. N.; Van Den Pol, A. N.; Bloom, F. E.; Gautvik, K. M.; Sutcliffe, J. G. The Hypocretins : Hypothalamus-Specific Peptides with Neuroexcitatory Activity. *Proc. Natl. Acad. Sci.* **1998**, *95*, 322–327.

(45) Sakurai, T.; Amemiya, A.; Ishii, M.; Matsuzaki, I.; Chemelli, R.; Tanaka, H.; Williams, S.; Richardson, J.; Kozlowski, G.; Wilson, S.; Arch, J.; Buckingham, R.; Haynes, A.; Carr, S.; Annan, R.; McNulty, D.; Liu, W.-S.; Terret, J.; Elshourbagy, N.; Bergsma, D.; Yanagisawa, M. Orexins and Orexin Receptors: A Family of Hypothalamic Neuropeptides and G Protein-Coupled Receptors That Regulate Feeding Behavior. *Cell* **1998**, *92* (4), 573–585.

(46) Takai, T.; Takaya, T.; Nakano, M.; Akutsu, H.; Nakagawa, A.; Aimoto, S.; Nagai, K.; Ikegami, T. Orexin-A Is Composed of a Highly Conserved C-Terminal and a Specific, Hydrophilic N-Terminal Region, Revealing the Structural Basis of Specific Recognition by the Orexin-1 Receptor. *J. Pept. Sci.* **2006**, *12* (7), 443–454.

(47)   Lee, J.-H.; Bang, E.; Chae, K.-J.; Kim, J.-Y.; Lee, D. W.; Lee, W. Solution Structure of a New Hypothalamic Neuropeptide, Human Hypocretin-2/Orexin-B. *Eur. J. Biochem.* **1999**, *266* (3), 831–839.

(48)   Ammoun, S.; Holmqvist, T.; Shariatmadari, R.; Oonk, H. B.; Detheux, M.; Parmentier, M.; Åkerman, K. E. O.; Kukkonen, J. P. Distinct Recognition of OX1 and OX2 Receptors by Orexin Peptides. *J. Pharmacol. Exp. Ther.* **2003**, *305* (2), 507–514.

(49)   Asahi, S.; Egashira, S. I.; Matsuda, M.; Iwaasa, H.; Kanatani, A.; Ohkubo, M.; Ihara, M.; Morishima, H. Development of an Orexin-2 Receptor Selective Agonist, [Ala11, D-Leu15]Orexin-B. *Bioorganic Med. Chem. Lett.* **2003**, *13* (1), 111–113.

(50)   German, N. A.; Decker, A. M.; Gilmour, B. P.; Thomas, B. F.; Zhang, Y. Truncated Orexin Peptides : Structure – Activity Relationship Studies. *ACS Medichinal Chem. Lett.* **2013**, *4*, 1224–1227.

(51)   Darker, J. G.; Porter, R. A.; Eggleston, D. S.; Smart, D.; Brough, S. J.; Sabido-David, C.; Jerman, J. C. Structure-Activity Analysis of Truncated Orexin-A Analogues at the Orexin-1 Receptor. *Bioorganic Med. Chem. Lett.* **2001**, *11* (5), 737–740.

(52)   Lang, M.; Söll, R. M.; Dürrenberger, F.; Dautzenberg, F. M.; Beck-Sickinger, A. G. Structure-Activity Studies of Orexin A and Orexin B at the Human Orexin 1 and Orexin 2 Receptors Led to Orexin 2 Receptor Selective and Orexin 1 Receptor Preferring Ligands. *J. Med. Chem.* **2004**, *47* (5), 1153–1160.

(53)   Karhu, L.; Weisell, J.; Turunen, P. M.; Leino, T. O.; Pätsi, H.; Xhaard, H.; Kukkonen, J. P.; Wallén, E. A. A. Stapled Truncated Orexin Peptides as Orexin Receptor Agonists. *Peptides* **2018**.

(54)   Yin, J.; Babaoglu, K.; Brautigam, C. A.; Clark, L.; Shao, Z.; Scheuermann, T. H.; Harrell, C. M.; Gotter, A. L.; Roecker, A. J.; Winrow, C. J.; Renger, J. J.; Coleman, P. J.; Rosenbaum, D. M. Structure and Ligand-Binding Mechanism of the Human OX1 and OX2 Orexin Receptors. *Nat. Struct. Mol. Biol.* **2016**, *23* (4), 293–299.

(55)   Yin, J.; Mobarec, J. C.; Kolb, P.; Rosenbaum, D. M. Crystal Structure of the Human OX2 Orexin Receptor Bound to the Insomnia Drug Suvorexant. *Nature* **2015**, *519* (7542), 247–250.

(56)   Suno, R.; Kimura, K. T.; Nakane, T.; Yamashita, K.; Wang, J.; Fujiwara, T.; Yamanaka, Y.; Im, D.; Horita, S.; Tsujimoto, H.; Tawaramoto, M. S.; Hirokawa, T.; Nango, E.; Tono, K.; Kameshima, T.; Hatsui, T.; Joti, Y.; Yabashi, M.; Shimamoto, K.; Yamamoto, M.; Rosenbaum, D. M.; Iwata, S.; Shimamura, T.; Kobayashi, T. Crystal Structures of Human Orexin 2 Receptor Bound to the Subtype-Selective Antagonist EMPA Article Crystal Structures of Human Orexin 2 Receptor Bound to the Subtype-Selective Antagonist EMPA. *Structure* **2018**, *26* (1), 7–19.e5.

(57)   Malherbe, P.; Roche, O.; Marcuz, A.; Kratzeisen, C.; Wettstein, J. G.; Bissantz, C. Mapping the Binding Pocket of Dual Antagonist Almorexant to Human Orexin 1 and Orexin 2 Receptors: Comparison with the Selective OX1 Antagonist SB-674042 and the Selective OX2 Antagonist N-Ethyl-2-[(6-Methoxy-Pyridin-3-Yl)-(Toluene-2-Sulfonyl)-Amino]-N-P. *Mol. Pharmacol.* **2010**, *78* (1), 81–93.

(58)   Tran, D. T.; Bonaventure, P.; Hack, M.; Mirzadegan, T.; Dvorak, C.; Letavic, M.; Carruthers, N.; Lovenberg, T.; Sutton, S. W. Chimeric, Mutant Orexin Receptors Show Key Interactions between Orexin Receptors, Peptides and Antagonists. *Eur. J. Pharmacol.* **2011**, *667* (1–3), 120–128.

(59)   Putula, J.; Kukkonen, J. P. Mapping of the Binding Sites for the OX1 Orexin Receptor Antagonist, SB-334867, Using Orexin/Hypocretin Receptor Chimaeras. *Neurosci. Lett.* **2012**, *506* (1), 111–115.

(60)   Heifetz, A.; Morris, G. B.; Biggin, P. C.; Barker, O.; Fryatt, T.; Bentley, J.; Hallett, D.; Manikowski, D.; Pal, S.; Reifegerste, R.; Slack, M.; Law, R. Study of Human Orexin-1 and -2 G-Protein-Coupled Receptors with Novel and Published Antagonists by Modeling, Molecular Dynamics Simulations, and Site-Directed Mutagenesis. *Biochemistry* **2012**, *51* (15), 3178–3197.

(61)   Ballesteros, J.; Weinstein, H. Integrated Methods for the Construction of Three-Dimensional Models and Computational Probing of Structure-Function Relations in G Protein-Coupled Receptors. *Methods Neurosci.* **1995**, *25*, 366–428.

(62)   Xhaard, H.; Nyrönen, T.; Rantanen, V. V.; Ruuskanen, J. O.; Laurila, J.; Salminen, T.; Scheinin, M.; Johnson, M. S. Model Structures of α-2 Adrenoceptors in Complex with Automatically Docked Antagonist Ligands Raise the Possibility of Interactions Dissimilar from Agonist Ligands. *J. Struct. Biol.* **2005**, *150* (2), 126–143.

(63)   Wu, B.; Chien, E. Y. T.; Mol, C. D.; Fenalti, G.; Liu, W.; Katritch, V.; Abagyan, R.; Brooun, A.; Wells, P.; Bi, F. C.; Hamel, D. J.; Kuhn, P.; Handel, T. M.; Cherezov, V.; Stevens, R. C. Structures of the CXCR4 Chemokine. *Science (80-.).* **2010**, *330* (6007), 1066–1071.

(64)   Chen, J.; Zhang, R.; Chen, X.; Wang, C.; Cai, X.; Liu, H.; Jiang, Y.; Liu, C.; Bai, B. Heterodimerization of Human Orexin Receptor 1 and Kappa Opioid Receptor Promotes Protein Kinase A/CAMP-Response Element Binding Protein Signaling via a Gαs-Mediated Mechanism. *Cell. Signal.* **2015**, *27* (7), 1426–1438.

(65)   Granier, S.; Manglik, A.; Kruse, A. C.; Kobilka, T. S.; Thian, F. S.; Weis, W. I.; Kobilka, B. K. Structure of the δ-Opioid Receptor Bound to Naltrindole. *Nature* **2012**, *485* (7398), 400–404.

(66)   Thompson, A. A.; Liu, W.; Chun, E.; Katritch, V.; Wu, H.; Vardy, E.; Huang, X. P.; Trapella, C.; Guerrini, R.; Calo, G.; Roth, B. L.; Cherezov, V.; Stevens, R. C. Structure of the Nociceptin/Orphanin FQ

Receptor in Complex with a Peptide Mimetic. *Nature* **2012**, *485* (7398), 395–399.

(67) Wheatley, M.; Wootten, D.; Conner, M. T.; Simms, J.; Kendrick, R.; Logan, R. T.; Poyner, D. R.; Barwell, J. Lifting the Lid on GPCRs: The Role of Extracellular Loops. *Br. J. Pharmacol.* **2012**, *165* (6), 1688–1703.

(68) Wu, H.; Wacker, D.; Mileni, M.; Katritch, V.; Han, G. W.; Vardy, E.; Liu, W.; Thompson, A. A.; Huang, X. P.; Carroll, F. I.; Mascarella, S. W.; Westkaemper, R. B.; Mosier, P. D.; Roth, B. L.; Cherezov, V.; Stevens, R. C. Structure of the Human κ-Opioid Receptor in Complex with JDTic. *Nature* **2012**, *485* (7398), 327–332.

(69) Voisin, T.; Rouet-Benzineb, P.; Reuter, N.; Laburthe, M. Orexins and Their Receptors: Structural Aspects and Role in Peripheral Tissues. *Cell. Mol. Life Sci.* **2003**, *60* (1), 72–87.

(70) Milasta, S.; Evans, N. A.; Ormiston, L.; Wilson, S.; Lefkowitz, R. J.; Milligan, G. The Sustainability of Interactions between the Orexin-1 Receptor and Beta-Arrestin-2 Is Defined by a Single C-Terminal Cluster of Hydroxy Amino Acids and Modulates the Kinetics of ERK MAPK Regulation. *Biochem. J.* **2005**, *387* (Pt 3), 573–584.

(71) Smart, D.; Jerman, J. C.; Brough, S. J.; Rushton, S. L.; Murdock, P. R.; Jewitt, F.; Elshourbagy, N. A.; Ellis, C. E.; Middlemiss, D. N.; Brown, F. Characterization of Recombinant Human Orexin Receptor Pharmacology in a Chinese Hamster Ovary Cell-Line Using FLIPR. *Br. J. Pharmacol* **1999**, *128* (1), 1–3.

(72) Lund, P. E.; Shariatmadari, R.; Uustare, A.; Detheux, M.; Parmentier, M.; Kukkonen, J. P.; Åkerman, K. E. O. The Orexin OX1 Receptor Activates a Novel Ca2+ Influx Pathway Necessary for Coupling to Phospholipase C. *J. Biol. Chem.* **2000**, *275* (40), 30806–30812.

(73) Holmqvist, T.; Åkerman, K. E. O.; Kukkonen, J. P. Orexin Signaling in Recombinant Neuron-like Cells. *FEBS Lett.* **2002**, *526* (1–3), 11–14.

(74) Kukkonen, J. P. OX2 Orexin/Hypocretin Receptor Signal Transduction in Recombinant Chinese Hamster Ovary Cells. *Cell. Signal.* **2016**, *28* (2), 51–60.

(75) Turunen, P. M.; Jantti, M. H.; Kukkonen, J. P. OX1 Orexin/Hypocretin Receptor Signaling through Arachidonic Acid and Endocannabinoid Release. *Mol Pharmacol* **2012**, *82* (2), 156–167.

(76) Holmqvist, T.; Johansson, L.; Östman, M.; Ammoun, S.; Åkerman, K. E. O.; Kukkonen, J. P. OX1 Orexin Receptors Couple to Adenylyl Cyclase Regulation via Multiple Mechanisms. *J. Biol. Chem.* **2005**, *280* (8), 6570–6579.

(77) Jäntti, M. H.; Putula, J.; Somerharju, P.; Frohman, M.; Kukkonen, J. P. OX1 Orexin/Hypocretin Receptor Activation of Phospholipase D.

Br. J. Pharmacol. **2012**, *165* (4b), 1109–1123.

(78) Kukkonen, J. P. G-Protein-Dependency of Orexin/Hypocretin Receptor Signalling in Recombinant Chinese Hamster Ovary Cells. *Biochem. Biophys. Res. Commun.* **2016**, *476* (4), 379–385.

(79) Leonard, C. S.; Kukkonen, J. P. Orexin / Hypocretin Receptor Signalling : A Functional Perspective. *Br. J. Pharmacol.* **2014**, *171*, 294–313.

(80) Xu, T.; Yang, Y.; Ward, R.; Gao, L.; Liu, Y. Orexin Receptors : Multi-Functional Therapeutic Targets for Sleeping Disorders , Eating Disorders , Drug Addiction , Cancers and Other Physiological Disorders. *Cell. Signal.* **2013**, *25* (12), 2413–2423.

(81) Konieczny, V.; Keebler, M. V.; Taylor, C. W. Spatial Organization of Intracellular Ca2+ Signals. *Semin. Cell Dev. Biol.* **2012**, *23* (2), 172–180.

(82) Yang, Y. R.; Follo, M. Y.; Cocco, L.; Suh, P. G. The Physiological Roles of Primary Phospholipase C. *Adv. Biol. Regul.* **2013**, *53* (3), 232–241.

(83) Gamper, N.; Shapiro, M. S. Regulation of Ion Transport Proteins by Membrane Phosphoinositides. *Nat. Rev. Neurosci.* **2007**, *8* (12), 921–934.

(84) Suh, B.-C.; Hille, B. PIP2 Is a Necessary Cofactor for Ion Channel Function: How and Why? *Annu. Rev. Biophys.* **2008**, *37* (1), 175–195.

(85) Newton, A. C. Protein Kinase C: Poised to Signal. *AJP Endocrinol. Metab.* **2010**, *298* (3), E395–E402.

(86) Ammoun, S.; Johansson, L.; Ekholm, M. E.; Holmqvist, T.; Danis, A. S.; Korhonen, L.; Sergeeva, O. A.; Haas, H. L.; Åkerman, K. E. O.; Kukkonen, J. P. OX1 Orexin Receptors Activate Extracellular Signal-Regulated Kinase in Chinese Hamster Ovary Cells via Multiple Mechanisms : The Role of Ca2+ Influx in OX1 Receptor Signaling. *Mol. Endocrinol.* **2006**, *20* (1), 80–99.

(87) Xia, J. X.; Fan, S. Y.; Yan, J.; Chen, F.; Li, Y.; Yu, Z. P.; Hu, Z. A. Orexin A-Induced Extracellular Calcium Influx in Prefrontal Cortex Neurons Involves L-Type Calcium Channels. *J. Physiol. Biochem.* **2009**, *65* (2), 125–136.

(88) Nakajima, Y.; Nakajima, S. *Measurement of Orexin (Hypocretin) and Substance P Effects on Constitutively Active Inward Rectifier K+ Channels in Brain Neurons*, 1st ed.; Elsevier Inc., 2010; Vol. 484.

(89) Uramura, K.; Funahashi, H.; Muroya, S.; Shioda, S.; Takigawa, M.; Yada, T. Orexin-A Activates Phospholipase C- and Protein Kinase C-Mediated Ca2+ Signaling in Dopamine Neurons of the Ventral Tegmental Area. *Mol. Neurosci.* **2001**, *12* (9), 1885–1889.

(90) Malendowicz, L. K.; Tortorella, C.; Nussdorfer, G. G. Orexins Stimulate Corticosterone Secretion of Rat Adrenocortical Cells,

through the Activation of the Adenylate Cyclase-Dependent Signaling Cascade. *J. Steroid Biochem. Mol. Biol.* **1999**, *70* (4–6), 185–188.

(91) Randeva, H. S.; Karteris, E.; Grammatopoulos, D.; Hillhouse, E. W. Expression of Orexin-a and Functional Orexin Type 2 Receptors in the Human Adult Adrenals: Implications for Adrenal Function and Energy Homeostasis. *J. Clin. Endocrinol. Metab.* **2001**, *86* (10), 4808–4813.

(92) Mazzocchi, G.; Malendowicz, L. K.; Gottardo, L.; Aragona, F.; Nussdorfer, G. G. Orexin A Stimulates Cortisol Secretion from Human Adrenocortical Cells through Activation of the Adenylate Cyclase-Dependent Signaling Cascade. *J. Clin. Endocrinol. Metab.* **2001**, *86* (2), 778–782.

(93) Karteris, E.; Machado, R. J.; Chen, J.; Zervou, S.; Hillhouse, E. W.; Randeva, H. S. Food Deprivation Differentially Modulates Orexin Receptor Expression and Signaling in Rat Hypothalamus and Adrenal Cortex. *Am. J. Physiol. - Endocrinol. Metab.* **2005**, *288*, E1089–E1100.

(94) Tang, J.; Chen, J.; Ramanjaneya, M.; Punn, A.; Conner, A. C.; Randeva, H. S. The Signalling Profile of Recombinant Human Orexin-2 Receptor. *Cell. Signal.* **2008**, *20* (9), 1651–1661.

(95) Sunahara, R. K. Isoforms of Mammalian Adenylyl Cyclase: Multiplicities of Signaling. *Mol. Interv.* **2002**, *2* (3), 168–184.

(96) Lytton, J. Na $^+$ /Ca $^{2+}$ Exchangers: Three Mammalian Gene Families Control Ca $^{2+}$ Transport. *Biochem. J.* **2007**, *406* (3), 365–382.

(97) Putula, J.; Pihlajamaa, T.; Kukkonen, J. P. Calcium Affects OX1 Orexin (Hypocretin) Receptor Responses by Modifying Both Orexin Binding and the Signal Transduction Machinery. *Br. J. Pharmacol.* **2014**, *171*, 5816–5828.

(98) Lund, P. E.; Shariatmadari, R.; Uustare, A.; Detheux, M.; Parmentier, M.; Kukkonen, J. P.; Åkerman, K. E. O. The Orexin OX1 Receptor Activates a Novel CA2+ Influx Pathway Necessary for Coupling to Phospholipase C. *J. Biol. Chem.* **2000**, *275* (40), 30806–30812.

(99) Turunen, P. M.; Ekholm, M. E.; Somerharju, P.; Kukkonen, J. P. Arachidonic Acid Release Mediated by OX 1 Orexin Receptors. *Br. J. Pharmacol.* **2010**, *159* (1), 212–221.

(100) Johansson, L.; Ekholm, M. E.; Kukkonen, J. P. Regulation of OX 1 Orexin/Hypocretin Receptor-Coupling to Phospholipase C by Ca 2+ Influx. *Br. J. Pharmacol.* **2007**, *150* (1), 97–104.

(101) Maggio, R.; Innamorati, G.; Parenti, M. G Protein-Coupled Receptor Oligomerization Provides the Framework for Signal Discrimination. *J. Neurochem.* **2007**, *103* (5), 1741–1752.

(102) Milligan, G. G Protein-Coupled Receptor Hetero-Dimerization: Contribution to Pharmacology and Function. *Br. J. Pharmacol.*

2009, *158* (1), 5–14.

(103)   Wang, C.; Pan, Y.; Zhang, R.; Bai, B.; Chen, J.; Randeva, H. S. Heterodimerization of Mouse Orexin Type 2 Receptor Variants and the Effects on Signal Transduction. *Biochim. Biophys. Acta - Mol. Cell Res.* **2014**, *1843* (3), 652–663.

(104)   Jäntti, M. H.; Mandrika, I.; Kukkonen, J. P. Human Orexin/Hypocretin Receptors Form Constitutive Homo- and Heteromeric Complexes with Each Other and with Human CB1cannabinoid Receptors. *Biochem. Biophys. Res. Commun.* **2014**, *445* (2), 486–490.

(105)   Xu, T.-R.; Ward, R. J.; Pediani, J. D.; Milligan, G. The Orexin OX 1 Receptor Exists Predominantly as a Homodimer in the Basal State: Potential Regulation of Receptor Organization by Both Agonist and Antagonist Ligands. *Biochem. J.* **2011**, *439* (1), 171–183.

(106)   Ward, R. J.; Pediani, J. D.; Milligan, G. Heteromultimerization of Cannabinoid CB 1 Receptor and Orexin OX 1 Receptor Generates a Unique Complex in Which Both Protomers Are Regulated by Orexin A. *J. Biol. Chem.* **2011**, *286* (43), 37414–37428.

(107)   Jäntti, M. H.; Putula, J.; Turunen, P. M.; Nasman, J.; Reijonen, S.; Lindqvist, C.; Kukkonen, J. P. Autocrine Endocannabinoid Signaling through CB1 Receptors Potentiates OX1 Orexin Receptor Signaling. *Mol. Pharmacol.* **2013**, *83* (3), 621–632.

(108)   Robinson, J. D.; McDonald, P. H. The Orexin 1 Receptor Modulates Kappa Opioid Receptor Function via a JNK-Dependent Mechanism. *Cell. Signal.* **2015**, *27* (7), 1449–1456.

(109)   Davies, J.; Chen, J.; Pink, R.; Carter, D.; Saunders, N.; Sotiriadis, G.; Bai, B.; Pan, Y.; Howlett, D.; Payne, A.; Randeva, H.; Karteris, E. Orexin Receptors Exert a Neuroprotective Effect in Alzheimer's Disease (AD) via Heterodimerization with GPR103. *Sci. Rep.* **2015**, *5* (November 2014), 1–12.

(110)   Navarro, G.; Quiroz, C.; Moreno-Delgado, D.; Sierakowiak, A.; McDowell, K.; Moreno, E.; Rea, W.; Cai, N.-S.; Aguinaga, D.; Howell, L. A.; Hausch, F.; Cortes, A.; Mallol, J.; Casado, V.; Lluis, C.; Canela, E. I.; Ferre, S.; McCormick, P. J. Orexin-Corticotropin-Releasing Factor Receptor Heteromers in the Ventral Tegmental Area as Targets for Cocaine. *J. Neurosci.* **2015**, *35* (17), 6639–6653.

(111)   Kroemer, G.; Galluzzi, L.; Vandenabeele, P.; Abrams, J.; Alnemri, E. S.; Baehrecke, E. H.; Blagosklonny, M. V.; El-Deiry, W. S.; Golstein, P.; Green, D. R.; Hengartner, M.; Knight, R. A.; Kumar, S.; Lipton, S. A.; Malorni, W.; Nuñez, G.; Peter, M. E.; Tschopp, J.; Yuan, J.; Piacentini, M.; Zhivotovsky, B.; Melino, G. Classification of Cell Death: Recommendations of the Nomenclature Committee on Cell Death 2009. *Cell Death Differ.* **2009**, *16* (1), 3–11.

(112)   Silva, M. T. Secondary Necrosis: The Natural Outcome of the

Complete Apoptotic Program. *FEBS Lett.* **2010**, *584* (22), 4491–4499.

(113) Ammoun, S.; Lindholm, D.; Wootz, H.; Åkerman, K. E. O.; Kukkonen, J. P. G-Protein-Coupled OX1orexin/Hcrtr-1 Hypocretin Receptors Induce Caspase-Dependent and -Independent Cell Death through P38 Mitogen-/Stress- Activated Protein Kinase. *J. Biol. Chem.* **2006**, *281* (2), 834–842.

(114) Rouet-Benzineb, P.; Rouyer-Fessard, C.; Jarry, A.; Avondo, V.; Pouzet, C.; Yanagisawa, M.; Laboisse, C.; Laburthe, M.; Voisin, T. Orexins Acting at Native OX1 Receptor in Colon Cancer and Neuroblastoma Cells or at Recombinant OX1 Receptor Suppress Cell Growth by Inducing Apoptosis. *J. Biol. Chem.* **2004**, *279* (44), 45875–45886.

(115) Voisin, T.; El Firar, A.; Rouyer-Fessard, C.; Gratio, V.; Laburthe, M. A Hallmark of Immunoreceptor, the Tyrosine-Based Inhibitory Motif ITIM, Is Present in the G Protein-Coupled Receptor OX1R for Orexins and Drives Apoptosis: A Novel Mechanism. *FASEB J.* **2008**, *22* (6), 1993–2002.

(116) Voisin, T.; El Firar, A.; Fasseu, M.; Rouyer-Fessard, C.; Descatoire, V.; Walker, F.; Paradis, V.; Bedossa, P.; Henin, D.; Lehy, T.; Laburthe, M. Aberrant Expression of OX1 Receptors for Orexins in Colon Cancers and Liver Metastases: An Openable Gate to Apoptosis. *Cancer Res.* **2011**, *71* (9), 3341–3351.

(117) Voisin, T.; El Firar, A.; Avondo, V.; Laburthe, M. Orexin-Induced Apoptosis: The Key Role of the Seven-Transmembrane Domain Orexin Type 2 Receptor. *Endocrinology* **2006**, *147* (10), 4977–4984.

(118) Peyron, C.; Tighe, D. K.; van den Pol, a N.; de Lecea, L.; Heller, H. C.; Sutcliffe, J. G.; Kilduff, T. S. Neurons Containing Hypocretin (Orexin) Project to Multiple Neuronal Systems. *J. Neurosci.* **1998**, *18* (23), 9996–10015.

(119) Marcus, J. N.; Aschkenasi, C. J.; Lee, C. E.; Chemelli, R. M.; Saper, C. B.; Yanagisawa, M.; Elmquist, J. K. Differential Expression of Orexin Receptors 1 and 2 in the Rat Brain. *J. Comp. Neurol.* **2001**, *435* (1), 6–25.

(120) Trivedi, P.; Yu, H.; MacNeil, D. J.; Van der Ploeg, L. H.; Guan, X. M. Distribution of Orexin Receptor MRNA in the Rat Brain. *FEBS Lett.* **1998**, *438* (1–2), 71–75.

(121) Mieda, M.; Hasegawa, E.; Kisanuki, Y. Y.; Sinton, C. M.; Yanagisawa, M.; Sakurai, T. Differential Roles of Orexin Receptor-1 and -2 in the Regulation of Non-REM and REM Sleep. *J. Neurosci.* **2011**, *31* (17), 6518–6526.

(122) Roecker, A. J.; Cox, C. D.; Coleman, P. J. Orexin Receptor Antagonists: New Therapeutic Agents for the Treatment of Insomnia. *J. Med. Chem.* **2016**, *59* (2), 504–530.

(123) Heinonen, M. V.; Purhonen, A. K.; Mäkelä, K. A.; Herzig, K. H. Functions of Orexins in Peripheral Tissues. *Acta Physiol.* **2008**, *192* (4), 471–485.

(124) Scammell, T. E.; Arrigoni, E.; Lipton, J. O. Neural Circuitry of Wakefulness and Sleep. *Neuron* **2017**, *93* (4), 747–765.

(125) Adamantidis, A. R.; Zhang, F.; Aravanis, A. M.; Deisseroth, K.; De Lecea, L. Neural Substrates of Awakening Probed with Optogenetic Control of Hypocretin Neurons. *Nature* **2007**, *450* (7168), 420–424.

(126) Sasaki, K.; Suzuki, M.; Mieda, M.; Tsujino, N.; Roth, B.; Sakurai, T. Pharmacogenetic Modulation of Orexin Neurons Alters Sleep/Wakefulness States in Mice. *PLoS One* **2011**, *6* (5).

(127) Brisbare-Roch, C.; Dingemanse, J.; Koberstein, R.; Hoever, P.; Aissaoui, H.; Flores, S.; Mueller, C.; Nayler, O.; van Gerven, J.; de Haas, S. L.; Hess, P.; Qiu, C.; Buchmann, S.; Scherz, M.; Weller, T.; Fischli, W.; Clozel, M.; Jenck, F. Promotion of Sleep by Targeting the Orexin System in Rats, Dogs and Humans. *Nat. Med.* **2007**, *13* (2), 150–155.

(128) NINDS. Narcolepsy Fact Sheet.

(129) Chemelli, R. M.; Willie, J. T.; Sinton, C. M.; Elmquist, J. K.; Scammell, T.; Lee, C.; Richardson, J. a.; Clay Williams, S.; Xiong, Y.; Kisanuki, Y.; Fitch, T. E.; Nakazato, M.; Hammer, R. E.; Saper, C. B.; Yanagisawa, M. Narcolepsy in Orexin Knockout Mice: Molecular Genetics of Sleep Regulation. *Cell* **1999**, *98* (4), 437–451.

(130) Willie, J. T.; Chemelli, R. M.; Sinton, C. M.; Tokita, S.; Williams, S. C.; Kisanuki, Y. Y.; Marcus, J. N.; Lee, C.; Elmquist, J. K.; Kohlmeier, K. A.; Leonard, C. S.; Richardson, J. A.; Hammer, R. E.; Yanagisawa, M. Distinct Narcolepsy Syndromes in Orexin Receptor-2 and Orexin Null Mice. *Neuron* **2003**, *38* (5), 715–730.

(131) Lin, L.; Faraco, J.; Li, R.; Kadotani, H.; Rogers, W.; Lin, X.; Qiu, X.; De Jong, P. J.; Nishino, S.; Mignot, E. The Sleep Disorder Canine Narcolepsy Is Caused by a Mutation in the Hypocretin (Orexin) Receptor 2 Gene. *Cell* **1999**, *98* (3), 365–376.

(132) Mieda, M.; Willie, J. T.; Hara, J.; Sinton, C. M.; Sakurai, T.; Yanagisawa, M. Orexin Peptides Prevent Cataplexy and Improve Wakefulness in an Orexin Neuron-Ablated Model of Narcolepsy in Mice. *Proc. Natl. Acad. Sci. U. S. A.* **2004**, *101* (13), 4649–4654.

(133) Weinhold, S. L.; Seeck-Hirschner, M.; Nowak, A.; Hallschmid, M.; G??der, R.; Baier, P. C. The Effect of Intranasal Orexin-A (Hypocretin-1) on Sleep, Wakefulness and Attention in Narcolepsy with Cataplexy. *Behav. Brain Res.* **2014**, *262*, 8–13.

(134) Irukayama-Tomobe, Y.; Ogawa, Y.; Tominaga, H.; Ishikawa, Y.; Hosokawa, N. Nonpeptide Orexin Type-2 Receptor Agonist Ameliorates Narcolepsy-Cataplexy Symptoms in Mouse Models. *PNAS* **2017**, *114* (22), 5731–5736.

(135) Nishino, S.; Ripley, B.; Overeem, S.; Lammers, G. J.; Mignot, E. Hypocretin (Orexin) Deficiency in Human Narcolepsy. *Lancet* **2000**, *355* (9197), 39–40.

(136) Peyron, C.; Faraco, J.; Rogers, W.; Ripley, B.; Overeem, S.; Charnay, Y.; Nevsimalova, S.; Aldrich, M.; Reynolds, D.; Albin, R.; Li, R.; Hungs, M.; Pedrazzoli, M.; Padigaru, M.; Kucherlapati, M.; Jun, F.; Maki, R.; Lammers, G. J.; Bouras, C.; Kucherlapati, R.; Nishino, S.; Mignot, E. A Mutation in a Case of Early Onset Narcolepsy and a Generalized Absence of Hypocretin Peptides in Human Narcoleptic Brains. *Nat. Med.* **2000**, *6* (9), 991–997.

(137) Nutt, D. J.; Stahl, S. M. Searching for Perfect Sleep: The Continuing Evolution of GABAAreceptor Modulators as Hypnotics. *J. Psychopharmacol.* **2010**, *24* (11), 1601–1612.

(138) Jacobson, L. H.; Chen, S.; Mir, S.; Hoyer, D. Orexin OX2 Receptor Antagonists as Sleep Aids. In *Behavioral Neuroscience of Orexin/Hypocretin. Current Topics in Behavioral Neurosciences*; Lawrence, A., de Lecea, L., Eds.; Springer, Cham, 2017.

(139) Ripley, B.; Fujiki, N.; Okura, M.; Mignot, E.; Nishino, S. Hypocretin Levels in Sporadic and Familial Cases of Canine Narcolepsy. *Neurobiol. Dis.* **2001**, *8* (3), 525–534.

(140) Nishino, S.; Mignot, E. Pharmacological Aspects of Human and Canine Narcolepsy. *Prog. Neurobiol.* **1997**, *52* (1), 27–78.

(141) James, M. H.; Mahler, S. V.; Moorman, D. E.; Aston-Jones, G. A Decade of Orexin/Hypocretin and Addiction: Where Are We Now? In *Behavioral Neuroscience of Orexin/Hypocretin. Current Topics in Behavioral Neurosciences*; Lawrence, A., de Lecea, L., Eds.; Springer, Cham, 2017.

(142) Harris, G. C.; Wimmer, M.; Aston-Jones, G. A Role for Lateral Hypothalamic Orexin Neurons in Reward Seeking. *Nature* **2005**, *437* (7058), 556–559.

(143) Boutrel, B.; Kenny, P. J.; Specio, S. E.; Martin-Fardon, R.; Markou, A.; Koob, G. F.; de Lecea, L. Role for Hypocretin in Mediating Stress-Induced Reinstatement of Cocaine-Seeking Behavior. *Proc. Natl. Acad. Sci.* **2005**, *102* (52), 19168–19173.

(144) Mahler, S. V.; Moorman, D. E.; Smith, R. J.; James, M. H.; Aston-Jones, G. Motivational Activation: A Unifying Hypothesis of Orexin/Hypocretin Function. *Nat. Neurosci.* **2014**, *17* (10), 1298–1303.

(145) Yang, G.; Sau, C.; Lai, W.; Cichon, J.; Li, W. Orexin-1 Receptor Signaling Increases Motivation for Cocaine- Associated Cues. **2015**, *344* (6188), 1173–1178.

(146) Shoblock, J. R.; Welty, N.; Aluisio, L.; Fraser, I.; Motley, S. T.; Morton, K.; Palmer, J.; Bonaventure, P.; Carruthers, N. I.; Lovenberg, T. W.; Boggs, J.; Galici, R. Selective Blockade of the Orexin-2

Receptor Attenuates Ethanol Self-Administration, Place Preference, and Reinstatement. *Psychopharmacology (Berl)*. **2011**, *215* (1), 191–203.

(147) Srinivasan, S.; Simms, J. A.; Nielsen, C. K.; Lieske, S. P.; Bito-Onon, J. J.; Yi, H.; Hopf, F. W.; Bonci, A.; Bartlett, S. E. The Dual Orexin/Hypocretin Receptor Antagonist, Almorexant, in the Ventral Tegmental Area Attenuates Ethanol Self-Administration. *PLoS One* **2012**, *7* (9), 1–12.

(148) Uslaner, J. M.; Winrow, C. J.; Gotter, A. L.; Roecker, A. J.; Coleman, P. J.; Hutson, P. H.; Le, A. D.; Renger, J. J. Selective Orexin 2 Receptor Antagonism Blocks Cue-Induced Reinstatement, but Not Nicotine Self-Administration or Nicotine-Induced Reinstatement. *Behav. Brain Res*. **2014**, *269*, 61–65.

(149) Monteiro, S.; Monteiro, B.; Paes, F.; Egídio, A.; Nuno, N. Neurobiological Role of Hypocretin in Regulation of Psychiatric Disorders. *Sleep Vigil*. **2018**, No. 0123456789.

(150) James, M. H.; Campbell, E. J.; Dayas, C. V. Role of the Orexin/Hypocretin System in Stress-Related Psychiatric Disorders. In *Behavioral Neuroscience of Orexin/Hypocretin. Current Topics in Behavioral Neurosciences*; Lawrence, A., de Lecea, L., Eds.; Springer, Cham, 2017.

(151) Johnson, P. L.; Truitt, W.; Fitz, S. D.; Minick, P. E.; Dietrich, A.; Sanghani, S.; Träskman-Bendz, L.; Goddard, A. W.; Brundin, L.; Shekhar, A. A Key Role for Orexin in Panic Anxiety. *Nat. Med*. **2010**, *16* (1), 111–115.

(152) Johnson, P. L.; Samuels, B. C.; Fitz, S. D.; Federici, L. M.; Hammes, N.; Early, M. C.; Truitt, W.; Lowry, C. A.; Shekhar, A. Orexin 1 Receptors Are a Novel Target to Modulate Panic Responses and the Panic Brain Network. *Physiol. Behav*. **2012**, *107* (5), 733–742.

(153) Abbas, M. G.; Shoji, H.; Soya, S.; Hondo, M.; Miyakawa, T.; Sakurai, T. Comprehensive Behavioral Analysis of Male Ox1r−/− Mice Showed Implication of Orexin Receptor-1 in Mood, Anxiety, and Social Behavior. *Front. Behav. Neurosci*. **2015**, *9* (December), 1–10.

(154) Steiner, M. a.; Gatfield, J.; Brisbare-Roch, C.; Dietrich, H.; Treiber, A.; Jenck, F.; Boss, C. Discovery and Characterization of ACT-335827, an Orally Available, Brain Penetrant Orexin Receptor Type1 Selective Antagonist. *ChemMedChem* **2013**, *8* (6), 898–903.

(155) Rotter, A.; Asemann, R.; Decker, A.; Kornhuber, J.; Biermann, T. Orexin Expression and Promoter-Methylation in Peripheral Blood of Patients Suffering from Major Depressive Disorder. *J. Affect. Disord*. **2011**, *131* (1–3), 186–192.

(156) Salomon, R. M.; Ripley, B.; Kennedy, J. S.; Johnson, B.; Schmidt, D.; Zeitzer, J. M.; Nishino, S.; Mignot, E. Diurnal Variation of Cerebrospinal Fluid Hypocretin-1 (Orexin-A) Levels in Control and

Depressed Subjects. *Biol. Psychiatry* **2003**, *54* (2), 96–104.

(157) Scott, M. M.; Marcus, J. N.; Pettersen, A.; Birnbaum, S. G.; Mochizuki, T.; Scammell, T. E.; Nestler, E. J.; Elmquist, J. K.; Lutter, M. Hcrtr1 and 2 Signaling Differentially Regulates Depression-like Behaviors. *Behav. Brain Res.* **2011**, *222* (2), 289–294.

(158) Goforth, P. B.; Myers, M. G. Roles for Orexin/Hypocretin in the Control of Energy Balance and Metabolism. In *Behavioral Neuroscience of Orexin/Hypocretin. Current Topics in Behavioral Neurosciences*; Lawrence, A., de Lecea, L., Eds.; Springer, Cham, 2017.

(159) Marjan, B.; Hosseinzadeh, H. A Review of the Role of Orexin System in Pain Modulation. *Biomed. Pharmacother.* **2017**, *90*, 187–193.

(160) Bingham, S.; Davey, P. T.; Babbs, A. J.; Irving, E. A.; Sammons, M. J.; Wyles, M.; Jeffrey, P.; Cutler, L.; Riba, I.; Johns, A.; Porter, R. A.; Upton, N.; Hunter, A. J.; Parsons, A. A. Orexin-A, an Hypothalamic Peptide with Analgesic Properties. *Pain* **2001**, *92* (1–2), 81–90.

(161) Boss, C.; Roch, C. Expert Opinion on Therapeutic Patents Orexin Research : Patent News from 2016 Orexin Research : Patent News from 2016. *Expert Opin. Ther. Pat.* **2017**, 1–11.

(162) Cox, C. D.; Breslin, M. J.; Whitman, D. B.; Schreier, J. D.; McGaughey, G. B.; Bogusky, M. J.; Roecker, A. J.; Mercer, S. P.; Bednar, R. a.; Lemaire, W.; Bruno, J. G.; Reiss, D. R.; Harrell, C. M.; Murphy, K. L.; Garson, S. L.; Doran, S. M.; Prueksaritanont, T.; Anderson, W. B.; Tang, C.; Roller, S.; Cabalu, T. D.; Cui, D.; Hartman, G. D.; Young, S. D.; Koblan, K. S.; Winrow, C. J.; Renger, J. J.; Coleman, P. J. Discovery of the Dual Orexin Receptor Antagonist [(7 R)-4-(5-Chloro-1,3-   Benzoxazol-2-Yl)-7-Methyl-1,4-Diazepan-1-Yl][5-Methyl-2-(2 H -1,2,3-Triazol-2-Yl)Phenyl]Methanone (MK-4305) for the Treatment of Insomnia. *J. Med. Chem.* **2010**, *53* (14), 5320–5332.

(163) Heifetz, A.; Chudyk, E.; Gleave, L.; Aldeghi, M.; Cherezov, V.; Fedorov, D. G.; Biggin, P. C.; Bodkin, M. The Fragment Molecular Orbital Method Reveals New Insight into the Chemical Nature of GPCR-Ligand Interactions. *J. Chem. Inf. Model.* **2016**, *56* (1), 159–172.

(164) Nagase, H.; Yamamoto, N.; Yata, M.; Ohrui, S.; Okada, T.; Ogawa, Y.; Hirayama, S.; Kuroda, D.; Watanabe, Y.; Gouda, H. Design and Synthesis of Potent and Highly Selective Orexin 1 Receptor Antagonists with a Morphinan Skeleton and Their Pharmacologies. *J. Med. Chem.* **2017**, *60* (3), 1018–1040.

(165) Nagahara, T.; Saitoh, T.; Kutsumura, N.; Irukayama-Tomobe, Y.; Ogawa, Y.; Kuroda, D.; Gouda, H.; Kumagai, H.; Fujii, H.; Yanagisawa, M.; Nagase, H. Design and Synthesis of Non-Peptide, Selective Orexin Receptor 2 Agonists. *J. Med. Chem.* **2015**, *58* (20),

7931–7937.

(166) Heifetz, A.; Bodkin, M. J.; Biggin, P. C. Discovery of the First Selective, Nonpeptidic Orexin 2 Receptor Agonists. *J. Med. Chem.* **2015**, *58*, 7928–7930.

(167) Porter, R. a.; Chan, W. N.; Coulton, S.; Johns, A.; Hadley, M. S.; Widdowson, K.; Jerman, J. C.; Brough, S. J.; Coldwell, M.; Smart, D.; Jewitt, F.; Jeffrey, P.; Austin, N. 1,3-Biarylureas as Selective Non-Peptide Antagonists of the Orexin-1 Receptor. *Bioorganic Med. Chem. Lett.* **2001**, *11* (14), 1907–1910.

(168) Smart, D.; Sabido-David, C.; Brough, S. J.; Jewitt, F.; Johns, A.; Porter, R. A.; Jerman, J. C. SB-334867-A: The First Selective Orexin-1 Receptor Antagonist. *Br. J. Pharmacol.* **2001**, *132*, 1179–1182.

(169) American Chemical Society. SciFinder search "SB-334867."

(170) McElhinny, C. J.; Lewin, A. H.; Mascarella, S. W.; Runyon, S.; Brieaddy, L.; Carroll, F. I. Hydrolytic Instability of the Important Orexin 1 Receptor Antagonist SB-334867: Possible Confounding Effects on in Vivo and in Vitro Studies. *Bioorganic Med. Chem. Lett.* **2012**, *22* (21), 6661–6664.

(171) Gotter, A. L.; Roecker, A. J.; Hargreaves, R.; Coleman, P. J.; Winrow, C. J.; Renger, J. J. Orexin Receptors as Therapeutic Drug Targets. *Prog. Brain Res.* **2012**, *198*, 163–196.

(172) Langmead, C. J.; Jerman, J. C.; Brough, S. J.; Scott, C.; Porter, R. a; Herdon, H. J. Characterisation of the Binding of [3H]-SB-674042, a Novel Nonpeptide Antagonist, to the Human Orexin-1 Receptor. *Br. J. Pharmacol.* **2004**, *141* (2), 340–346.

(173) Perrey, D. A.; German, N. A.; Gilmour, B. P.; Li, J.-X.; Harris, D. L.; Thomas, B. F.; Zhang, Y. Substituted Tetrahydroisoquinolines as Selective Antagonists for the Orexin 1 Receptor. *J. Med. Chem.* **2013**, *56* (17), 6901–6916.

(174) Hirose, M.; Egashira, S. I.; Goto, Y.; Hashihayata, T.; Ohtake, N.; Iwaasa, H.; Hata, M.; Fukami, T.; Kanatani, A.; Yamada, K. N-Acyl 6,7-Dimethoxy-1,2,3,4-Tetrahydroisoquinoline: The First Orexin-2 Receptor Selective Non-Peptidic Antagonist. *Bioorganic Med. Chem. Lett.* **2003**, *13* (24), 4497–4499.

(175) McAtee, L. C.; Sutton, S. W.; Rudolph, D. a.; Li, X.; Aluisio, L. E.; Phuong, V. K.; Dvorak, C. a.; Lovenberg, T. W.; Carruthers, N. I.; Jones, T. K. Novel Substituted 4-Phenyl-[1,3]Dioxanes: Potent and Selective Orexin Receptor 2 (OX2R) Antagonists. *Bioorganic Med. Chem. Lett.* **2004**, *14* (16), 4225–4229.

(176) Dugovic, C.; Shelton, J. E.; Aluisio, L. E.; Fraser, I. C.; Jiang, X.; Sutton, S. W.; Bonaventure, P.; Yun, S.; Li, X.; Lord, B.; Dvorak, C. A.; Carruthers, N. I.; Lovenberg, T. W. Blockade of Orexin-1 Receptors Attenuates Orexin-2 Receptor Antagonism-Induced Sleep Promotion in the Rat. *J. Pharmacol. Exp. Ther.* **2009**, *330* (1), 142–

151.

(177) Malherbe, P.; Borroni, E.; Gobbi, L.; Knust, H.; Nettekoven, M.; Pinard, E.; Roche, O.; Rogers-Evans, M.; Wettstein, J. G.; Moreau, J. L. Biochemical and Behavioural Characterization of EMPA, a Novel High-Affinity, Selective Antagonist for the OX 2 Receptor. *Br. J. Pharmacol.* **2009**, *156* (8), 1326–1341.

(178) Fujimoto, T.; Kunitomo, J.; Tomata, Y.; Nishiyama, K.; Nakashima, M.; Hirozane, M.; Yoshikubo, S.; Hirai, K.; Marui, S. Discovery of Potent, Selective, Orally Active Benzoxazepine-Based Orexin-2 Receptor Antagonists. *Bioorg. Med. Chem. Lett.* **2011**, *21* (21), 6414–6416.

(179) Roecker, A. J.; Mercer, S. P.; Schreier, J. D.; Cox, C. D.; Fraley, M. E.; Steen, J. T.; Lemaire, W.; Bruno, J. G.; Harrell, C. M.; Garson, S. L.; Gotter, A. L.; Fox, S. V.; Stevens, J.; Tannenbaum, P. L.; Prueksaritanont, T.; Cabalu, T. D.; Cui, D.; Stellabott, J.; Hartman, G. D.; Young, S. D.; Winrow, C. J.; Renger, J. J.; Coleman, P. J. Discovery of 5″-Chloro-n-[(5,6-Dimethoxypyridin-2- Yl)Methyl]-2,2′:5′,3″-Terpyridine-3′-Carboxamide (Mk-1064): A Selective Orexin 2 Receptor Antagonist (2-Sora) for the Treatment of Insomnia. *ChemMedChem* **2014**, *9* (2), 311–322.

(180) Roecker, A. J.; Reger, T. S.; Mattern, M. C.; Mercer, S. P.; Bergman, J. M.; Schreier, J. D.; Cube, R. V.; Cox, C. D.; Li, D.; Lemaire, W.; Bruno, J. G.; Harrell, C. M.; Garson, S. L.; Gotter, A. L.; Fox, S. V.; Stevens, J.; Tannenbaum, P. L.; Prueksaritanont, T.; Cabalu, T. D.; Cui, D.; Stellabott, J.; Hartman, G. D.; Young, S. D.; Winrow, C. J.; Renger, J. J.; Coleman, P. J. Discovery of MK-3697: A Selective Orexin 2 Receptor Antagonist (2-SORA) for the Treatment of Insomnia. *Bioorganic Med. Chem. Lett.* **2014**, *24* (20), 4884–4890.

(181) Raheem, I. T.; Breslin, M. J.; Bruno, J.; Cabalu, T. D.; Cooke, A.; Cox, C. D.; Cui, D.; Garson, S.; Gotter, A. L.; Fox, S. V.; Harrell, C. M.; Kuduk, S. D.; Lemaire, W.; Prueksaritanont, T.; Renger, J. J.; Stump, C.; Tannenbaum, P. L.; Williams, P. D.; Winrow, C. J.; Coleman, P. J. Discovery of Piperidine Ethers as Selective Orexin Receptor Antagonists (SORAs) Inspired by Filorexant. *Bioorganic Med. Chem. Lett.* **2015**, *25* (3), 444–450.

(182) Letavic, M. A.; Bonaventure, P.; Carruthers, N. I.; Dugovic, C.; Koudriakova, T.; Lord, B.; Lovenberg, T. W.; Ly, K. S.; Mani, N. S.; Nepomuceno, D.; Pippel, D. J.; Rizzolio, M.; Shelton, J. E.; Shah, C. R.; Shireman, B. T.; Young, L. K.; Yun, S. Novel Octahydropyrrolo[3,4- c]Pyrroles Are Selective Orexin-2 Antagonists: SAR Leading to a Clinical Candidate. *J. Med. Chem.* **2015**, *58* (14), 5620–5636.

(183) Fujimoto, T.; Tomata, Y.; Kunitomo, J.; Hirozane, M.; Marui, S. Discovery of Spiropiperidine-Based Potent and Selective Orexin-2 Receptor Antagonists. *Bioorganic Med. Chem. Lett.* **2011**, *21* (21),

6409–6413.

(184) Koberstein, R.; Aissaoui, H.; Bur, D.; Clozel, M.; Fischli, W.; Jenck, F.; Mueller, C.; Nayler, O.; Sifferlen, T.; Treiber, A.; Weller, T. Tetrahydroisoquinolines as Orexin Receptor Antagonists: Strategies for Lead Optimization by Solution-Phase Chemistry. *Chimia (Aarau).* **2003**, *57* (5), 270–275.

(185) Hoch, M.; Van Gorsel, H.; Van Gerven, J.; Dingemanse, J. Entry-into-Humans Study with ACT-462206, a Novel Dual Orexin Receptor Antagonist, Comparing Its Pharmacodynamics with Almorexant. *J. Clin. Pharmacol.* **2014**, *54* (9), 979–986.

(186) Di Fabio, R.; Pellacani, A.; Faedo, S.; Roth, A.; Piccoli, L.; Gerrard, P.; Porter, R. a; Johnson, C. N.; Thewlis, K.; Donati, D.; Stasi, L.; Spada, S.; Stemp, G.; Nash, D.; Branch, C.; Kindon, L.; Massagrande, M.; Poffe, A.; Braggio, S.; Chiarparin, E.; Marchioro, C.; Ratti, E.; Corsi, M. Discovery Process and Pharmacological Characterization of a Novel Dual Orexin 1 and Orexin 2 Receptor Antagonist Useful for Treatment of Sleep Disorders. *Bioorg. Med. Chem. Lett.* **2011**, *21* (18), 5562–5567.

(187) Whitman, D. B.; Cox, C. D.; Breslin, M. J.; Brashear, K. M.; Schreier, J. D.; Bogusky, M. J.; Bednar, R. a; Lemaire, W.; Bruno, J. G.; Hartman, G. D.; Reiss, D. R.; Harrell, C. M.; Kraus, R. L.; Li, Y.; Garson, S. L.; Doran, S. M.; Prueksaritanont, T.; Li, C.; Winrow, C. J.; Koblan, K. S.; Renger, J. J.; Coleman, P. J. Discovery of a Potent, CNS-Penetrant Orexin Receptor Antagonist Based on an N,N-Disubstituted-1,4-Diazepane Scaffold That Promotes Sleep in Rats. *ChemMedChem* **2009**, *4* (7), 1069–1074.

(188) Winrow, C. J.; Gotter, A. L.; Cox, C. D.; Doran, S. M.; Tannenbaum, P. L.; Breslin, M. J.; Garson, S. L.; Fox, S. V; Harrell, C. M.; Stevens, J.; Reiss, D. R.; Cui, D.; Coleman, P. J.; Renger, J. J. Promotion of Sleep by Suvorexant-a Novel Dual Orexin Receptor Antagonist. *J. Neurogenet.* **2011**, *25* (1–2), 52–61.

(189) Winrow, C. J.; Gotter, A. L.; Cox, C. D.; Tannenbaum, P. L.; Garson, S. L.; Doran, S. M.; Breslin, M. J.; Schreier, J. D.; Fox, S. V.; Harrell, C. M.; Stevens, J.; Reiss, D. R.; Cui, D.; Coleman, P. J.; Renger, J. J. Pharmacological Characterization of MK-6096 - A Dual Orexin Receptor Antagonist for Insomnia. *Neuropharmacology* **2012**, *62* (2), 978–987.

(190) Boss, C.; Brisbare-Roch, C.; Jenck, F.; Aissaoui, H.; Koberstein, R.; Sifferlen, T.; Weller, T. Orexin Receptor Antagonism: A New Principle in Neuroscience. *Chim. Int. J. Chem.* **2008**, *62* (12), 974–979.

(191) Yoshida, Y.; Naoe, Y.; Terauchi, T.; Ozaki, F.; Doko, T.; Takemura, A.; Tanaka, T.; Sorimachi, K.; Beuckmann, C. T.; Suzuki, M.; Ueno, T.; Ozaki, S.; Yonaga, M. Discovery of (1R,2S)-2-{[(2,4-

Dimethylpyrimidin-5-Yl)Oxy]Methyl}-2-(3-Fluorophenyl)-N-(5-Fluoropyridin-2-Yl)Cyclopropanecarboxamide (E2006): A Potent and Efficacious Oral Orexin Receptor Antagonist. *J. Med. Chem.* **2015**, *58* (11), 4648–4664.

(192) Cox, C. D.; McGaughey, G. D.; Bogusky, M. J.; Whitman, D. B.; Ball, R. G.; Winrow, C. J.; Renger, J. J.; Coleman, P. J. Conformational Analysis of N,N-Disubstitued-1,4-Diazepane Orexin Receptor Antagonists and Implications for Receptor Binding. *Bioorganic Med. Chem. Lett.* **2009**, *19*, 2997–3001.

(193) Coleman, P. J.; Schreier, J. D.; Roecker, A. J.; Mercer, S. P.; McGaughey, G. B.; Cox, C. D.; Hartman, G. D.; Harrell, C. M.; Reiss, D. R.; Doran, S. M.; Garson, S. L.; Anderson, W. B.; Tang, C.; Prueksaritanont, T.; Winrow, C. J.; Renger, J. J. Discovery of 3,9-Diazabicyclo[4.2.1]Nonanes as Potent Dual Orexin Receptor Antagonists with Sleep-Promoting Activity in the Rat. *Bioorganic Med. Chem. Lett.* **2010**, *20* (14), 4201–4205.

(194) Mould, R.; Brown, J.; Marshall, F. H.; Langmead, C. J. Binding Kinetics Differentiates Functional Antagonism of Orexin-2 Receptor Ligands. *Br. J. Pharmacol.* **2014**, *171* (2), 351–363.

(195) Lindstrom, E.; Mentzer, B. Von; Påhlman, I.; Ahlstedt, I.; Uvebrant, A.; Kristensson, E.; Martinsson, R.; Nove, A.; Verdier, J. De. Neurokinin 1 Receptor Antagonists : Correlation between in Vitro Receptor Interaction and in Vivo Efficacy. *J. Pharmacol. Exp. Ther.* **2007**, *322* (3), 1286–1293.

(196) Coleman, P. J.; Schreier, J. D.; Cox, C. D.; Breslin, M. J.; Whitman, D. B.; Bogusky, M. J.; McGaughey, G. B.; Bednar, R. a.; Lemaire, W.; Doran, S. M.; Fox, S. V.; Garson, S. L.; Gotter, A. L.; Harrell, C. M.; Reiss, D. R.; Cabalu, T. D.; Cui, D.; Prueksaritanont, T.; Stevens, J.; Tannenbaum, P. L.; Ball, R. G.; Stellabott, J.; Young, S. D.; Hartman, G. D.; Winrow, C. J.; Renger, J. J. Discovery of [(2R,5R)-5-{[(5-Fluoropyridin-2-Yl)Oxy]Methyl}-2-Methylpiperidin-1-Yl][5-Methyl-2-(Pyrimidin-2-Yl)Phenyl]Methanone (MK-6096): A Dual Orexin Receptor Antagonist with Potent Sleep-Promoting Properties. *ChemMedChem* **2012**, *7* (3), 415–424.

(197) J. Yin; D.M. Rosenbaum. The Human Orexin/Hypocretin Receptor Crystal Structures. In *Current Topics in Behavioral Neurosciences, vol 33., Behavioral Neuroscience of Orexin/Hypocretin.*; A., L., L., de L., Eds.; Springer, Cham, 2017; pp 1–15.

(198) Karhu, L.; Turku, A.; Xhaard, H. Modeling of the OX1R–orexin-A Complex Suggests Two Alternative Binding Modes. *BMC Struct. Biol.* **2015**, *15* (1), 1–17.

(199) Lee, J.; Reddy, M. M.; Kodadek, T. Discovery of an Orexin Receptor Positive Potentiator. *Chem. Sci.* **2010**, *1* (1), 48–54.

(200) Yanagisawa, M. Small-Molecule Agonist for Type-2 Orexin Receptor.

Patent US20100150840A1, 2010.

(201) Cano, M.; Grima, P. M.; Palomer Benet, A. 2-(2-Aminophenoxy)-3-Chloronaphthalene-1,4-Dione Compounds Having Orexin 2 Receptor Agonist Activity. Patent WO2014198880, 2014.

(202) Vuorinen, A.; Schuster, D. Methods for Generating and Applying Pharmacophore Models as Virtual Screening Filters and for Bioactivity Profiling. *Methods* **2015**, *71*, 113–134.

(203) Accelrys Software Inc. Discovery Studio Modeling Environment, Release 3.5. Accelrys Software Inc.: San Diego 2007.

(204) Schrödinger. Small-Molecule Drug Discovery Suite 2013-2: Schrödinger Suite 2013-2 Induced Fit Docking Protocol; Glide Version 5.9; Prime Version 3.2. Schrödinger, LLC: New York, NY 2013.

(205) Dassault Systèmes BIOVIA. Discovery Studio Modeling Environment. San Diego: Dassault Systèmes 2015.

(206) Lagorce, D.; Sperandio, O.; Galons, H.; Miteva, M. a; Villoutreix, B. O. FAF-Drugs2: Free ADME/Tox Filtering Tool to Assist Drug Discovery and Chemical Biology Projects. *BMC Bioinformatics* **2008**, *9*, 1–9.

(207) Cheng, T.; Li, Q.; Zhou, Z.; Wang, Y.; Bryant, S. H. Structure-Based Virtual Screening for Drug Discovery: A Problem-Centric Review. *AAPS J.* **2012**, *14* (1), 133–141.

(208) Schrödinger. Small-Molecule Drug Discovery Suite 2015-3: Schrödinger Suite 2015-3 Induced Fit Docking Protocol; Glide Version 6.8; Prime Version 4.1. Schrödinger, LLC: New York, NY 2015.

(209) Friesner, R. A.; Banks, J. L.; Murphy, R. B.; Halgren, T. A.; Klicic, J. J.; Mainz, D. T.; Repasky, M. P.; Knoll, E. H.; Shelley, M.; Perry, J. K.; Shaw, D. E.; Francis, P.; Shenkin, P. S. Glide: A New Approach for Rapid, Accurate Docking and Scoring. 1. Method and Assessment of Docking Accuracy. *J. Med. Chem.* **2004**, *47* (7), 1739–1749.

(210) Schrödinger. Small-Molecule Drug Discovery Suite 2016-3: Schrödinger Suite 2016-3 Induced Fit Docking Protocol; Glide Version 7.2, Prime Version 4.5. Schrödinger, LLC: New York, NY 2016.

(211) Leino, T. O.; Baumann, M.; Yli-Kauhaluoma, J.; Baxendale, I. R.; Wallén, E. A. A. Synthesis of 1,3,6-Trisubstituted Azulenes. *J. Org. Chem.* **2015**, *80*, 11513–11520.

(212) Leino, T. O.; Devisscher, L.; Sipari, N.; Yli-Kauhaluoma, J.; Wallén, E. A. A. Synthesis of 1,3,6-Trisubstituted Azulenes Based on the 1-Acyloxyazulene Scaffold. *Eur. J. Org. Chem.* **2016**, 5539–5544.

(213) Schrödinger. Small-Molecule Drug Discovery Suite 2015-1: Schrödinger Suite 2015-1 Induced Fit Docking Protocol; Glide

Version 6.6; Prime Version 3.9. Schrödinger, LLC: New York, NY 2015.

(214) Brown, A. C.; Fraser, T. R. V.—On the Connection between Chemical Constitution and Physiological Action. Part. I.—On the Physiological Action of the Salts of the Ammonium Bases, Derived from Strychnia, Brucia, Thebaia, Codeia, Morphia, and Nicotia. *Trans. R. Soc. Edinburgh* **1867**, *25* (1), 151–203.

(215) Putula, J.; Turunen, P. M.; Jäntti, M. H.; Ekholm, M. E.; Kukkonen, J. P. Agonist Ligand Discrimination by the Two Orexin Receptors Depends on the Expression System. *Neurosci. Lett.* **2011**, *494* (1), 57–60.

(216) Bergman, J. M.; Roecker, A. J.; Mercer, S. P.; Bednar, R. a.; Reiss, D. R.; Ransom, R. W.; Meacham Harrell, C.; Pettibone, D. J.; Lemaire, W.; Murphy, K. L.; Li, C.; Prueksaritanont, T.; Winrow, C. J.; Renger, J. J.; Koblan, K. S.; Hartman, G. D.; Coleman, P. J. Proline Bis-Amides as Potent Dual Orexin Receptor Antagonists. *Bioorganic Med. Chem. Lett.* **2008**, *18* (4), 1425–1430.

(217) Cheng, Y.-C.; Prusoff, W. H. Relationship between the Inhibition Constant (Ki) and the Concentration of Inhibitor Which Causes 50 per Cent Inhibition (I50) of an Enzymatic Reaction. *Biochem. Pharmacol.* **1973**, *22* (23), 3099–3108.

(218) Löber, S.; Hübner, H.; Buschauer, A.; Sanna, F.; Argiolas, A.; Melis, M. R.; Gmeiner, P. Novel Azulene Derivatives for the Treatment of Erectile Dysfunction. *Bioorg. Med. Chem. Lett.* **2012**, *22* (23), 7151–7154.

(219) Hong, B.-C.; Jiang, Y.-F.; Kumar, E. S. Microwave-Assisted [6+4]-Cycloaddition of Fulvenes and Alpha-Pyrones to Azulene – Indoles : Facile Syntheses of Novel Antineoplastic Agents. *Bioorg. Med. Chem. Lett.* **2001**, *11*, 1981–1984.

(220) Ikegai, K.; Imamura, M.; Suzuki, T.; Nakanishi, K.; Murakami, T.; Kurosaki, E.; Noda, A.; Kobayashi, Y.; Yokota, M.; Koide, T.; Kosakai, K.; Ohkura, Y.; Takeuchi, M.; Tomiyama, H.; Ohta, M. Synthesis and Biological Evaluation of C-Glucosides with Azulene Rings as Selective SGLT2 Inhibitors for the Treatment of Type 2 Diabetes Mellitus : Discovery of YM543. *Bioorg. Med. Chem.* **2013**, *21* (13), 3934–3948.

(221) Chen, C.; Lee, O.; Yao, C.; Chuang, M.; Chang, Y.; Chang, M.; Wen, Y.; Yang, W.; Ko, C.; Chou, N.; Lin, M.; Lai, C.; Sun, C.; Wang, L.; Chen, Y.; Hseu, T.; Chang, C.; Hsu, H.; Lin, H.; Chang, Y.; Shih, Y.; Chou, S.; Hsu, Y.; Tseng, H.; Liu, C.; Tu, C.; Hu, T.; Tsai, Y.; Chen, T.; Lin, C.; Chiou, S.; Liu, C.; Hwang, C. Novel Azulene-Based Derivatives as Potent Multi-Receptor Tyrosine Kinase Inhibitors. *Bioorg. Med. Chem. Lett.* **2010**, *20* (20), 6129–6132.

(222) Zhang, H.; Unal, H.; Gati, C.; Han, G. W.; Liu, W.; Zatsepin, N. A.; James, D.; Wang, D.; Nelson, G.; Weierstall, U.; Sawaya, M. R.; Xu,

Q.; Messerschmidt, M.; Williams, G. J.; Boutet, S.; Yefanov, O. M.; White, T. A.; Wang, C.; Ishchenko, A.; Tirupula, K. C.; Desnoyer, R.; Coe, J.; Conrad, C. E.; Fromme, P.; Stevens, R. C.; Katritch, V.; Karnik, S. S.; Cherezov, V. Structure of the Angiotensin Receptor Revealed by Serial Femtosecond Crystallography. *Cell* **2015**, *161* (4), 833–844.

(223) Takashima, H.; Mimura, N.; Ohkubo, T.; Yoshida, T.; Tamaoki, H.; Kobayashi, Y. Distributed Computing and NMR Constraint-Based High-Resolution Structure Determination: Applied for Bioactive Peptide Endothelin-1 to Determine C-Terminal Folding. *J. Am. Chem. Soc.* **2004**, *126* (14), 4504–4505.

(224) Lu, S.; Zhang, J. Small Molecule Allosteric Modulators of G‑Protein-Coupled Receptors: Drug–Target Interactions. *J. Med. Chem.* **2018**.

Recent Publications in this Series